DNA DEGRADATION AS AN INDICATOR OF POST-MORTEM INTERVAL

William J. Watson, B.S., M.S.

Dissertation Prepared for the Degree of

DOCTOR OF PHILOSOPHY

UNIVERSITY OF NORTH TEXAS

August 2010

APPROVED:

Robert C. Benjamin, Major Professor
H. Gill-King, Committee Member
Gerard A. O'Donovan, Committee Member
Joseph Warren, Committee Member
John Knesek, Committee Member
Arthur J. Goven, Chair of the Department of Biological Sciences
James D. Meernik, Acting Dean of the Robert B. Toulouse School of Graduate Studies

Watson, William J., DNA degradation as an indicator of post-mortem interval. Doctor of Philosophy (Molecular Biology), August 2010, 174 pp., 3 tables, 42 figures, 280 reference items.

The question of post-mortem interval (PMI) or time since death is often the most sought after piece of information associated with a medical death investigation. Based on the observation that DNA degradation disproportionately affects the analysis of larger genetic loci, it was proposed that DNA degradation, as a result of autolysis or putrefaction, could prove suitable as a potential rate-of-change indicator of PMI.

Nine randomly amplified polymorphic DNA (RAPD) analysis primers and three sets of directed amplification primers were evaluated to determine their suitability for use in assessing the degree of DNA fragmentation in tissue samples. They were assessed for amplicon specificity, total DNA target sensitivity, allele monomorphism and the observance of degradation-based profile changes. Markers meeting the requisite criteria were then used to assess a range samples degraded under controlled and uncontrolled conditions. Tissue samples collected from seven domestic pigs (*Sus scrofa*) were incubated under controlled laboratory or uncontrolled field conditions to produce samples simulating those potentially collected in a forensic case. DNA samples isolated from these specimens were then analyzed at those loci which had been determined to meet the requisite criteria. Collectively, data generated from these analyses indicate that genetic profiles generated by this approach can provide information useful for estimating the post-mortem interval, with the locus and amplicons used being most useful during the first 72 hours after death.

ACKNOWLEDGEMENTS

I wish to thank both Dr. Miguel Castro, of BioSynthesis Inc, and Bruce Boeko, of Orchid Cellmark Inc, for providing many of the reagents, supplies and equipment used to carry out this project.

Since no project of this type can be completed alone, I would also like to thank the people who helped me finish the final stretch. My friends and lab mates Tracy Kim and Aaron Binder, thank you both for making the hours spent in the laboratory easier by your presence. Heath Wessler, thank you for bringing a deskbound administrator back into the laboratory. Dr. Meredith Turnbough, thank you for always being ready with a colorful suggestion for overcoming my latest obstacle. Ron Fazio, thank you for your support through the years. Dr. Joseph Warren, thank you for starting me down this road so many years ago. I owe you each a special debt of thanks.

In addition to those who helped and supported me along the way, there were those whose support made the completion of this project possible. To my major professor and his wife, Dr Robert Benjamin and Toni Benjamin, I owe you a debt that I can never repay; but I look forward to a long and close friendship and the opportunity to try.

Finally, and most importantly, I wish to thank my wife, Melany and my sons, Matthew and Joseph. Your love, support and strength made it difficult to leave you, possible for me to be gone from you, and anxious to come home to you. Thank you.

TABLE OF CONTENTS

Page

LIST OF TABLES

Page

LIST OF FIGURES

Page

CHAPTER 1

INTRODUCTION

> "Watson, can you determine cause and time of death?"
>
> I knelt over the woman and began a cursory examination... "*Rigor mortis* has set in, so I'd estimate she's been dead about 10 to 12 hours."
>
> Holmes stood up and brushed himself off with his hands. "So, that puts her death between midnight and 2 AM."
>
> *Sir Arthur Conan Doyle*

After the question of cause of death; the question of time of death is often the most sought after piece of information associated with a medical death investigation. As a consequence, death investigators find themselves in need of a means of ascertaining the period of time between when an individual's body is found and when they died, sometimes referred to as the post mortem interval. Establishing the time of death through the determination of post mortem interval may have a direct bearing on the legal question of guilt or innocence by confirming that a suspect's alibi covers the period when the victim died, or demonstrating that it does not. If the time of death can be established to within hours, days, months or even years, a suspect may be able to prove that they were at some other place at that time. On the other hand, if the suspect is known to have been in the vicinity of the victim during the appropriate time period, then they can be shown to have had an opportunity to commit the crime. The determination of postmortem interval in natural deaths can also have legal implications in issues of insurance and inheritance (266)

Currently, there are multiple techniques for determining post mortem interval that incorporate methods in almost every discipline of forensic science. Depending upon the circumstances, these techniques can yield results that vary from a narrow accurate

estimate (video of the victim, the victim's stopped watch etc.) to a wide range estimate (counting tree rings on trees growing over or through the remains). Regardless of the of the method used, the calculation of post mortem interval is generally at best an estimate and should not be accepted as accurate without considering all of the factors that can potentially impact the result.

Post Mortem Interval Estimation

> For everything there is a season,
> And a time for every matter under heaven:
> A time to be born, and a time to die…
>
> *Ecclesiastes 3:1-2*

The techniques currently utilized for estimating post mortem interval can be broken down into two broad categories based upon the methodology used (197). The first of these categories are the concurrence-based methodologies. Concurrence based methods relate or compare the occurrence of a known event, which took place at a known time, with the occurrence of death, which took place at an unknown time. Examples of concurrence-based methods include determining the year(s) of manufacture of clothing found on a body, tree ring development, dates on personal effects, etc. Concurrence based methods rely on both evidence associated with the body, and anamnestic evidence such as the deceased's normal pattern of movements. The second grouping of techniques includes rate of change methodologies. Rate-of-change based methodologies measure some aspect of evidence, directly associated with the body, which changes at a known or predictable rate and is started or stopped at the time of death. Examples of the rate-of-change based methods include body temperature, tissue decomposition, insect succession and bone weathering. Some of

methodologies can in fact be considered to fall into both of these categories. Examples of approaches that fall into both categories would be tree ring development (52) and insect succession (4).

Traditional Post Mortem Interval Estimation Methods

The variety of approaches for estimating post mortem interval spring from the varied expertise and experiences of their proponents, and as such the different methods tend to be focused on the immediate needs of the investigator, and are limited to a particular stage of the post mortem interval or type of observation. As a consequence, the period of time for which a specific procedure is effective will overlap the useful window of others.

Assessing Algor*,* Rigor *and* Livor Mortis

> Tis after death that we measure men.
> *James Barron Hope*

The earliest recorded method for estimating early post mortem interval was a rate-of-change methodology based on the most easily observed changes. The cooling of the body after death (*algor mortis*), the gradual stiffening of the body (*rigor mortis*) and the fixed pooling of the blood resulting in discoloration of the lower portions of the body (*livor mortis*) can be easily assessed with minimal instrumentation. Since the time of the ancient Greeks when the following rule of thumb was developed:

> Warm and not stiff: Not dead more than three hours;
> Warm and stiff: Dead between 3 and 8 hours;
> Cold and stiff: Dead between 8 and 36 hours;
> Cold and not stiff: Dead more than 36 hours (226)

From then until modern times, the basis of most temperature based post mortem interval analyses is the assumption that the human body, which averages 98.2^{o}F +/- 1.3^{o}F (160), was at 98.6^{o}F (150) at death and that after death the body loses heat in a predictable manner.

There have been many temperature based methods for estimating post mortem interval. As early as the 1800s, Dr. John Davy had developed a method using the fall in body temperature (*algor mortis*), measured rectally, to determine the post mortem interval (98). This method was refined by De Saram et al. by recording detailed temperature measurements collected from executed prisoners (54). More recent approaches to this technique have included measuring rectal temperature, body surface temperature, ear canal temperature, eye socket temperature and liver temperature (9, 99, 127, 220).

Improvements to these techniques have included multiple progressive sampling, and the introduction of concepts such as the initial temperature plateau, core temperature, heat gradients, the effects of insulation, the ratio of surface area to volume, the effects of humidity, the effect of conductive surfaces, microclimates and postmortem skin cooling (87, 177, 183).

However, most methods that attempt to use body temperature changes to determine the post mortem interval are hampered by individual variability. Even when complex calculations and algorithms have been designed to model for tissue signal, initial temperature distribution, post mortem exothermic reactions and heat loss, the results have not appreciably narrowed the estimate window for post mortem interval. Multiple studies outlining instances of initial temperature increase of a body soon after

death (109) associated with post mortem chemical changes such as *rigor mortis*, cell lysis and the conversion of cellular energy production to anaerobic respiration (177); variations in the core body temperature ranging from 0.5 - 1.2°C during a 24 hour period (46, 150); the effect of variable environmental temperatures (87, 88); and the effect of environmental temperature on overall body surface temperatures (161) have all contributed to limit the usefulness of body temperature as a consistent indicator of post mortem interval. Additionally, once the body has reached ambient temperature, temperature ceases to be a factor. As noted by Henssage and Knight, ‘‘It would seem that the timing of death by means of temperature can never be more than an approximation’’(99).

Assessing Soft and Hard Tissue Decomposition

> Now, a corpse, poor thing, is an untouchable and the process of decay is, of all pieces of bad manners, the vulgarest imaginable…
>
> *Aldous Huxley*

Cadaveric decomposition is a complex process that begins immediately following death and proceeds beyond the time when recognizable human remains have ceased to exist. Decomposition can be broken down into two major stages. The first stage, soft-tissue decomposition, is caused by autolysis and putrefaction. Autolysis is the digestion of tissue by cellular enzymes and digestive processes normally present in the organism. Putrefaction is the digestion of whole tissue systems caused by the enzymatic activity of fungi and bacteria, present in the organism or the environment, that opportunistically invade the tissue. Both autolysis and the microorganisms responsible for putrefaction are normally held in check in living organisms. However,

when an organism dies, the cellular and systemic mechanisms responsible for regulating autolysis and inhibiting putrefying microorganisms stop. "Without these controlling processes the body becomes fancy [bacterial] culture media" (L. Carayannopoulos, personal communication). These early postmortem changes in soft tissues can be used to provide an estimate of the post mortem interval until skeletonization is reached. However, the rate of soft tissue decomposition can be dramatically affected by both internal and external factors that have an impact on the body (i.e. ambient temperature, cause of death, scavenging, trauma, environmental conditions, clothing, body size, mummification and adipocere formation) (38, 137, 162, 170, 206, 257). There are reported instances of accelerated decomposition associated with acute illness (76) and I am personally aware of an instance of a post mortem interval of less than eleven days resulting in complete skeletalization of an individual that died of complications related to acquired immunodeficiency syndrome (262) . Additionally, there are a number of examples of bodies remaining unusually intact for decades after death (13).

Beyond gross observation for assessing decomposition, researchers have developed multiple morphometric and chemical methods for assessing soft tissue decomposition. Early (ca.1800s) methods such as the Brouardel method, examined the shift in flammability of putrefaction gases in the early post-mortem interval, and the Westernhoffer-Rocha-Valverde method examined the formation of crystals in the blood formed after the third day of putrefaction (41). More modern methods such as ultrasound assessments of organ condition (251) and the use of electron microscopy have been used to examine measurable physical changes in mitochondria (173) and

platelet count (244). Chemical methods used to assess time since death include the assessment of volatile organic compound formation (55, 227, 228, 257), the concentrations of non-protein nitrogen (78, 211) and creatinine (33, 78).

Bony tissue decomposition, the second major stage of decomposition, results from a combination of surface weathering due to environmental conditions (temperature, humidity, sunlight) and erosion from soil conditions (pH, mineral content, etc.) (18, 116). While few detailed studies have been completed to identify exactly how and to what extent environmental factors affect bony tissue breakdown, it has been established that factors such as pH, oxygenation, hydrology and soil flora and fauna can influence the long term stability of collagen (19, 79, 97). Collagen, the primary proteinaceous component of bone, slowly hydrolyzes to peptides, and then to amino acids, leading to the breakdown of the collagen-mineral bonds and subsequent weakening of the overall bone structure. This, in turn, leaves it more susceptible to environmental weathering (97). By examining the effects of related changes (cracking, flaking, vacuole formation, UV-fluorescence of compact bone) the investigator can estimate the period of time a bone sample has been exposed to weathering (19, 116, 268, 276). Current methods of assessing time since death using bone weathering rely heavily upon the experience of the investigator (134) and are limited to immediately post skeletalization to 10 to 100 years based on environmental conditions (90).

As with the assessment of soft tissue decomposition for time since death estimation, investigators examining bone decomposition have supplemented observational methods with quantifiable testing techniques that analyze changes that are not directly affected by the physical environment (148). Radiocarbon dating of

carbon-14 and strontium-90 has been used to group remains pre and post 1950 (151, 242). Neis et al. suggested that, with further study of strontium-90 distributions, determination of times since death should be possible (176). Bradley suggested that measuring the distribution of ^{210}Pb and ^{210}Po in marrow and calcified bone could prove forensically significant (31). This work was built upon by Swift who evaluated using ^{210}Pb and ^{210}Po distribution in conjunction with trace element analysis to provide a meaningful estimate of the post-mortem interval (237, 238). Maclaughlin-Black et al. demonstrated that chemical changes due to the environment could measurably affect isotope levels (151). In addition to radionucleotide studies, investigators have also measured the changes in both organic (amino acids, urea, proteins, DNA) and inorganic compounds (nitrogen, potassium, sulfur, phosphorus) in bone (117, 200).

Assessing Stomach Contents/Rate of Digestion

> Govern well thy appetite, lest sin surprise thee, and her black attendant Death.
>
> *John Milton*

The presence or absence of food in the stomach is often used as an indicator of post mortem interval. Its use as an indicator of post mortem interval is predicated on the assumption that, under normal circumstances, the stomach digests and empties at a predictable rate, taking from 2 to 6 hours to eliminate a full meal (115). If a person had eaten a light meal the stomach would empty in about 1.5-2 hours. For a medium-sized meal the stomach would be expected to take about 3 to 4 hours to empty. A large meal would take about 4 to 6 hours to exit the stomach. Regardless, it would take from 6 to 8 hours for the initial portion of the meal to reach the large intestine (91). This

information, coupled with reliable ante-mortem information relating to when an individual last ate, is used by some pathologists when providing an estimate of the time since death within hours. It is for this reason, among others, that comprehensive autopsies usually include an examination of the stomach contents (15, 219).

Although it provides another useful indicator of time since death, there are serious limitations to the assessment of the stomach contents as an accurate indicator of time since death. Its reliance on reliable anamnestic evidence limits its usefulness to a small number of cases (115). Researchers have found that variations in how the food was eaten such as the extent to which the victim chews their food (190), the types of food eaten (protein vs. fiber vs. fat) (63, 245) and the amount of liquid and/or alcohol consumed with the meal can influence stomach emptying. Additionally, the physiological (118, 143, 194, 247) and the psychological (115) state of the victim can dramatically affect stomach emptying. As if pre- and perimortem factors did not complicate the estimation process, there is significant evidence that digestion can continue after death (136), making the assessment of the condition of the stomach contents related to post mortem interval difficult at best.

Assessing Insect Succession

Buzzards gotta eat same as worms.
Josey Wales

Insect colonization of a body begins within hours of death and proceeds until remains cease to be a viable insect food source. Throughout this period, multiple waves of colonization by different insect species, as well as multiple generations of previously established species can exist. Forensic entomologists can use the waves of

succession and generation time to estimate the postmortem interval based on the variety and stage of development of the insects, or insect remnants, present on the body (7). In addition to information regarding time since death, forensic entomology can provide useful information about the conditions to which the body was exposed. Most insects have a preference for specific conditions and habitats when colonizing a body and laying their eggs. Modifications to that optimal habitat can interrupt the expected insect colonization and succession. The presence of insects or insect larva that would typically be found on bodies colonized indoors or in shade on a body discovered outside in direct sunlight may indicate that the body was moved after death (217). Aquatic insects found on bodies discovered on land could indicate the body was originally in water (201, 260).

Although insect succession varies by season, geographic location and local environmental conditions, it is commonly assumed to follow a predictable sequence within a defined habitat. While there are a multitude of studies that have examined regional succession patterns (7, 65, 163, 217, 239, 240), these studies use different approaches to define habitat and assess insect succession and thus make cross-comparisons of their data difficult. Also, the majority of these studies do not rigorously address the statistical predictability of a species occurrence, making their results of limited use as post mortem interval indicators (168). Additionally, beyond the presence or absence of clothing, the majority of the post mortem entomological studies conducted do not examine non-habitat external factors that may affect succession. For example, only a few studies have been conducted that assess the effect of drug ingestion (81) or the presence of chemicals (bleach, lye, acid etc.) used to “cover-up” evidence (42) on

the insect life cycle. As with other means of assessing time since death, more extensive studies with different insect species and drugs in a wider variety of habitats are necessary.

Assessing Electrolyte Concentration

Death is a low chemical trick played on everybody…
J.J. Furnas

Cellular activity does not immediately cease when an organism dies. Rather, individual cells will continue to function at varying metabolic rates until the loss of oxygen and metabolic substrates caused by the cessation of blood flow results in hypoxia (low oxygen). As cell metabolism shifts from aerobic to anaerobic, oxidative phosphorylation and ATP generation, the cellular processes powering the mechanisms that keep autolysis in check, begin to decrease and eventually cease entirely. Without energy to maintain osmotic and ionic gradients, fluid and reactive ions begin to build up in some areas of the cell and decrease in others. These changes in the cell physiology eventually result in the activation of cellular apoptosis (51). At the same time the shift from aerobic to anaerobic respiration results in the build-up of lactic acid in the cell. The decrease in the pH of the cytoplasm activates released lysosomal enzymes and the cell begins consuming itself from the inside out (30). With autolysis comes a cascade of released metabolic chemicals, originally sequestered in various cellular structures, that begins to diffuse down their respective concentration gradients (according to Fick's law) into the intracellular spaces (153). Forensic researchers have used the presence, absence or effects of inorganic ions such as potassium, phosphate, calcium, sodium and chloride as a means of estimating time since death (213). In most instances the

higher the initial concentration gradient, the more suitable is the analyte for the estimation of the time since death. When analyzing body fluids for the purpose of estimating post mortem interval, early researchers tended to focus their studies on those such as, cerebrospinal fluid, blood and pericardial fluid (50, 99, 212, 270), with a few other researchers examining additional compartmentalized bodily fluids (157) and the largest numbers focusing on vitreous humor (71, 138, 156, 158, 243). Chemical methods used to assess these analytes in blood and spinal fluid as indicators of post mortem interval have failed to gain general acceptance because, for the most part, they failed to produce precise, reliable, and rapid results as required by the forensic community (148). Currently applied chemical methods, which have primarily focused on vitreous fluid, tend to suffer from the same limitations demonstrated by the fact that with notable exceptions (197) very few statistically rigorous field studies on the reliability and precision of estimating post mortem interval are available in the literature (49, 153).

Assessing Enzyme Activity

> Each of us, as with all living organisms, could be regarded
> as an orderly, integrated succession of enzyme reactions.
> *Humbart Santillo*

As previously discussed, cellular biochemical activities do not stop when clinical death occurs. In any circumstances where the cellular metabolism shifts from a homeostatic balanced state to an imbalanced state, additional biochemical changes occur. Changes in the levels or activity of proteins (i.e. cardiac troponin, c-reactive proteins, and G proteins) have long been used as indicators of cellular stress (129, 141, 250, 252). Assessing similar changes in cellular biochemistry as a function of time

since death provides investigators with a wide variety of tissues, testing methods and analytes for consideration. As a consequence, forensic investigators have assessed and suggested enzymes from heart, pancreas, muscle, blood and brain as potential amplicons for time since death (120, 128, 195, 264, 265). Comparisons of total ante and post mortem proteins as analyzed with two-dimensional gel electrophoresis and Matrix Assisted Laser Desorption/ Ionization Time-of-Flight (MALDI-TOF) have demonstrated changes in metabolic enzymes levels, (108, 120). Assessing the changes in enzyme levels provides examiners a means to assess time since death, in many instances long before visible cellular changes occur. However, in at least a few of these studies, results indicate that enzyme degradation during extraction and partial enzyme activity observed with degradation products makes these amplicons better suited for qualitative analyses rather than quantitative analyses (208).

Assessing Muscle/Nerve Excitation

Our nature consists in motion; complete rest is death.
Blaise Pascal

Both neurons and myocytes retain the ability to respond to electrical stimulation for at least a short period of time after organism death. (34, 210, 233). The response of nervous and muscle tissue to external electric stimulation has also been investigated and proposed as a means to estimate time since death (133, 232).

Methods developed to investigate myocyte excitability assess the relative magnitude and duration of the muscle contraction during the application of external stimulation. To assess the contractile response, a combination of observational based

assessments (123, 154) and measurement based assessments (100, 152) have been suggested and reported.

Similar investigations have examined post mortem excitation of nervous tissue by measuring a variety of neurological reactions to stimuli. These include the alteration of Compound Muscle Action Potential (CMAP) (66, 67, 182), lengthen of the refractory or non-propagating period immediately following the CMAP (164), the extracellular impedance/resistance (204), the chronaxie measurement or the time over which a current double that necessary to produce a contraction is applied before the contraction occurs (232) and the changes in the amplitude of the F-wave (the secondary CMAP observed after the initial CMAP) have all been examined, and been suggested as potential indicators of time since death.

The results of studies examining the response of excitable tissue to electric stimulation have been consistent in that the stimulation response varies predictably relative to time. However, suitability for absolute indicators of time since death remains in question as investigators have reported contradictory results related to the effect of the manner of death on the stimulation response (67, 155).

Assessing RNA Degradation

> Faith in chemistry is so touching in origins of life studies.
>
> *Adam Crowl*

RNA degradation, both antemortem and postmortem, is a complex process that is not well understood. Unlike with DNA degradation, continuous degradation of inducible mRNAs by endogenous ribonucleases is used as a means of translational control. After cell death these ribonucleases, no longer kept in check by the

mechanisms of cellular homeostasis, combine with exogenous ribonucleases from bacteria and fungi to begin the un-inhibited digestion of all cellular RNA. Investigators have noted extensive variability in RNA degradation rates in different tissues (16). Not surprisingly, such variability appears to be related to the antemortem ribonuclease activity of the tissue; with relatively "ribonuclease poor" tissues such as brain and retina exhibiting greater RNA stability (122, 159) when compared to ribonuclease rich tissues such as liver, stomach and pancreas (17, 72, 107). Additionally, but also not surprisingly, some constitutively expressed mRNAs have been shown to be more stable, or perhaps simply more prevalent, than inducible mRNAs (111). Additionally, while mRNA levels are fairly constant when comparing regions within a brain, levels vary considerably when making comparisons between brains (199). As a consequence of these observations, RNA (total and/or mRNA) has been suggested as a potential degradation analyte to assess time since death.

Researchers examining the effect of post mortem interval on RNA stability have examined a variety of targets (mRNA, both tissue specific and constitutively expressed, and total RNA) with an assortment of methods including Reverse Transcriptase (RT) PCR(73, 92, 185, 277), RNA (cDNA) microarrays (10, 40, 196, 223) and quantitative RT-qPCR (256). Based on these studies, there are indications that beyond time and temperature, factors such as hypoxia, tissue pH, antemortem physiological conditions (coma, seizure activity and injury) postmortem transcriptional activity and RNA sequence can dramatically affect the stability and measurable levels of RNA (16, 37, 40, 94, 185). When examining the seminal question regarding time since death and temperature some researchers have reported temperature and time as significant

factors affecting mRNA levels (37), while others have reported the reverse (94, 198). These contradictory data are not surprising given the changes in the specificity, sensitivity and application of the assays used; however, the ultimate question has not been resolved. What is clear from the research is that RNA degradation (mRNA or total) is a complex process (96, 198, 199) affected by multiple factors indicating more study will be required before RNA degradation can be considered a reliable indicator of time since death.

DNA Degradation and Its Effect on DNA Typing

> DNA is an abbreviation for deoxyribonucleicantidisestablishmentarianism, a complex string of syllables.
>
> *Dave Barry*

Since the initial application of molecular biology techniques to samples of forensic significance in the latter half of the 1980s, forensic scientists have noted that increased exposure to environmental insult can result in DNA degradation. Developmental validation studies performed to evaluate the efficacy of new typing techniques (236) have found that environmental variables such as heat, high humidity, direct moisture, fungal/bacterial contamination and ultraviolet radiation can impact the quantity or quality of the DNA sample, making it unsuitable for DNA analysis (20, 86, 165, 181, 214, 241). During transitions in technology from Restriction Fragment Length Polymorphism (RFLP) analysis to Polymerase Chain Reaction (PCR) based testing, researchers noted that samples too degraded to produce an RFLP pattern could still yield profiles using a variety of PCR-based amplicons that evaluated loci shorter in length (102). This finding supports the hypothesis that degradation in the forensic

setting is (not surprisingly) processive. Additional research found that, while the DNA in some samples like cadaveric blood and kidney tissue could degrade to the point where it was no longer suitable for DNA fingerprinting after as little as a week (147), other samples such as bone (75, 102) and teeth (193, 216) could under most conditions provide DNA that can be typed for months or even years.

The fact that DNA degradation has a disproportionate detrimental effect on larger genetic loci, and occurs in different tissues at different rates, is considered to be of extraordinary forensic significance. This is evidenced by the number of studies that seek to examine, and overcome the effects of degradation on DNA typing analyses (42 forensic validation studies specifically mentioning DNA degradation from 1995-2009 in Pub Med). This interest makes perfect sense when the observer considers the impact that degradation can have on selecting suitable samples, choosing the profiling technique(s) used and evaluating the resultant DNA profiles. However, a number of researchers have looked beyond the simple question of how degradation affects the typing of samples to address broader questions such as the mechanisms of postmortem degradation (53, 74) and synthesis (184) and how that knowledge can be used to assist in the assessment of time since death.

Assessing DNA Degradation by RFLP

Since Sir Alec Jeffreys first applied Southern blotting (224) techniques to the testing of forensically significant samples in 1985 (119), DNA analysis has revolutionized forensic science. Restriction Fragment Length Polymorphism DNA analysis relies on variations in the lengths of DNA fragments generated by restriction

enzymes. With restriction fragments generated from the chosen loci ranging from approximately from 0.5 to 33 kilobase pairs (11), successful typing and analysis requires high quality (un-fragmented) DNA. Researchers noted from the outset that in some cases involving older and/or postmortem samples that DNA degradation resulted in the gradual disappearance of the longer fragments and thus reduced the potential evidentiary value of older samples (12). At about the same time, researchers interested in assessing time since death were building on this work by comparing DNA degradation in rib bone from multiple individuals using Southern blotting and radioactive probe detection techniques. Results of this early work indicated that variation in the rate of DNA degradation between individuals was not as significant as between samples exposed to different postmortem intervals and temperatures (191).

Assessing DNA Degradation by DNA Flow Cytometric Analysis

Flow cytometry is a method that can be used to determine the relative nuclear DNA content in individual cells. Flow cytometer analyses involve moving cells or chromosomes in suspension through units where they are excited by a source of light (U.V. or laser) and in turn emit a signal. The signal is captured and converted into a graphical representation of the intensity of the fluorescence emitted. By using a DNA specific fluorescent dye and analyzing the amount of fluorescence emitted by a cell, the analyst can evaluate the DNA content. The results of this measurement can be used to assess the amount of DNA in a cell even when to fragment sizes from about 1-150 kilobases (70, 272).

Utilizing flow cytometry, researchers have investigated the effects of time related

degradation/fragmentation on DNA in postmortem eukaryotic cells (1) with at least one investigator demonstrating no significant differences in DNA degradation between fresh splenic tissue and tissue degraded up to 36 hours (58). Forensic investigators have proposed using a variety of different tissues as sources of samples that would demonstrate the best correlation between DNA degradation and postmortem interval. Splenic cells have been recommended by several investigators (29, 47, 57). Other internal organs evaluated include blood and liver, with hepatic tissue showing an almost linear correlation between the time since death and the level of DNA degradation (57). "Non-organ" tissues suggested as suitable samples for flow cytometry evaluations of time since death include costicartilage cells and dental pulp (29, 145).

While investigators have found good correlations between time since death and DNA degradation measured using flow cytometry, limitations to the procedure as it was originally proposed have proven difficult to overcome for forensic samples. Flow cytometry requires a suspension for staining and analysis. This makes solid tissue difficult to analyze without extensive manipulation. Additionally, the assay measures total DNA, making the differentiation between intact human DNA and bacterial or fungal DNA difficult. While several modifications to flow cytometry have made it more specific and sensitive (85), the approaches have not gained the same general acceptance as has, for example, DNA amplification in DNA profiling techniques.

Assessing DNA Degradation by Single Cell Electrophoresis

Single cell gel electrophoresis (SCGE), sometimes referred to as a comet assay, uses migration of DNA from cells encapsulated in agarose to measure the level of DNA

fragmentation. A tissue sample is encapsulated in agarose and the DNA within the tissue is denatured. The DNA is electrophoresed through the encapsulating agarose and samples with degraded DNA generate smeared tails (hence the name comet assay). The stronger the signal from the tail, the more DNA damage present. Tail length is directly influenced by the size of the DNA fragments with more degraded DNA generating longer tails. The tail moment is the product of the fraction of DNA in the tail and the tail length and is related to the proportion of non-fragmented to fragmented DNA.

Forensic investigators have evaluated SCGE as a means of assessing time since death, analyzing DNA from skeletal muscle, heart muscle, liver and kidney with increasing postmortem intervals (121, 278). Measurement of tail-length has provided the strongest statistical correlation based upon regression analysis. (121). While a promising technology, SCGE lacks specificity, being unable to differentiate between eukaryotic and prokaryotic DNA mixtures. It is relatively insensitive, requiring microgram quantities of DNA and exhibits excessive interlaboratory variability due to a lack of consistent protocols and analysis techniques (56). Despite these issues, several investigators have suggested SCGE as a useful quantitative assay to pair with RT-PCR (2). As with flow cytometry, however, SCGE has not gained the same general acceptance that PCR- based assay's have.

Assessing Measurement of DNA Degradation by In Situ Labeling

Fluorescence in situ hybridization (FISH) is a technique used to detect specific DNA sequences on chromosomes. FISH uses a fluorescently labeled probe that is

complementary to the DNA sequence of interest. Once bound, the probe can be detected using fluorescence microscopy or other fluorescence sensitive instrumentation.

Forensic FISH techniques using centromeric probes for sex chromosomes were developed to identify the sex of contributors to bloodstains (192) and for the selection and microdissection of male cells on slides with male/female cellular mixtures (255).

Assessing DNA Degradation by Image Analysis/Staining

A variety of different nucleic acid staining techniques have been applied to the analysis of forensic evidence. As is often the case with technology, the use of nucleic acid staining as a means of assessing medico legally significant aspects of a case has been cyclical. Early applications of nucleic acid/chromatin staining such as the use of Kernechtrot-Picroindigocarmine (KPIC) staining, sometimes referred to as Christmas tree staining (267), and the Feulgen method with Schiff's reagent (135) were first applied to the detection of sperm in evidence associated with sexual assaults. Modifications to these techniques further refined their efficacy in criminal cases allowing the determination of the sex of hairs (174). With the advent of DNA analysis protocols for the determination of paternity (119) and for forensic testing (83), nucleic acid staining moved from the forefront of forensic testing to a secondary position as an ancillary analysis technique used with RFLP (139, 263) and PCR (36).

However, even as the majority of forensic scientists began moving away from staining nucleic acid as an analysis technique in and of itself, other researchers were developing new staining assays that had the potential to provide information still very

useful to the forensic investigator. Researchers investigating DNA damage developed specialized staining techniques using fluorochromes that, under the proper conditions, interact preferentially with double-stranded DNA (dsDNA), allowing them to make measurements of DNA denaturation/damage (14). Other researchers have developed new applications for the Feulgen method that combine staining with micro densitometry, allowing increased sensitivity and accuracy for this approach (93). By applying these methods to a variety of different cell types (44, 142) several investigators have reported both a linear relationship between DNA degradation and the early time since death window (43, 142, 144, 218) and a measurable effect of temperature on the rate of degradation (261). For the most part, however, general staining techniques lack specificity—most importantly being unable to differentiate between eukaryotic and prokaryotic DNA mixtures. This is very relevant for forensic samples and for time since death applications would thus require the use of intact tissues not exposed to bacteria, making the majority of postmortem forensic samples unsuitable for analysis by such techniques.

Assessing DNA Degradation by DNA Amplification

Polymerase chain reaction (PCR) (172, 209) is a process used to copy, or amplify, specific segments of a DNA fragment by many orders of magnitude. PCR performs this amplification by reproducing in a test tube the normal process of DNA replication that occurs in the cell. Samples that start with only a few complete copies of template DNA can, with the aid of PCR, yield in a relatively short time tens of millions of copies of the sequence of interest suitable for genetic analysis. This is possible

because as PCR progresses, each replicated copy of the target loci produced by a previous copying cycle is replicated again and again in subsequent cycles, resulting in an exponential increase in DNA copies. The PCR process starts with an enzymatic reaction mix that contains an optimizing buffer, a thermostable DNA polymerase often from *Thermus aquaticus (Taq*), short DNA sequences (primers) complementary to the DNA target locus/loci and deoxyribonucleoside triphosphates (dNTPs, the individual building blocks used to assemble new DNA strands). This reaction mix is then combined with the extracted template DNA and placed in a thermalcycler. The thermalcycler unit alternately heats and cools (cycles) the mixture, allowing one complete round of the replication process to occur with each cycle. The initial step in each cycle is denaturation, where the reaction mix is heated to near boiling and the dsDNA template separates (melts) into two single strands. The reaction mix is then cooled to the optimal sequence-dependent temperature for the primers to bind or anneal to the DNA template. During the subsequent extension step the reaction mix is heated to the optimal extension temperature for *Taq* (or related thermophilic) polymerase to extend the primer, making a new copy of each of the targeted loci in the DNA sample.

Since the mid 1980s, all DNA-based methods for establishing human identity and/or kinship have relied on various methods of assessing length polymorphisms, sequence polymorphisms or both. As testing preferences shifted from large fragment analyses like RFLP (VNTR minisatellite loci having alleles with average sizes in the multiple kilobase pair range) to shorter allele loci such as STR microsatellites (having alleles ranging from <100 – 350 base pairs) there was a lessened need, and

concomitant lessened focus, on the condition/degradation level of the sample DNA. However, as PCR-STR analyses has became more widespread and applied in more varied types of case-work it became obvious that regardless of the fragment size assessed, DNA degradation can potentially have a negative effect on testing results. Most forensic scientists have viewed the issues associated with STR typing of degraded samples as a problem to be overcome, either with the development of complicated interpretation guidelines (2, 84), or new STR kits that type ever smaller DNA fragments (187). Other forensic scientists have seen the potential of using DNA fragment amplification as a means of assessing degradation (12).

Assessing DNA Degradation by Competitive PCR

Competitive PCR (c-PCR) is a quantitative PCR procedure where one adds a "competitor DNA fragment" with the same primer recognition sites as the target locus but that produces a unique/different sized PCR amplicon (279). Once the PCR amplification process in completed, the product amplicons are separated using slab gel (agarose or polyacrylamide) electrophoresis or capillary electrophoresis. The signal intensity from the target fragment amplicon (from the DNA sample being analyzed) and that from the "internal control" competitive fragment are compared to determine the concentration of the target sequence in the unknown DNA.

Researchers have used the competitive PCR process to develop quantitative PCR assays that use probes targeting the mitochondrial DNA hypervariable region I and the amelogenin locus. Using this approach, investigators were able to assess changes in the quantity of DNA in tissues exposed to different conditions for different periods of

time, finding that DNA was well preserved in bone and fingernails but rapidly decreased in soft tissues regardless of the exposure time or conditions (110).

Assessing DNA Degradation by Real-Time PCR

Real-time quantitative PCR (RT-qPCR) is an amplification process that allows the quantification of the number of copies of a specific DNA sequence present in a sample. The procedure relies on PCR but the amplification process is combined with a means to continuously monitor the increase in dsDNA PCR product. The initial publication describing quantitative PCR utilized the hybridization of radioactively labeled probes to the amplified product followed by exposure to X-ray film (130). Subsequent researchers proposed modifications to these quantitative techniques that used the 5'-3'-exonuclease activity of *Taq* polymerase to release the radioactive tags or fluorescent dyes associated with the bound primers. The released radioactive or fluorescent modifiers were assessed with either exposure to film (103) or capillary electrophoresis (68). However, while these assays were informative, they could not be considered "real-time" in that they each required post PCR manipulations to produce interpretable data. The initial publication suggesting a real-time method proposed the use of intercalating dyes combined with a video monitor to measure the increase in signal in real time (101). Subsequently, multiple researchers proposed adapting Holland's method for use with analytical thermalcyclers that could measure the increase in fluorescence by the sample as the amplification process progressed (45, 82, 95).

Over the last ten years RT-qPCR based methods have become the standard method for forensic sample DNA quantification (89). The Quantifiler™ human kit

produced by Applied Biosystems targets a 62 base amplicon within an intron in the human telomerase reverse transcriptase gene (hTERT) at chromosomal location 5p15.33 (179). The process uses standard oligonucleotide primers for amplification, a minor groove binding TaqMan® reporter probe (95) and the 5'-3' exonuclease activity of *Taq* polymerase as described by Holland above. The reporter probe has a fluorescent tag on the 5' end, a fluorescent signal quencher on its 3' end and binds in the minor groove of one strand of the target DNA. During amplification, as *Taq* extends the amplification primer bound to the strand with the reporter, the enzyme encounters and excises the 5'end of the reporter probe, releasing the fluorescent tag. Once the fluorescent tag is no longer in close proximity to the quencher it gives off a detectable signal when excited by UV radiation.

As the equipment necessary to perform RT-qPCR has become more prevalent in forensic laboratories, and forensic scientists have become more familiar with the procedure and results, forensic researchers began to recognize the potential for using RT-qPCR to assess both the quantity of DNA and the likelihood of successful genotyping of DNA isolated from forensic samples. To achieve this, researchers have proposed modifications to the procedure that would allow analysts to assess both total DNA and the degradation level of that DNA. The most straightforward modification was the incorporation of a longer amplicon (170-190 bp) to assess the level of degradation (234, 235). The short amplicon included in the Quantifiler® kit (62 bp) is much shorter than the amplification products obtained by commonly used genotyping kits (106-350 bp) resulting in instances where sufficient quantities of DNA are present to quantify but no profile can be obtained due to the quality of that DNA—the average fragment size

being too small to yield intact amplicons of the genotyping loci. Other researchers have proposed incorporating multiple probes to assess gender, degradation and inhibition (105). Niederstatter et al. have evaluated the incorporation of multiple varying sized amplicons that target both nuclear and mitochondrial DNA (180). Although, as noted in the RNA section above, some research has been conducted investigating the application of RT-qPCR combined with reverse transcription (RT-PCR) of RNA to assess time since death, using RT-qPCR to compare the rate of decomposition of RNA between tissues (246) and determining insect age to assess time since death (6), little or no work has been performed applying this approach to the direct assessment of DNA degradation to determine time since death .

Assessing DNA Degradation by Amplified Fragment Size Analysis

Competitive PCR and RT-qPCR techniques described above were both initially designed as quantitative PCR techniques with the goal to determine human DNA yield. These approaches were then adapted by investigators to assess degradation. Amplified Fragment Size Analysis, hereafter referred to as FSA-PCR is an approach where the investigator evaluates the size distribution of amplified fragments in order to assess the level of DNA fragmentation in a sample. In contrast to the two previously discussed methods, this method was specifically developed to allow the estimation of DNA "quality" and provides little information about the absolute DNA quantity. In this instance quality can be defined as a combination of the fragmentation level of the DNA as well as it's availability for amplification. As noted above, DNA that is fragmented to the point where few to none of the remaining fragments span the desired amplicon will

no longer produce amplified product, or produce products at a very reduced level. Additionally, samples with intact DNA but that contain PCR inhibitory contaminants that bind the DNA or co-purify with the DNA may also fail to amplify. Unlike quantitative PCR methods which typically utilize smaller amplicons to provide estimates of the absolute quantity of DNA but in the process can underestimate the quantity of DNA in the required larger amplicon ranges; FSA-PCR focuses on assessing DNA for fragments of sufficient size to allow for amplification of larger amplicons. Additionally, unlike RT-qPCR, an internal positive amplification control is used with each sample and the amplicon length for this control is ideally restricted to 50 – 150 bp (3) Additionally, in competitive PCR the competitor DNA must be pre-amplified, purified, quantified then added to the amplification (279). FSA-PCR is less complicated in that it does not require an internal standard/competitor and the fragment length possibilities are only limited by primer design, enzyme efficiency, GC content and detection method.

Several investigators have developed FSA-PCR assays specifically to assess DNA quality in forensic samples. One proposed assay developed by Von Wurmb-Schwark et al. used fluorescently labeled amplicons in the mid-range of STR analysis (164 bp) and mitochondrial sequencing (260 bp) assayed on a ABI Prism® 310 to predict the likelihood that a forensic sample (bone, formalin fixed tissue and casework) would produce a full STR profile (259). Kaiser et al. used the amplification of fragments of the beta-actin gene ranging from 150-750 bp to assess the quality of DNA in various layers of bone ranging in age from 1-200 years (126). Most recently, researchers in Australia used FSA PCR to examine the effect of time and temperature on the DNA in porcine skeletal muscle (140).

Research Objectives

Forensic scientists who perform DNA analysis are not only interested in the application of molecular biology techniques to the area of DNA analysis, but, are also interested in applying technology existing in their field to new areas of forensics. It has been well established that the degradation of DNA influences its ability to be typed using standard genotyping methods (48, 64). Further, studies using the controlled enzymatic degradation of purified DNA have shown that the capacity of a genotyping method to produce a profile is directly related to its minimum required DNA fragment length and the level of sample degradation and thus it varies from procedure to procedure and specimen to specimen. Such studies have been invaluable in establishing the limitations of a genotyping method related to the level of degradation exhibited by the DNA specimen under controlled conditions. Additional studies, examining the effects of various environmental insults have been performed on degraded tissues in order to shed light on the strengths and limitations of the genotyping method examined (132, 225, 254). Although instrumental in developing and understanding new genotyping methods, these studies have been limited to “naked” DNA, tissue specimens degraded under uncontrolled conditions or stains on cloth. While such samples simulate certain types of DNA evidence found at crime scenes, as with the enzymatic degradation studies, these samples typically are not degraded under controlled conditions and thus are of limited value as models in studying post mortem interval. Unlike anthropological studies designed to assess degradation in specimens under strictly controlled environmental conditions to determine post mortem interval

(58), most DNA validation studies that examine degraded DNA have not attempted to correlate typing data with the post mortem interval.

This study was designed to examine the effect of temperature and time on the degradation of DNA within soft tissue, and to determine if the type and degree of DNA degradation found in samples could be used to estimate post mortem interval.

To accomplish the objectives of this project the following aspects were addressed:

1. Suitable loci/amplicons were identified.
2. A PCR-based assay that allows the assessment of the fragmentation level of DNA was developed.
3. A method of controlling or eliminating microbial putrefaction was established.
4. Skeletal muscle was degraded and analyzed under the controlled conditions.
5. The relevant data were analyzed.

Oligonucleotide primers were designed to allow the PCR amplification of varying sized fragments of nuclear loci, mitochondrial loci and RAPD amplicons. An FSA PCR-based assay was developed initially using DNase I degraded DNA. Tissue samples, handled a manner designed to decrease or eliminate microbial putrefaction, were degraded under laboratory controlled conditions and assessed with the FSA PCR assay. The amplified fragments, obtained from samples exposed to varying conditions, were analyzed using gel electrophoresis. Differences in the quantities of the individual amplicon products were compared and assessed.

The application of FSA-PCR testing to samples degraded in a controlled fashion should provide a valuable technique for assessing time since death based on the

relative level of DNA fragmentation. However, even if the method is unable to provide definitive estimates of the postmortem interval, it should provide additional information regarding the rate of DNA degradation related to autolysis as well as providing a new approach for the assessment of the effects of varying conditions on the rate and extent of DNA degradation.

CHAPTER 2

MATERIALS AND METHODS

Tissue Selection

The nearest thing to the flesh of a man is the flesh of a pig.
William "Bill the butcher" Cutting

DNA and tissue used for all laboratory studies were prepared from muscle tissue (pig tongue, *Sus scrofa*). Tongues (designated Specimens 2-7) were collected from a local abattoir at or near (within 1 hour) the time of slaughter and stored on wet ice for not more than 1 hour before hard freezing at –80°C. Tissue used for all field samples included skin and blood collected from an intact animal. An intact animal (designated Specimen 1) was collected from a local abattoir at the time it was sacrificed using a penetrating captive bolt pistol. The head wound was sealed with silicone caulk and the animal transferred to a partially shaded location and placed in a wire mesh cage within two hours of death.

Field Location

Tissue sample sets were placed at 33.130694° N, 97.160127° W 689 ft elevation with temperatures collected at 33.206° N, 97.199° W 676 ft elevation. Intact animal field samples were placed and collected at 36.25877° N, 86.446524° W 479 ft elevation with temperatures collected at 36.125674° N, 86.678009° W 554 ft. Coordinates and elevations were plotted using Google maps and www.heywhatsthat.com.

Tissue Sampling

Tissue samples used for laboratory assessments were first collected from frozen

pig tongue using a 0.75 cm diameter brass cork boring tool. Previous studies indicate that freezing the tissue prior to use does not affect decomposition of the tissue (231). For sampling, the frozen tongue was removed from the freezer and placed on a surface pre-sterilized with a 1:10 dilution of regular strength (5.25%) household bleach (sodium hypochlorite). The sterilized cork boring tool was used to remove a 5-7 cm plug of tissue. A 2-3 mm length section was removed from end of the plug corresponding to the outer dermis of the tongue. The still frozen plug was placed in a pre-sterilized 50 mL screw-cap conical tube and placed in the –80°C freezer until needed. Sub samples of the tissue plug were prepared using a clean plastic weigh boat, clean razor blades and heat sterilized forceps. A 1-3 mm length section (approximately 0.1 g) of tissue was removed from the plug. Once a section was removed from the plug it was placed into a pre-sterilized 1.5 mL microcentrifuge tube or a pre-sterilized 15 mL screw-cap conical tube.

Laboratory Controlled Tissue Degradation

Tissue samples weighing approximately 0.1 g were placed in individual 1.5 mL polypropylene tubes. The tubes were closed and placed in a refrigerator (~13^{o}C), in a fume hood at room temperature (~23^{o}C) and in a drying oven (~37^{o}C). A control sample was immediately placed in the -80^{o}C freezer and subsequent samples were removed after 3 – 505 hours. Once removed, samples were placed in the -80^{o}C freezer until extracted.

Field Controlled Specimen Degradation

Duplicate tissue samples weighing approximately 0.1 g were placed in individual 1.5 mL polypropylene tubes. The tubes were closed and placed in a tube rack in a weighted cage 33.130694° N, 97.160127° W 689 ft elevation. Control samples were immediately placed in a BioRad Cryosafe freezer box in a -20^{o}C frost free freezer and remained there for the duration of sample collection. Subsequent samples were removed after 3 – 240 hours. Once removed samples were placed in a BioRad Cryosafe freezer box in a -20^{o}C frost-free freezer until extracted.

Intact Animal Field Specimen Degradation

Field samples collected from the intact animal were collected using three different procedures. Four positive control blood samples were collected from the head wound produced during the animal sacrifice using 4 inch sterile Dacron® applicators. The swabs were allowed to completely dry at room temperature and were stored in 15 mL screw-cap conical tubes at –20°C until needed. During the initial stages of decomposition (days 1-10) tissue samples were collected from the intact field specimen using a clean 0.75 cm diameter brass cork boring tool. An approximately 1-3 cm long plug was removed from muscle tissue by driving the boring tool through the dermis into underlying muscle. Once the plug was removed the hole was plugged with silicone caulk. Subsequent samples were collected approximately 0.5 cm away from previous sample sites. The tissue plug was placed into a pre-sterilized 50 mL conical tube with approximately 10 mL of isopropanol, transferred at room temperature to an intermediate storage freezer (–20°C, frost free) for not more than 24 hours and transferred to a long-

term storage freezer (–20°C, no defrost cycle) until sectioned for analysis. Sectioned samples of the tissue plug were prepared as noted above. During the second phase of decomposition (~days 11-25) drying of the dermis, breakdown in muscle connective tissue and insect activity made penetration of the skin and successful muscle tissue collection difficult using the cork boring tool. An alternative method using clean forceps and scissors was devised and used. The dermis was lifted away from the underlying tissue and scissors were used to excise a circular portion of the dermis and any adhering tissue. Once the tissue section was removed, the hole was plugged with silicone caulk. During the third phase of decomposition (~days 26-35) tissue breakdown and insect activity had advanced to the point that silicone plugs and "patches" failed to adhere to the surrounding tissue. Samples collected during the third phase of decomposition were collected using the same procedure as during phase two sample collection. However, no attempt was made to close tissue collection sites. The tissue sections were stored as noted above.

There were several issues noted with collection and documentation. Narrow rope or wire attached to the limbs at the outset of the experiment would make repositioning of the specimen easier when shifting due to bloat occurs. A means of measuring loss of mass of the specimen would have provided another data point. On-site high/low temperature data was lost for 18 days due to the loss of a digital file. The site was mowed 15 days after specimen placement, affecting insect succession.

Genomic DNA Isolation

DNA isolation consists of three primary steps. The first step, referred to as cell

lysis, consists of an enzymatic digestion of the cell proteins. Lysis is followed by purification or the removal of proteins and contaminants. The DNA is then recovered and if necessary concentrated and purified.

Cell Lysis Procedure 1

Tissue sample sets (approximately 50 mg dry wt. each sample) were prepared from tissue plugs as described above. While still frozen each sample was cut into wafer thin slices and transferred to a microcentrifuge tube.

A 500 µL aliquot of stain extraction buffer (10 mM Tris-HCl, 100 mM NaCl, 10 mM EDTA, 2% SDS), combined with 25 µL Proteinase K (20 mg/mL) and 50 µL 0.39 M DTT was added. The sample was vortexed to mix the contents and centrifuged at approximately 14,000 g for 5 – 10 seconds to force the solution and tissue sections to the bottom of the sample tube. Samples were incubated in a 56°C water bath for 24 hours. The digested sample was then subjected to the organic extraction procedure.

Cell Lysis Procedure 2

Tissue samples created from plugs or sections (approximately 100 -500 mg) were dropped into a mortar cooled to –196°C with liquid nitrogen and maintained at –79°C in a bed of crushed dry ice. Liquid nitrogen was poured into the mortar over the tissue, being careful not to wash the tissue out into the dry ice bed. The tissue, floating in the liquid nitrogen, was ground into powder using a pre-cooled pestle.

The tissue powder was scraped/poured into a 15 mL conical tube and mixed with 2 mL of tissue digestion buffer (100 mM NaCl, 10 mM Tris-HCl pH 8, 25 mM EDTA pH

8, 0.5% SDS tissue digestion buffer). Proteinase K was added to a final concentration of 0.1 mg/mL (8). The samples were digested overnight at 56°C in a shaking water bath. The samples were gently inverted to mix several times in the first few hours. Samples with more than 200 mg tissue were supplemented with an additional aliquot of Proteinase K after six hours of digestion.

Organic Purification

Samples were removed from the water bath and centrifuged for 3 minutes at 1000 rpm to collect any condensation at the bottom of the tube. An equal volume of phenol:chloroform:isoamyl alcohol (25:24:1) was added to the tube. The mixture was gently vortexed to achieve a milky emulsion and centrifuged for 5-15 minutes at 150 g. The upper aqueous layer was transferred to a 15 mL siliconized Clorex ™ tube using a new transfer pipette.

A 1/10 volume of a 3 M sodium acetate (NaOAC) solution was added to the aqueous phase and swirled to mix. Two volumes of cold 100% ethanol were added to the tube. The tube was sealed with Parafilm® and mixed by gently inverting the tube. The Parafilm® was pierced with a pipette tip and the tube was placed in the –80°C freezer for a minimum of one hour. The tube was removed from the freezer and centrifuged for 10 - 20 minutes at 7000 x g. The ethanol was immediately decanted taking care not to dislodge the pellet. The pellet was washed by the addition of 1 mL ice-cold 70% ethanol, inverting once, and centrifuging for 10 – 20 minutes at 7000 x g. The ethanol was immediately decanted, again taking care not to dislodge the pellet. The inverted tube was blotted on a Kimwipe® and placed upright in a tube rack. The

rack was placed in a vacuum concentrator for at least 10 minutes until the pellet was dry. The tube was removed from the vacuum concentrator and the pellet suspended in 100 – 200 µL of sterile deionized water. The DNA solution was further processed with either Microcon® microfiltration or Qiagen Qia-amp® column purification.

Microcon 100® Microfiltration Concentration

A variety organic and inorganic molecules can co-purify with DNA and inhibit subsequent PCR amplification (23, 188). In order to reduce the level of small molecular weight potential inhibitors, extracted samples were filtered using microfiltration. A Microcon 100® microfiltration device was assembled and labeled with the sample number. The Microcon 100® membrane was pre-wetted by the addition of 100 µL of sterile deionized water to the top of the membrane in the membrane unit. The water was forced through the membrane using a 2-3 minute centrifugation at 3500 rpm in a microcentrifuge. The DNA extract was then transferred to the Microcon 100® membrane and centrifuged in a microcentrifuge at 822 g for 10 minutes or until the liquid had filtered though the membrane. The membrane unit was removed from the Microcon 100® assembly and the filtrate discarded. The Microcon 100® was reassembled and 200 µL of sterile deionized water was added to the membrane unit as a wash step. The water was centrifuged in a microcentrifuge at 822 g for 10 minutes or until the liquid had filtered though the membrane. The wash step was repeated at least one time. One hundred microliters of water was then added to the membrane unit and the membrane unit was removed from the assembly and inverted into a retentate capture tube labeled with the sample number. The retentate assembly was centrifuged

in a microcentrifuge at 822 g for 5 minutes. The membrane unit was discarded. The filtered DNA was stored at -20°C until used.

Qiagen QIAamp Mini™ Column Purification

In order to improve the DNA recovery and remove potential enzymatic inhibitors, DNA extracts were further purified using the QIAamp Mini® columns. After the drying step of the organic extraction protocol, the DNA pellet was suspended in 160 µl of QIAamp digest buffer (ATL Buffer). A 40 µl aliquot of RNase A (10 mg/mL) was then added to the DNA solution. The sample was mixed by vortexing for 15 seconds and incubated at room temperature for 2 minutes. The sample was centrifuged at 67 g for ~5 seconds to remove liquid from the inside of the lid. After centrifugation 200 µl of binding buffer (AL buffer) was added to the tube. The sample was mixed by vortexing for 15 seconds and incubated at 70°C for 10 min. The sample was again centrifuged at low speed to remove liquid from the inside of the lid. After centrifugation, 200 µl of ethanol (96–100%) was added to the sample and mixed by vortexing for 15 seconds. The sample was once again centrifuged to remove liquid from the inside of the lid. The mixture, and any precipitate that may have formed, was applied to the QIAamp Mini® spin column. The column was centrifuged at 6000 x g (approximately 8000 rpm) for 1 minute. The QIAamp Mini® spin column was transferred to a clean 2 mL collection tube and initial filtrate tube and binding solution was discarded. After column transfer 500 µl of QIAamp buffer AW1 wash buffer was added to the column. The column was centrifuged at 6000 x g (8000 rpm) for 1 minute. The QIAamp Mini® spin column was transferred to a clean 2 mL collection tube and the initial wash filtrate tube and wash

solution were discarded. After column transfer, 500 µl of QIAamp AW2 wash buffer was added to the column. The column was centrifuged at 20,000 x g (approximately 14,000 rpm) for 3 minutes. The QIAamp Mini® spin column was transferred to a clean 1.5 – 2 mL microcentrifuge tube and the second filtrate tube and wash solution discarded. The DNA was eluted from the column by adding 200 µl of distilled water, incubating at room temperature for 5 minutes, and then centrifuging at 6000 x g (approximately 8000 rpm) for 1 minute. The elution step was repeated with an additional 200 µl of distilled water. Eluted DNA was stored at –20°C until used.

Quantitative Characterization of DNA Samples

The quantification (concentration determination) of nucleic acids is paramount for optimizing the dsDNA and/or single-strand DNA (ssDNA) to enzyme ratio utilized in many molecular procedures. Several methods were utilized during this study to measure the nucleic acid concentration in samples.

UV Absorbance A220 – A320

The most commonly used technique for assessing the concentration of nucleic acids is measurement of UV absorbance. Advantages to using UV absorbance for determining concentration are that it is fast, accurate and does not require expensive reagents. However, absorbance values are adversely affected by the presence of proteins, phenol and other contaminants. Additionally, the process is not very sensitive at very low DNA concentrations and is unable to differentiate between ssDNA, dsDNA and RNA. DNA and RNA both exhibit maximum absorbance at ~260 nm. Primarily

due to tryptophan residues, proteins exhibit a maximum absorbance at ~280 nm. Phenol exhibits a maximum absorbance at ~270 nm. The ratio of absorbance at 260 nm: 280 nm is often used as a means to assess DNA purity. When used to assess the concentration of a pure DNA sample, an A_{260} reading of 1 corresponds to a 50 µg/mL dsDNA or 33 µg/mL for ssDNA.

When oligonucleotides were received from the manufacturer (generously provided by Bio-Synthesis, Inc.), they were diluted and quantified with a BioRad spectrophotometer. A cursory analysis to determine yield and quality of the newly acquired oligonucleotide was routinely performed. First the oligonucleotide was reconstituted from its desiccated form in ddH_20 (330 µL for 5 OD units), and then a portion of this sample was diluted 1:100 by placing 10 µL oligonucleotide solution into 990 µL ddH_20 for spectrophotometer analysis. The diluted oligonucleotide was then placed into a 1 mL quartz cuvette for a wavelength scan from 220 nm to 320 nm. An absorbance reading of 1.0 in the range of 256 nm to 260 nm was assumed to represent approximately 33 µg/mL of ssDNA.

Experimental sample extracts were also diluted and scanned to determine absorbance. Sample extracts were quantified at either a 1:100 dilution by mixing 10 µL of extract with 990 µL ddH_2O, or a 1:10 dilution by mixing 100 µL of extract with 900 µL ddH_2O. Diluted samples were then placed into a 1 mL quartz cuvette and scanned over a range of 220 to 320 nm. An absorbance reading of 1.0 in the range of 256 to 260 nm was assumed to represent approximately 50 µg/mL of dsDNA. Phenol or protein contaminants are known to shift the absorbance maximum to the right (270 – 280 nm). Samples exhibiting a contamination shift were re-purified and re-quantified.

Fluorescent Dye DNA Quantification

Early in the project experimental dsDNA samples were quantified using a PicoGreen® ([2-[N-bis-(3-dimethylaminopropyl)-amino]-4-[2,3-dihydro-3-methyl-(benzo-1,3-thiazol-2-yl)-methylidene]-1-phenyl-quinolinium]+) based quantification assay (248).

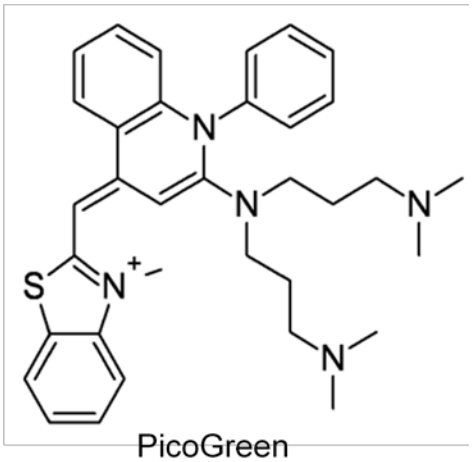

PicoGreen
(Ygonaar, 2006)

PicoGreen® is a fluorescent nucleic acid stain for quantifying dsDNA in solution. The structure of PicoGreen® (274) is such that once it binds dsDNA it exhibits a 1000-fold increase in fluorescent signal. The increase of signal allows samples ranging from 25 pg/mL – 1000 ng/mL to be quantified using a standard fluorescence microplate reader (221).

Fluorescent quantification calibrators were prepared from a 50 ng/μL dsDNA stock solution and sterile distilled water in the following concentrations:

Cal-0.0 ng/μL

Cal-20.0 ng/μL

Cal-15.0 ng/μL

Cal-10.0 ng/μL

Cal- 7.5 ng/μL

Cal-5.0 ng/μL

Cal-2.5 ng/μL

Cal-1.0 ng/μL

Cal-0.75 ng/μL

Cal-0.50 ng/μL

Cal-0.25 ng/μL

A 1:500 working stock of PicoGreen® was prepared using sterile distilled water. An optically clear microtiter scanning plate was prepared with 3 μL of calibrator or experimental dsDNA mixed with 97 μL of the PicoGreen® working stock. The scanning plate was incubated for five minutes at room temperature, protected from light. After incubation, the samples were exposed to ultraviolet light and the Relative Florescence Units (RFU) measured using a fluorescence microplate reader. RFU measurements were obtained using a BMG Labtech FLUOstar fluorescent plate reader with excitation and emission wavelengths of ~480 nm and ~520 nm, respectively. The plate was continuously agitated for 300 seconds and the fluorescence of each well was assayed five times with the reported RFU value representing an average of the 5 assayed values. In order to correct for background signal, the fluorescence value of the reagent blank was subtracted from the calibrator and sample values. The corrected calibrator data was used to generate the standard curve of RFU versus dsDNA concentration (Fig. 1). Relative fluorescence measurements of samples with unknown DNA concentrations were compared to the standard curve and assigned concentration values using regression analysis. The calibrators were verified by assessing the r^2. Calibrator sets with r^2 values less than 0.98 were repeated.

Quantitative/Qualitative Characterization of DNA Samples

Agarose gel separation was used to perform quantitative and qualitative DNA analysis of some dsDNA samples. After separation, nucleic acids were stained using

ethidium bromide (EtBr), a dsDNA intercalating agent. After staining, gels were evaluated by the use of a UV transilluminator, a hand-held UV light source or by scanning with the BioRad Molecular Imager FX. A visual comparison of the experimental samples to calibrator samples and/or ladders allowed for the estimation of fragment size, quality and DNA concentration based on the shape, size and location of the stained bands/material on treated gels.

DNA Fragment Reference Sizing Ladders

Four primary DNA fragment sizing ladders were used for this project. The *Hin*d III digest of Lambda phage (178) was used during the initial evaluation stages for agarose gel analysis. This digest includes eight discrete fragments with fragment sizes of 23130, 9416b, 6557, 4361, 2322, 2027, 564 and 125 bp. The *Hin*f I digest of pBR322 was used during the initial assay development stages in both agarose and acrylamide gels. This digest includes ten discrete fragments with fragment sizes of 1632, 517, 504, 396, 344, 298, 221, 220, 154 and 75 bp. The Fermentas ZipRuler™ Express DNA ladder Set (69) was used in some agarose and most acrylamide gels during the analysis of all samples degraded under laboratory controlled conditions. The ZipRuler™ Express DNA Ladder Set consists of two ladder sets composed of chromatography purified DNA fragments. The first set, used as the primary ladder in this study, is ZipRuler™ Express DNA Ladder 1, which consists of nine discrete fragments with fragment sizes of 100, 300, 500, 850 1200, 2000, 3000, 5000, and 10000 bp. The second set is ZipRuler™ Express DNA Ladder 2, which consists of nine discrete fragments with fragment sizes of 200, 400, 700, 1000, 1500, 2500, 4000, 7000, and 20000 bp. The Invitrogen Trackit™

100 bp Ladder is prepared from a plasmid containing repeats of a 100 bp DNA fragment. The Invitrogen Trackit™ 100 bp Ladder consists of sixteen discrete fragments with fragment sizes of 100, 200, 300, 400, 500, 600, 700, 800, 900, 100, 1100, 1200, 1300, 1400, 1500 and 2072 bp fragments.

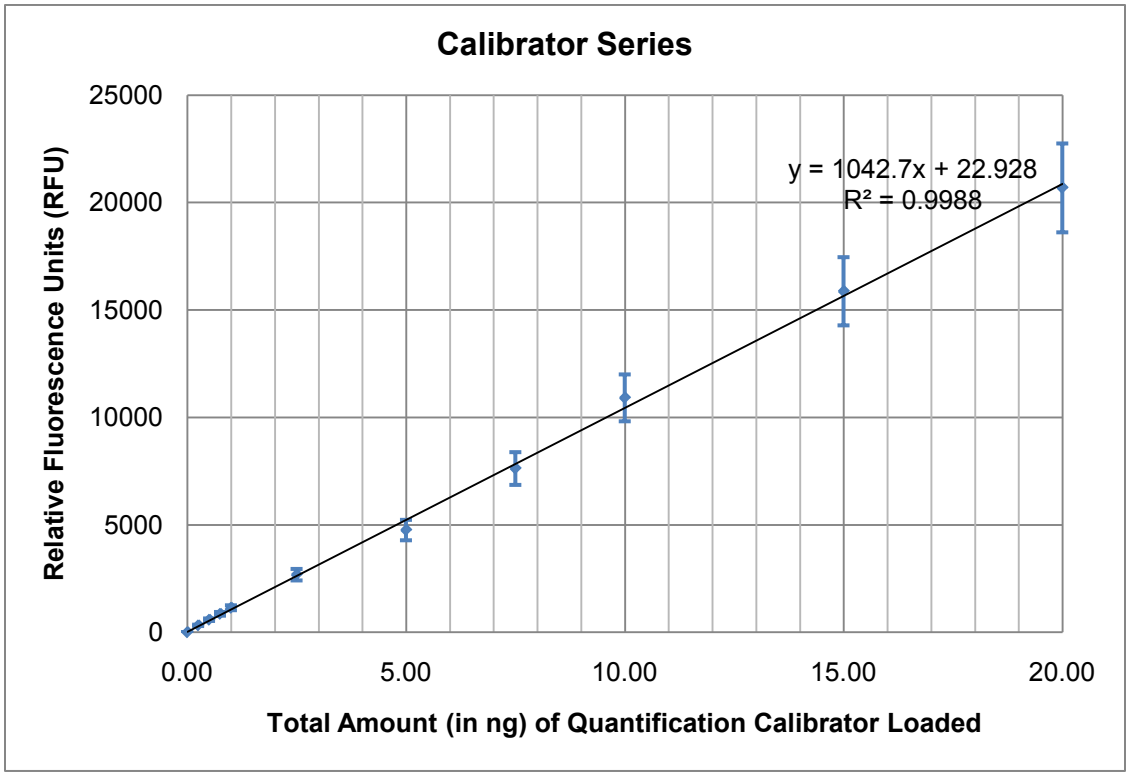

Fig. 1. Corrected standard quantification curve obtained using fluorescent quantification with known concentration calibrator dsDNA. Calibrator dsDNA (Invitrogen) of a known concentration was diluted to generate quantification standards corresponding to 0 ~ 7 ng/µL. Three microliters of each standard was added to an optically clear microtiter scanning plate with 97 µL of a 1:500 PicoGreen® solution. The plate was excited at ~480 nm and scanned at ~520 nm. A corrected value for each point was obtained by subtracting the RFU value obtained for the 0.0 ng/µL. The error between the calculated concentration (based on the slope of the line) and the known concentration ranged from 0.9% - 9.38%. The error bar is plus or minus 10%.

Preparation of Sizing Ladders, Calibrators and Experimental Samples

Prior to mixing with loading dye, ladders, calibrators and experimental samples were gently vortexed and centrifuged for 5 seconds at 67 g to mix and bring the contents to the bottom of the tube. Depending upon the final volume prepared (10 – 20 µL), 2 -4 µL of 5X loading buffer (10 mM Tris-HCl; 1 mM EDTA, pH 7.5; 0.005% bromophenol blue; and 0.005% xylene cyanol FF) was transferred to the bottom of a labeled microcentrifuge tube, PCR amplification plate well or PCR amplification tube. A volume of 2 – 4 µL of experimental sample, 2 – 4 µL of calibrator DNA, or 2 – 5 µL of ladder was then transferred to the loading buffer in the corresponding tube/well. Sample, calibrator and ladder volumes were adjusted to a final volume of 10 – 20 µL by the addition of 4 – 14 µL sterile distilled water to the bottom of the corresponding tube/well.

Preparation of Agarose Gel Solutions

Agarose gels were prepared by mixing agarose in a weight to volume ratio of 1.2 g:100 mL LE Agarose to 1X Tris Borate EDTA (TBE) buffer. Agarose gel stock (1.2%) was prepared in batches by mixing 4.8 g SeaChem LE Agarose (275) with 40 mL 10X TBE or 80 mL 5X TBE in a 500 mL bottle or flask. The final volume was adjusted to 400 mL using distilled water (makes 4 X 100 mL gels) and swirled gently to mix the contents.

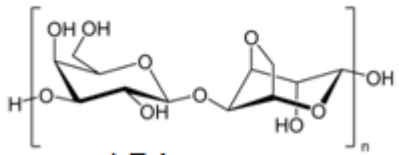

LE Agarose
(Yikrazuul, 2007)

Autoclave Agarose Melting Method

The bottom chamber of the autoclave was filled with deionized water until the level was just below the bottom ledge of the door. The bottle(s)/flask(s) of agarose were placed in the autoclave chamber. The door was closed, latched and the chamber exhausted on the slow setting. The agarose was autoclaved for 25 minutes. The agarose was allowed to cool at room temperature until the boiling stopped. The agarose was gently swirled to mix. The agarose was either used immediately to pour gels or cooled to room temperature and stored at 4°C until used.

Microwave Agarose Melting Method

The bottle(s)/flask(s) of agarose were placed in a microwave and boiled at the high setting for 6-8 minutes. The agarose was allowed to cool at room temperature until the boiling stopped. The agarose was gently swirled to mix. If the agarose was not completely melted the solution was heated for one minute intervals until the agarose was melted. The agarose was cooled at room temperature until the boiling stopped. The agarose was either used immediately to pour gels or cooled to room temperature and stored at 4°C until used.

Agarose Gel Casting

The agarose gel form was created using gel tape to seal the ends of an acrylic tray. One hundred grams of agarose gel stock was placed into a 250 mL flask and heated in a microwave until the agarose was completely melted. A 15 µL aliquot of 1% ethidium bromide (273) was added to the melted agarose which was swirled to mix.

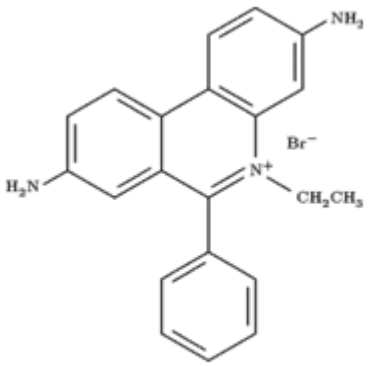

Ethidium Bromide
(Ygonaar , 2006)

The melted agarose solution was poured into the gel tray. A comb was placed in the top of the gel and the agarose was allowed to solidify for 30 minutes. Once the gel solidified, the tape was removed from the edges of the gel tray and the gel placed into the electrophoresis tank with the comb at the negative (black electrode) end of the gel. The gel tank was filled to just above the level of the gel surface with 1X TBE buffer. The comb(s) were removed taking care not to tear the wells.

Agarose Gel Loading

The ladders, calibrators and/or samples, prepared as noted above, were individually loaded into separate gel wells.

Electrophoresis of Agarose Gels

The gel tank lid was placed on the tank and the wire leads, red to (+) positive and black to (-) negative, were connected to the power supply. The current was set from 100 – 200 volts and the gel was electrophoresed for 10 - 30 minutes.

Film Documentation of Agarose Gels

The gel was removed from the base of the gel box and placed on the UV transilluminator. The gel was photographically documented using a shrouded gel camera with Polaroid 667 Black and White film for 1 second at f4.5 with an orange filter.

Gels exhibiting dark images were re-photographed using a longer exposure time. Gels exhibiting bright images were re-photographed using a shorter exposure time. The Polaroid 667 Black and White film was stripped from the camera and allowed to develop for approximately 45 seconds before being removed from the backing.

Digital Documentation of Agarose Gels

The gel was removed from the base of the gel box and placed on the UV transilluminator. The gel was documented using the UVP Doc it®LS system version 5.0.0 with an Olympus C5060 digital camera.

Invitrogen E-Gel®

E-Gel® pre-cast, pre-stained agarose gels are self-contained agarose gels that include electrodes packaged inside a dry, disposable, UV-transparent cassette. The E-Gel® agarose gels are electrophoresed in a specially designed device that is a base and power supply combined into one unit.

E-Gel® Pre-electrophoresis

The E-Gel® was removed from the package and inserted (with the comb in place) into the E-Gel® Powerbase™ (v.4) right edge first. Proper placement required that the Invitrogen logo be located at the bottom of the E-Gel® Powerbase™. The E-Gel® was pressed firmly at the top and bottom to seat the gel in the E-Gel® Powerbase™. The E-Gel® PowerBase™ was plugged into an electrical outlet using the adaptor plug on the base. A steady, red light on the base indicated when the gel was

correctly inserted into the base. The gel was pre-electrophoresed (with the comb in place) by pressing and holding either the 15 min or 30 min button until the red light turned to a flashing-green light indicating the start of a 2-minute pre-electrophoresis step. At the end of the pre-electrophoresis step, the current automatically shut off. The combs were removed from the E-Gel® cassette and the wells loaded.

E-Gel® Loading

The ladders, calibrators and/or samples, prepared as noted above, were loaded in the appropriate wells of the E-Gel®. Additional water was added to samples to bring their final volume to 20 – 25 µL. The entire ladder, calibrator and/or sample volume was then loaded into the precast well.

E-Gel® Electrophoresis

The 15 minute or 30 minute activation button on the E-Gel® PowerBase™ was pressed to begin electrophoresis. Once complete, the current automatically shut off and the power base signaled completion of electrophoresis with a flashing red light and rapid beeping. Either button was pressed to stop the beeping. The gel cassette was then removed and documented.

E-Gel® Documentation

The E-Gel® cassette was documented with film or digitally using the procedures noted above.

Preparation of Degraded DNA

Two methods were evaluated to generate fragmented control DNA for assay development.

DNase I Digestion Method 1

Degraded DNA samples were prepared by treating previously quantified high molecular weight dsDNA samples with DNase I. Extracted DNA samples (~0.5 – 1 mg total DNA) were digested for 5 minutes at 37^{o}C with varying concentrations of pancreatic DNase I (0 ug – 1 mg total enzyme) in the presence of a manganese buffered solution (50 mM Tris–HCl, pH 8; 10 mM $MnCl_2$) (167). Reactions were stopped using an EDTA stop solution (12.5 mM final concentration). Fifteen microliter reactions were set-up as follows:

DNase I Dilution	µL DNase I	µL DNA	Digest Conditions	µL Stop Solution
0 µg/mL	10 µL	5 µL DNA	5 min/37^{o}C	5 µL
100 µg/mL	10 µL	5 µL DNA	5 min/37^{o}C	5 µL
10 µg/mL	10 µL	5 µL DNA	5 min/37^{o}C	5 µL
1 µg/mL	10 µL	5 µL DNA	5 min/37^{o}C	5 µL
100 ng/mL	10 µL	5 µL DNA	5 min/37^{o}C	5 µL
10 ng/mL	10 µL	5 µL DNA	5 min/37^{o}C	5 µL
1 ng/mL	10 µL	5 µL DNA	5 min/37^{o}C	5 µL

Digested DNA samples were stored at –20°C until used.

DNase I Digestion Method 2

Degraded DNA samples were prepared by treating previously quantified high molecular weight dsDNA samples with pancreatic DNase I. Extracted DNA samples

(~0.5 mg total DNA) were incubated from 0 seconds to 120 minutes at 37°C with a fixed concentration of pancreatic DNase I (0.2 ng total enzyme) in the presence of a magnesium buffered solution (10 mM Tris–HCl, pH 8; 1 mM $MgCl_2$, 0.1 mM $CaCl_2$) (167). Reactions were stopped using an EDTA stop solution (10 mM final concentration). Reactions were set-up as follows:

1 µL	100 mM Tris–HCl, pH 8
1 µL	10 mM $MgCl_2$, 1 mM $CaCl_2$
5 µL	DNA (0.1 µg/µL)
2 µL	ddH_2O
1 µL	Pancreatic DNase I (2 ng/µL)
10 µL	Total Reaction Volume

DNase I was inactivated by the addition of 10 µL stop solution and heating (95°C for 10 minutes). Stop solution was prepared as follows:

2 µL	EDTA 100 mM
8 µL	Sterile Distilled Deionized Water
10 ul	Total Stop Solution Volume

Digested DNA samples were stored at –20°C until used.

RAPD Analysis

Random amplification of polymorphic DNA (RAPD) was performed using nine random decamer oligonucleotides previously reported for RAPD analysis (205, 269). The oligonucleotides were ordered from Applied Biosystems with a 6-FAM label on the

5'end in the hopes that they could eventually be assayed utilizing capillary electrophoresis.

Primer 1*	5'-GAACGGACTC-3'
Primer 2*	5'-AAAGCTGCGG-3'
Primer 3*	5'-TGTCATCCCC-3'
Primer 4*	5'-CACACTCCAG-3'
Primer 5*	5'-GTTGCCAGCC-3'
Primer 6*	5'-GTGCCTAACC-3'
Primer 7*	5'-TCACGTCCAC-3'
Primer 8*	5'-CTCTCCGCCA-3'
Primer 9*	5'-GGATGAGACC-3'

* = 5' labeled with 6-FAM

PCR amplification reactions were set up using the following reaction. A new set of thin-wall (PCR) reaction tubes was set up with each containing the following:

10 µL	DNA (3 ng/µL)
2.5 µL	Promega Gold ST*R 10X Buffer™ (w/dNTP Mix)
2.0 µL	RAPD primer 1-9 (10 µM)
0.2 µL	*Taq* polymerase (5 U/µL)
10.3 µL	ddH_2O
25 µL	Total volume

Promega's Gold ST*R 10X Buffer™ (catalog # DM2411) was used for all project related amplifications. Gold ST*R Buffer ™ has been optimized to work with Life Technologies AmpliTaq Gold® DNA polymerase. Gold ST*R 10X Buffer™ components

include 500 mM KCl, 100 mM Tris-HCl (pH 8.3), 15 mM $MgCl_2$, 1 % Triton® X-100, 1,600 µg/mL BSA, 2 mM each dNTP (~pH 8.3) (202).

Prior to implementation with degraded samples, RAPD primers were assessed for sensitivity to total DNA amplification target. Each primer set evaluated was assessed with a serial dilution of 30 ng - 0.029 ng total target DNA. The resulting PCR amplification products were stored at -20°C until analyzed by agarose or acrylamide gel electrophoresis.

The parameters for the RAPD thermal cycling reaction were as follows:

	94°C for 11 minutes
3 cycles of	94°C for 30 seconds
	34 °C for 30 seconds
	72°C for 90 seconds
35 cycles of	94°C for 15 seconds
	34 °C for 30 seconds
	72°C for 90 seconds
	72°C for 7 minutes
	4°C hold

The resulting PCR amplification products were stored at -20°C until analyzed by agarose or acrylamide gel electrophoresis.

Directed PCR Amplification Primer Design

Primers for directed amplification of amplicons were ordered from a variety of suppliers. Primer design consisted of the selection of a single “anchor” primer with three or four fragment primers on the opposite strand producing amplicons of increasing length. All primers were initially designed using Primer 3 (v. 0.4.0) primer design program (207). The optimal PCR annealing temperature was determined using an MJ Research PTC-200 Gradient Cycler ™ thermalcycler. A 12°C annealing temperature

gradient bracketing the calculated primer melting point (Tm) was used with each directed primer set (113). Subsequent assays utilized the established optimal annealing temperature.

Group Component Primers

Primers for the directed amplification of group component (125) were ordered from Operon. The anchor oligonucleotide was manufactured with a fluorescein label on label on the 5'end in the hopes that amplified fragments could eventually be assayed utilizing capillary electrophoresis.

Primer GC A* 5'-AGGACTTGCCAGCAGAAAAA-3'

Primer GC B1 5'-TCTGGAAGCTCAGGTCTTGG-3'

Primer GC B2 5'-CCAAATTCGCAGTAGGCACT-3'

Primer GC B3 5'-CCTTGGGGTCTTTCCTGAAT-3'

Primer GC B4 5'-AGCAGGCTTCTGTCAAGGAC-3'

Primer GC B5 5'-TGCTACAGCAAGCAGGAAAA-3'

* = 5' labeled with fluorescein (FL)

Mitochondrial Cytochrome B Primers

Primers for the directed amplification of *Sus scrofa* mitochondrial cytochrome b (CBM, encoded by mtDNA) gene (131) were ordered from and generously provided by Biosynthesis, Inc. in Lewisville, Texas. All oligonucleotide primers were unlabeled.

Primer CBM R 5'-AATGGGTGTTCTACGGGTTG-3'

Primer CBM L1 5'-TCCTGCCCTGAGGACAAATA-3'

Primer CBM L2 5’-GCAGGAAACCGGATCCAA-3’

Primer CBM L3 5’-TAAACACCCCACCCCATATT-3’

Nuclear Cytochrome B5 Primers

Primers for the directed amplification of the *Sus scrofa* cytochrome b-5 (CB5) gene on chromosome 1 (24) were ordered from and generously provided by Biosynthesis in Lewisville, Texas. All oligonucleotide primers were unlabeled.

Primer CB5 L 5’-TGGAAGAAAAGACTGCTCTGG-3’

Primer CB5 R1 5’-ATGCAGGAGGAAAAGGAAAC-3’

Primer CB5 R2 5’-AGATTGTGCCCACACTAAGC-3’

Primer CB5 R3 5’-GGGCTTTTCATATTTCCCTTGG-3’

Primer CB5 R4 5’-TAGCACGCCAATGGACAATC-3’

PCR Amplification

PCR amplification reactions were set up using the following reaction scheme. A new set of thin-wall (PCR) reaction tubes, or a PCR amplification plate, was set up with each containing the following:

1 µL	DNA extract
1 µL	Promega Gold ST*R 10x Buffer™ (w/dNTP Mix)
0.1-0.4 µL	Directed Primer Left (10 µM)
0.1-0.4 µL	Directed Primer Right (10 µM)
0.2 µL	*Taq* polymerase (5 U/µL)
7-7.6 µL	ddH_2O (volume depends on primer quantity)

10 µL Total volume

Promega's Gold ST*R 10X Buffer™ (catalog # DM2411) was used for all project related amplifications. Gold ST*R Buffer ™ has been optimized to work with Life Technologies AmpliTaq Gold® DNA polymerase. Gold ST*R 10X Buffer™ components include 500 mM KCl, 100 mM Tris-HCl (pH 8.3), 15 mM $MgCl_2$, 1 % Triton® X-100, 1,600 µg/mL BSA, 2 mM each dNTP (~pH 8.3) (202).

The directed PCR thermal cycling parameters were as follows:

	94°C for 4 minutes
29 cycles of	94°C for 30 seconds
	64°C for 45 seconds
	72°C for 1 minute
	72°C for 7 minutes
	4°C hold

Prior to implementation with degraded samples, directed primer sets were optimized for annealing temperature using temperature gradient amplification. Each primer set evaluated was assessed with a 12^{o}C temperature gradient bracketing the projected primer annealing temperature.

Prior to implementation with degraded samples, directed primer sets were assessed for sensitivity to total DNA amplification target. Each primer set evaluated was assessed with a serial dilution of 30 ng - 0.029 ng total target DNA. The resulting PCR amplification products were stored at -20^{o}C until analyzed by agarose or acrylamide gel electrophoresis.

Vertical Non-Denaturing Polyacrylamide Gel Electrophoresis

Separation of dsDNA products created by PCR amplification was routinely

performed using non-denaturing polyacrylamide gel electrophoresis (N-PAGE). N-PAGE analysis procedures were optimized to allow differentiation of amplicons ranging from 50 – 1500 bp. The procedure to assemble the polyacrylamide gel cassette is outlined below.

A 20 x 20 cm gel cassette with 8% non-denaturing polyacrylamide gel was used in these experiments. Two glass plates, one 20 x 20 cm and the other 20 x 22 cm, were soaked for 30 minutes in 1 M NaOH to strip contaminants from the plates. After stripping, the plates were washed with Alconox™ detergent and distilled water. Once dry, both plates were coated on one side with a thin layer of 5% dichloro-dimethylsilane dissolved in heptane. The plates were allowed to dry and were then wiped with Kimwipes® before completing the cassette assembly. The silinating was performed in a vented fume hood to prevent inhalation of the potential carcinogen. Two spacers, 1.5 mm thick and 1.5 cm wide, were placed on either side of one of the plates. The other plate was then carefully placed on top of the spacers with clamps added to hold the plates together. The cassette assembly was placed on a flat surface taped across the bottom using yellow gel tape. Non-denaturing acrylamide gel solution was then prepared.

A ten milliliter volume of 40% acrylamide (29:1 acrylamide/bis-acrylamide) was added to a fifty milliliter conical tube. Ten milliliters of 5X non-denaturing buffer (500 mM Tris, pH set to 8.3 with solid boric acid, 10.0 mM EDTA, ethylenediaminetetra-acetate, disodium form) was mixed with the acrylamide/bis-acrylamide solution. Thirty milliliters of de-ionized water was used to bring the volume up to 50 mL, producing an 8% polyacrylamide solution. Ammonium persulfate, 0.06 g, was added to the solution

and the mixture was filtered through a Whatman Number 1 filter into a side-arm flask. A vacuum was applied (2-10 minutes) to remove dissolved gases from the mixture. A polymerization catalyst, 8 µL TEMED (*N,N,N',N'*-tetramethylethylenediamine), was added and the solution gently swirled before being transferred into the cassette using a 25 mL glass pipette and powered vacuum pipettor. The comb was inserted after it was determined that no bubbles, which would inhibit polymerization, were present in the assembly. Clamps were used to clamp the comb, like a spacer, ensuring uniform gel thickness. The cassette was left in a horizontal position to prevent leakage and help promote uniform gel thickness. Polymerization was considered complete after 0.5 - 1 hour. The top of the cassette was wrapped with plastic wrap if it was to be allowed to sit overnight and the gel electrophoresed the next day.

Prior to electrophoresis, the comb was removed and wells straightened with a thin wire and rinsed. The cassette was then placed into a vertical electrophoresis chamber and 1 liter of 1X TBE buffer was equally dispensed into the upper and lower reservoirs. The gel was pre-electrophoresed for 10 minutes at 400 volts.

N-PAGE Sample Loading

Polyacrylamide gels were loaded using two different processes. Initial developmental gels were loaded using a porous 0.2 mm thick 96 well membrane comb (The Gel Company catalog number CAJ96). One microliter of each set of directed PCR amplicons was combined into a single tube. One microliter of the combination was mixed with one microliter of 5X loading buffer (15% ficoll, 0.1% bromophenol blue, 0.1% xylene cyanol FF, 50 mM EDTA). One microliter of the mix was pipetted into a well in a

96 well loading block. A 96 tooth porous comb was inserted, one tooth per well, into the loading block and the sample was allowed to absorb into the membrane. The Gel was pre-electrophoresed for 5 minutes, turned off and the trough well thoroughly rinsed. The membrane comb was inserted into the trough well and the gel was electrophoresed for 3-5 minutes to run the DNA out of the membrane and into the gel. The current was turned off and the membrane comb was removed. The current was turned back on and the gel was electrophoresed to completion. Membrane combs provide the advantages of rapid loading and a higher sample signal when compared to traditional well-forming combs (39).

However, based on the developmental data showing ladder carry-over (data not shown) and the necessity of quantifying distinct amplicon values, it was decided to switch to a traditional flat bottom comb with well dividers once the developmental gels were complete. Loading of the flat bottom wells was similar to that of the membrane comb in that one microliter of each set of directed PCR amplicons was combined. However, for loading flat bottom wells the entire mix was combined with two microliters of 5X loading buffer (15% ficoll, 0.1% bromophenol blue, 0.1% xylene cyanol FF, 50 mM EDTA). The solution was brought up to a total volume of 10 µL using distilled water before loading in a washed well of the gel. Ladders consisting of 25 ng of Fermentas ZipRuler™ Express DNA Ladder Set I or 50 ng of pBR322 *Hin*f I digested DNA was mixed with 2 µL of 5X loading buffer and the volume was brought up to 10 µL using distilled water before loading in a washed well of the gel. The gel was pre-electrophoresed at 100 V for 15 minutes to stack the PCR products in the gel. The gel voltage was then adjusted to 400 V and electrophoresed for 80 minutes.

DNA Detection by SYBR Green®/Gel Red™ Staining

Polyacrylamide gels were stained with either SYBR Green® (SG) or Gel Red™ (GR).

SG is a positively charged synthetic fluorescent dye that binds with a high affinity to dsDNA (280). It was initially marketed as a non, or less, mutagenic (222) but more sensitive alternative to Ethidium Bromide (EtBr) staining (146) that exhibited a greater binding affinity (5). Although SG does interact with ssDNA its fluorescence is approximately 11-fold less than that seen when it is bound to dsDNA (280). SG produces it maximal emission at 521 nm when excited at 494 nm (146).

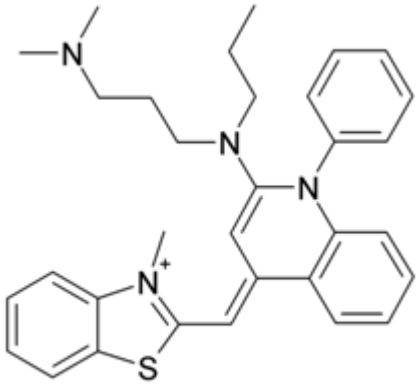

SYBR Green I
(Hoffmeier, K 2006)

Gel Red™ is a non-mutagenic, more sensitive fluorescent dye designed to replace EtBr and Sybr dyes in agarose and polyacrylamide gels (25). The manufacturers have modified GR's™ structure such that it is "…non-mutagenic or substantially so by denying its chance to be in contact with genomic DNA in living cells." (25, 27). Additionally GR has almost the same fluorescent spectra as EtBr, emitting at 600 nm when excited at 300nm, making a direct but more sensitive replacement (26).

The polyacrylamide gel cassette was removed and disassembled to leave the gel on one plate. The teeth were removed from the top of the gel and the gel was rolled off of the plate into a shallow plastic tray with between 500 mL and 1 L of SG or GR (1:10,000). The tray was placed on a slowly rocking platform for 15 – 30 minutes. The gel was removed from the bath and transferred to the BioRad Molecular Imager FX

using a 35 x 60 cm piece of flexible nylon window screening as support. The gel was scanned using a Bio-Rad Laboratories Molecular Imager FX set for either Sybr Green® or EtBr.

Gel Data Analysis

Once scanned the gel lanes must be defined and the peaks identified and quantified. Bio-Rad Laboratories' Quantity One® software, designed to analyze 1-D gel images obtained using different imaging systems, was used to analyze all gels produced during this project. The gel analysis process used had four primary steps:

- Lane definition – Lanes were defined using the Auto Frame Lanes command which recognizes and delineates the lanes. When necessary, individual lanes were defined, adjusted or deleted manually using individual lane tools.
- Background subtraction – Once lanes were defined, gel background noise was subtracted using rolling disk subtraction which removed background on a lane by lane basis. The user defined "rolling disk" traced the baseline removing background.
- Band identification – Once the background was removed bands were detected using the Detect Bands command which automatically recognized bands. Bands were also defined adjusted or deleted manually using individual band tools. Each band was delineated by brackets which were also adjusted when necessary.
- Band signal quantification – Bands were quantified by calculating the average intensity of the signal within the band brackets.

Once quantified, the band signals within a specimen were assessed and compared.

Temperature Tracking

The daily temperature at the field site was monitored using a manual hi-low thermometer situated near the carcass and published temperature data using temperature recordings obtained using a manual minimum/maximum thermometer situated next to the carcass. On site temperature averages, calculated as an average of the minimum plus maximum, were compared to daily average published temperatures from the National Center for Atmospheric Research and the National Climactic Data Center sites nearest the carcass placement. Published temperature data was accessed at the following websites:

http://www.rap.ucar.edu/weather/surface/

http://www.ncdc.noaa.gov/oa/climate/stationlocator.html

Calculation of Degree Hours and Degree Days

Degree/hour and degree/day calculations should in theory allow the assay to be applied to samples with unknown PMIs. Once controlled data has been used to set-up the points of comparison, questioned sample can be tested, and compared to the controlled data. Assuming a good match the comparison should produce a degree/hours or degree/day value. Local temperature data available through the National Weather Service or National Oceanic and Atmospheric Administration can then be used to determine approximate PMI.

As noted above no location related temperature correction was used for the calculation of Accumulated Degree Hours (ADH) or Accumulated Degree Days (ADD). The degree hour value for a single hour was calculated using the following formula:

$$\text{Hourly Temperature} - \text{Minimum Threshold} = \text{DH}$$

The ADH was calculated by adding together the hourly values (80, 166).

The degree day value for a single day was calculated using the following formula:

$$\frac{\text{Maximum Daily Temperature} + \text{Minimum Daily Temperature}}{2} - \text{Minimum Threshold} = \text{DD}$$

The ADD were calculated by adding together the single day values (140).

For this study, the minimum thresholds of 0°C and 4°C were evaluated when calculating DH and DD (169, 257).

CHAPTER 3

RESULTS AND DISCUSSION

Using a rate of change process to assess the time since death is a complex process that in most instances has produced mixed results. The present study was conducted to determine the relationship between DNA degradation and time since death and to evaluate the efficacy of several molecular biology testing techniques in evaluating DNA degradation in the early post mortem interval. DNA was prepared from tissue collected from the domestic pig exposed to a variety of environmental conditions and processed using several different molecular biology testing techniques. Results were evaluated to determine which, if any, of the methods provided data demonstrating a link between DNA degradation and post-mortem interval. The majority of the laboratory processing and specimen testing was performed in the Biology Department of the University of North Texas in Denton, Texas. Field conditions were assessed in middle Tennessee and North Texas.

Animal Model Selection

The domestic pig, (Fig. 2) *Sus scrofa* (referred to by some taxonomists as *Sus domestica*) was selected as the human tissue analog for this study in order to by-pass regulations associated with the Human Tissue Act of 1983. Additionally, domestic pigs have been widely used in forensic anthropological studies for assessing time since death. Although there are some investigators who have questioned the use of domestic pigs as a human tissue analog (124), others have found pigs to be reliable models for human corpses (106, 215, 230). Like humans, pigs are omnivorous, possess a similar

digestion system, similar intestinal flora and similar distributions of body hair and skin tissue (60, 169). With a North American yearly production of approximately 1.5 million animals, domestic pigs are available in most areas. Finally, the use of whole pigs, humanely slaughtered for food, or pig tissue processed during the preparation of food or food products eliminates regulatory issues associated with the care and use of research animals under the Animal Welfare Act of 1966.

Fig. 2. A domestic pig on an organic farm in Solothurn, Switzerland (149).

Over the course of five years tissue samples from three sets of unrelated domestic pigs, totaling eight separate specimens were collected. These specimens were exposed to a variety of controlled laboratory environments and uncontrolled field environments.

Cell Lysis, Purification and Quantification of DNA

The primary focus of this project was to develop a suitable FSA-PCR based assay for assessing degradation of DNA. However, during the course of the project it

became necessary to evaluate a variety of processing techniques in order to improve sample DNA yield and quality.

During the initial stages of assay development, tissue specimens were lysed using cell lysis procedure 1. Cell lysates were organically extracted with phenol chloroform, concentrated with ethanol precipitation (combined with Microcon 100™ concentration if necessary) and quantified using fluorescent dye quantification. This combination of procedures is commonly used for forensic applications and was thought to produce DNA of a quality and quantity sufficient for use in this project. Specimens extracted using this combination of procedures produced DNA yields within an acceptable range (Table 1).

TABLE 1. Approximate DNA concentrations for Specimen numbers 2-7 obtained by comparison to the standard calibrator curve. Three microliters of undiluted specimen, 1:10 diluted specimen and 1:100 diluted specimen were added to an optically clear microtiter scanning plate with 97 µL of a 1:500 PicoGreen® solution. The plate was excited at ~480 nm and scanned at ~520 nm. Undiluted specimen concentration values exceeded the standard curve maximum value of 7 ng/µL dsDNA producing incorrect values due to RFU signal saturation. The calculated approximate DNA concentration value represents an average of the 1:10 and 1:100 dilutions.

Specimen #	Undiluted Quantification Value	1:10 Quantification Value	1:100 Quantification Value	Assessed DNA Concentration
2	8.99 ng/µL	2.61 ng/µL	0.19 ng/µL	~ 23 ng/µL
3	9.44 ng/µL	3.47 ng/µL	0.30 ng/µL	~ 33 ng/µL
5	9.23 ng/µL	2.89 ng/µL	0.34 ng/µL	~ 32 ng/µL
5	8.29 ng/µL	1.69 ng/µL	0.14 ng/µL	~ 16 ng/µL
6	8.21 ng/µL	1.77 ng/µL	0.14 ng/µL	~ 16 ng/µL
7	8.27 ng/µL	1.16 ng/µL	0.11 ng/µL	~ 12 ng/µL
Blank	0.01 ng/µL	0.01 ng/µL	0.01 ng/µL	~0.01 ng/µL

However, test data obtained using these samples (discussed in more detail in the RAPD

Analysis section below) were inconsistent with the assessed DNA quantity. Yield gel analysis was incorporated into the processing scheme to provide data allowing the evaluation of the quality of the DNA produced using the selected extraction procedure. The results of the yield gel analysis of the specimens extracted using cell lysis procedure 1 indicated that tissue samples processed with this procedure had a tendency to become degraded making them unsuitable for this project (Fig. 3). Although the cause of this degradation was not determined, it is believed that it was related to the procedures reliance on thin slicing of tissue sections to ensure even distribution of lysis buffer and proteinase K (pro k). Since complete tissue lysis with minimal DNA degradation requires complete pro K penetration, and penetration was slowed due to the thickness of the tissue slices, it is likely that native cellular nucleases had sufficient time to degrade the DNA before they could be digested by the pro K.To address this issue a second cell lysis procedure was assessed. Cell lysis procedure 2, unlike the first, included a liquid nitrogen freeze/mortar and pestle grind step to ensure the maximum surface area for distribution of Pro K in lysis buffer. The addition of this step had the added benefit of ensuring complete lysis of all calibrator curve tissue. Once it was established that high molecular weight DNA could be produced, an RNase A digest was added to eliminate RNA interference with quantification and potential PCR inhibition (Fig. 4). Although cell lysis procedure 2 ultimately proved to be more complicated and time consuming, it consistently produced DNA of the quantity and quality necessary to complete these studies (Fig. 5).

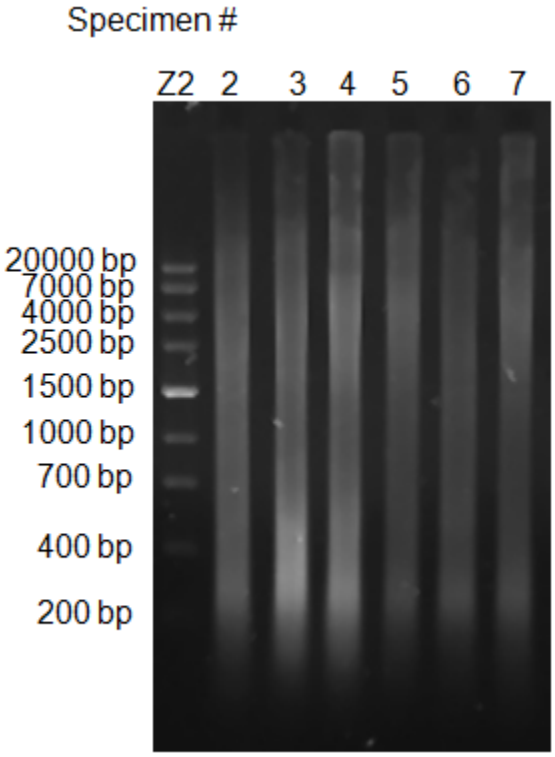

Fig. 3. Agarose gel electrophoretic analysis to assess the condition of genomic DNA in extracts from Specimens 2 – 7 (extract 071108). Approximately 100 ng of DNA from Specimens 2 – 7, extracted using cell lysis method 1 electrophoresed to evaluate the intactness of the DNA. Two microliters of each extract was loaded into each lane as noted above. Two microliters of ZipRuler™ Express DNA Ladder 2 (0.5 ug/µL) was loaded in lane 1. Samples were electrophoresed in 1.2% agarose gel for 50 minutes.

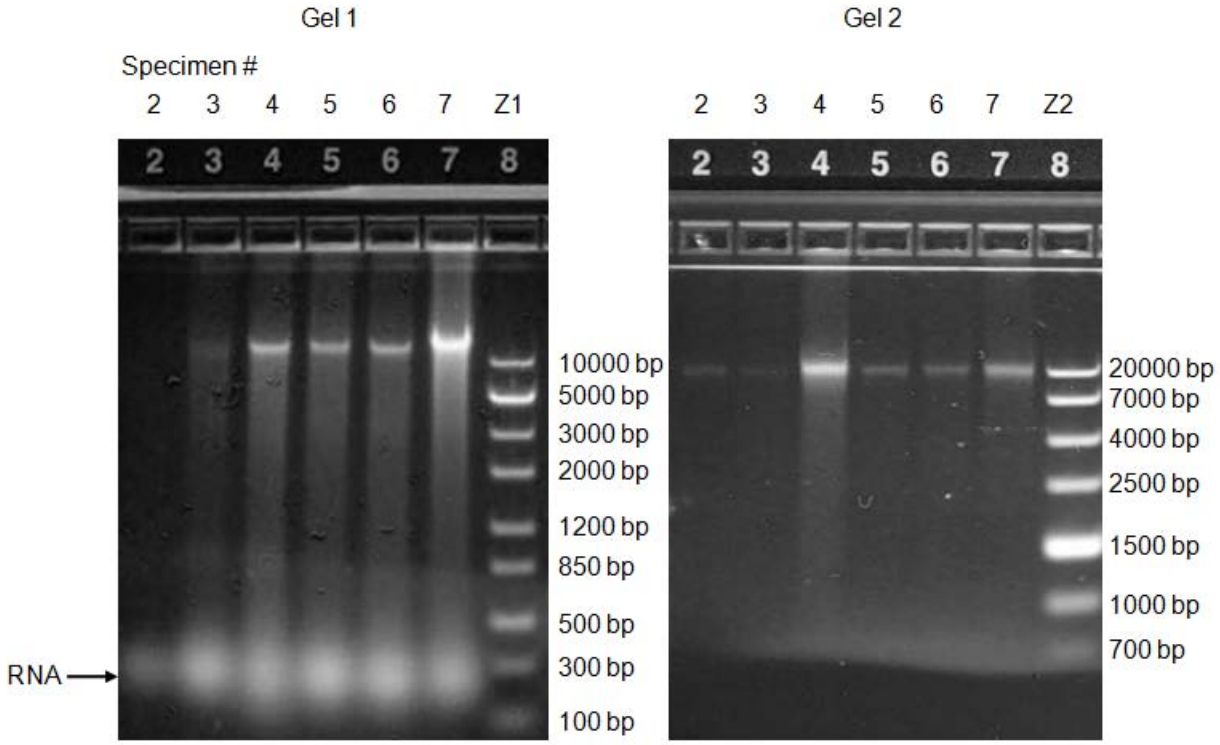

Fig. 4. Agarose gel electrophoretic analysis to assess the intactness of genomic DNA extracts from Specimens 2-7 (extract 021509 Gel 1 and subsequent clean-up **Gel 2).** High molecular weight DNA from Specimens 2-7 electrophoresed pre (Gel 1) and post

(Gel 2) RNase treatment. The intra-gel variability between identical specimens was likely due to incomplete pellet re-suspension of the specimens analyzed in Gel 1 (10 minute re-suspension in Gel 1 vs. overnight in Gel 2) combined with a higher pellet re-suspension volume in the samples analyzed in Gel 2 (100 µL for samples in Gel 1 vs. 500 µL for samples in Gel 2).

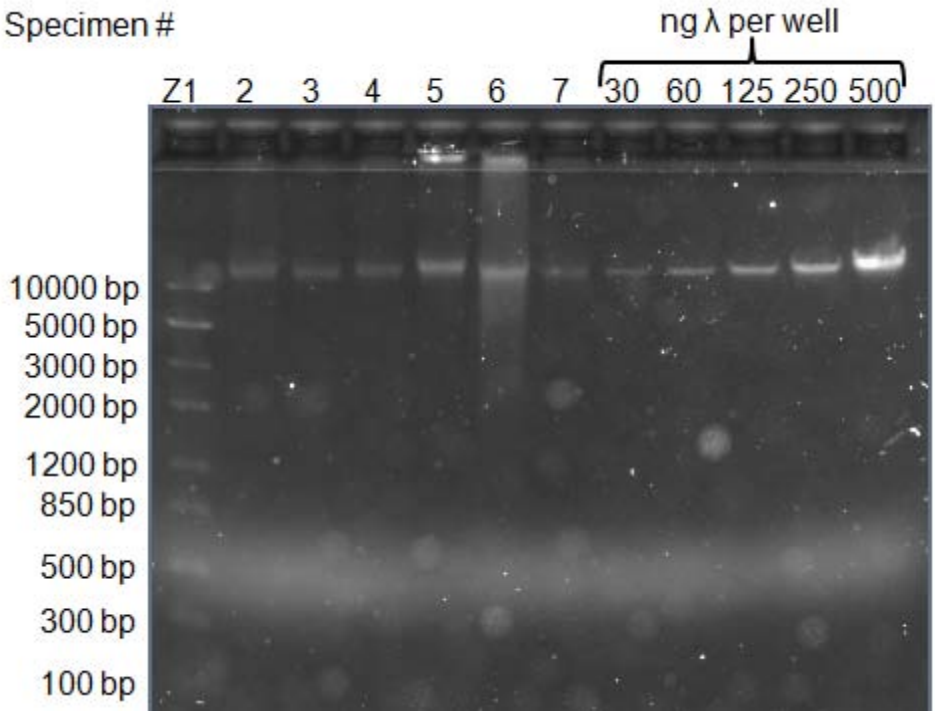

Fig. 5. Agarose gel electrophoretic analysis to assess the condition of genomic DNA extracts from Specimens 2-7 (Extract 021609). Two microliters of DNA from Specimens 2 – 7, extracted genomic DNA isolation method 2, were electrophoresed to evaluate the intactness of the DNA. The 1.2% Invitrogen E-Gel was electrophoresed for 30 minutes. ZipRuler™ Express DNA Ladder 1 was loaded in lane 1.

In addition to changes in specimen lysis, changes to the DNA purification were also implemented. Once intact DNA was produced, attempts were made to amplify the DNA and produce enzymatically fragmented DNA. However, initial attempts to amplify or digest the DNA using pancreatic DNase I were not successful (discussed in more detail in the Laboratory Assessment of Amplicons section below). To address the possibility that inhibitors to amplification and digestion were co-purifying with the DNA, an additional purification step was added. Qiagen QIAamp Mini® columns were used

to re-purify the DNA extracts re-suspended from pellets produced during the ethanol precipitation step. The addition of this step after the phenol chloroform extraction and ethanol precipitation ensured that both native inhibitors (lipids, proteins, etc.) that carried over during purification and non-native inhibitors introduced during extraction (phenol, NaCl, ethanol, etc.) would be removed. In addition to improving the overall quality of the DNA (purity and intactness) these modifications resulted in a significant improvement in DNA recovery (Table 2).

TABLE 2. Average DNA recovery by extraction procedure. Average total DNA recovery from six separate extracts using three variations of the DNA extraction process.

Total Quantity of Tissue Extracted	Average Total DNA Recovery	Description of Extraction Procedure
2.0 g	4.37 µg	Cell lysis Procedure 1/Organic Extraction/Ethanol Precipitation
0.6 g*	5.73 µg	Cell lysis Procedure 2/Organic Extraction/Ethanol Precipitation/Microcon microfiltration
0.1 g	36.07 µg	Cell lysis Procedure 2/Organic Extraction/Ethanol Precipitation/Qiagen QIAamp Mini® columns

Based on the inability of fluorescent DNA quantification to detect the DNA degradation noted when samples were extracted using cell lysis procedure 1, subsequent extracts were quantified using UV absorbance and were assessed using agarose gel electrophoresis when DNA intactness was at question.

Laboratory Assessment of Amplicons

To evaluate the suitability of a proposed directed primer set or RAPD primer for inclusion in this project, each was assessed in a two stage process. The initial stage of amplicon locus testing was designed to determine if a locus could be successfully

amplified (primer concentration, annealing temperature), if it was monomorphic, if it was sufficiently sensitive for use with forensic samples and if it produced a amplicon pattern suitable for assessing actual DNA degradation. Loci that were determined to meet the criteria outlined in stage one of the evaluation were advanced to stage two where they were evaluated using DNA extracted from tissue samples degraded under a variety of controlled laboratory and field conditions.

Assessing Amplifiability

With the exception of the RAPD primers, all locus primer sets were designed using published *Sus scrofa* sequence data. However, none of the exact primer sets including the RAPD primers had previously been used with reported DNA. In order to establish the primer or primer set viability, they were initially assessed using temperature gradient amplification and DNA target gradient amplification.

Temperature Gradient Amplification

Each primer set was designed with an annealing temperature between 58°C – 62°C using Primer 3 (v. 0.4.0) (207). However, in order to determine the optimal annealing temperature, and give the best chance for amplification, temperature gradient PCR was used. Primer sets were amplified at a fixed concentration of 0.2 µM and 0.4 µM using an MJ Research PTC-200 Gradient Cycler™ thermalcycler and a 12 °C temperature gradient from 55°C – 67°C. Once the amplification temperature was established each primer set's concentration was optimized by trial and error. RAPD

primers, unlike directed primer sets, rely on a low annealing temperature to produce a pattern and were not optimized using temperature gradient amplification.

Target Gradient Amplification

Before new DNA typing methods are implemented, they are evaluated to determine their sensitivity to the quantity of DNA amplified. The appropriate level of sensitivity is critical in a forensic genetic system to ensure that it can provide useful information. Overly sensitive genetic systems may be susceptible to low level contamination while systems requiring large quantities of DNA may not produce a usable profile with forensic samples that often contain limited quantities of DNA. Sensitivity to total DNA for genetic systems used for assessing time since death is generally less critical. Since they are applied in instances where the investigator is presented with a body or portion of a body there is usually sufficient tissue (soft or bony) from which to extract DNA. Additionally, since these assays usually rely on the presence of, absence of, or ratio of intact to non-intact DNA, the overall sensitivity is less of an issue. These generalizations hold true in the case of the genetic amplicons examined in this project since they were developed to assess DNA fragments that range from ~55 bp - ~1500 bp. However, because it is still necessary to understand the effects total DNA amount has on a genetic test and a minimum level of sensitivity is necessary, in this case arbitrarily selected as 30 ng – 3 ng of total DNA, RAPD primer's and directed primer sets were assessed against this quantity.

Once optimal annealing temperatures were established RAPD primers and directed primer sets that reliably produced specific and reproducible amplicons were

assessed to determine their sensitivity to the concentration of DNA.

Inter-specimen Polymorphism

At the outset of this project it was clear that there were a variety of DNA testing approaches that could be used for the development of a degradation-based assay for assessing time since death. The decision to focus on FSA-PCR based techniques was based on observations that sample fragmentation, presumably due to degradation, could have a detrimental effect on short tandem repeat (STR) analysis used in forensic science (84). However, unlike the process of selecting genetic amplicons for identity testing which focuses on polymorphic loci, degradation studies used to assess time since death require non-polymorphic amplicons to ensure consistent results between unrelated specimens.

With the exception of instances of point mutations within the primer binding sites, polymorphism was not a concern with directed primer sets. However, RAPD primers are notorious for exhibiting high levels of polymorphism. In order to ensure that RAPD primers were suitably un-polymorphic, those that successfully amplified DNA were assessed using DNA extracted from five separate animals. Specimens were collected over the course of several years from two different sources in the Middle Tennessee region.

Suitability for Assessing DNA Degradation

DNA degradation is the result of a combination of DNA fragmentation caused by autolysis and putrefaction. When using PCR to amplify DNA, the success of the

amplification can be dramatically affected by the fragmentation state of the template DNA. Depending on the number of copies of a locus within a genome, and the size of the target amplicon, fragmentation of the DNA can dramatically affect the ability of the locus to be amplified. As the DNA degrades to the point that all of the remaining fragments are smaller than the full-sized target amplicon, the yield of the resulting amplification product decreases to the point that successful amplification is no longer detectable using DNA staining.

Prior to their use with DNA degraded within limited samples (i.e. tissue samples degraded under controlled conditions and in field environments) the directed amplification primer sets found to be suitably sensitive and polymorphic were assessed using enzymatically degraded DNA. Although DNA within necrotic tissue does not degrade in the same manner as DNA digested with DNase I (253) (59) (175), it was felt that controlled digestion provided the best in vitro substitute for in vivo degradation.

DNase I Digestion in Manganese Buffer

The initial method evaluated used bovine pancreatic DNase I digestion in the presence of a Mn_2- buffered solution and was designed to produce DNA fragments with blunt ends. Digestion of DNA with bovine pancreatic DNase I in the presence of manganese has been demonstrated to produce blunt end or single base overhang fragments (167). However, samples digested using the manganese digest buffer failed to produce digested DNA (Fig. 6).

DNase I Digestion in Magnesium Buffer

A second DNA digestion was attempted using DNase I digestion with a Mg^{2+} buffered solution. DNase I in the presence of magnesium ions has been demonstrated to introduce random single-strand nicks into dsDNA. With both procedures digestion was allowed to proceed for 5 minutes using varying amounts of DNase I (Fig. 6). Once the optimal DNase I concentration was established, specimen DNA extracts were digested for varying lengths of time from 0 seconds to 120 minutes before testing with subject primer sets.

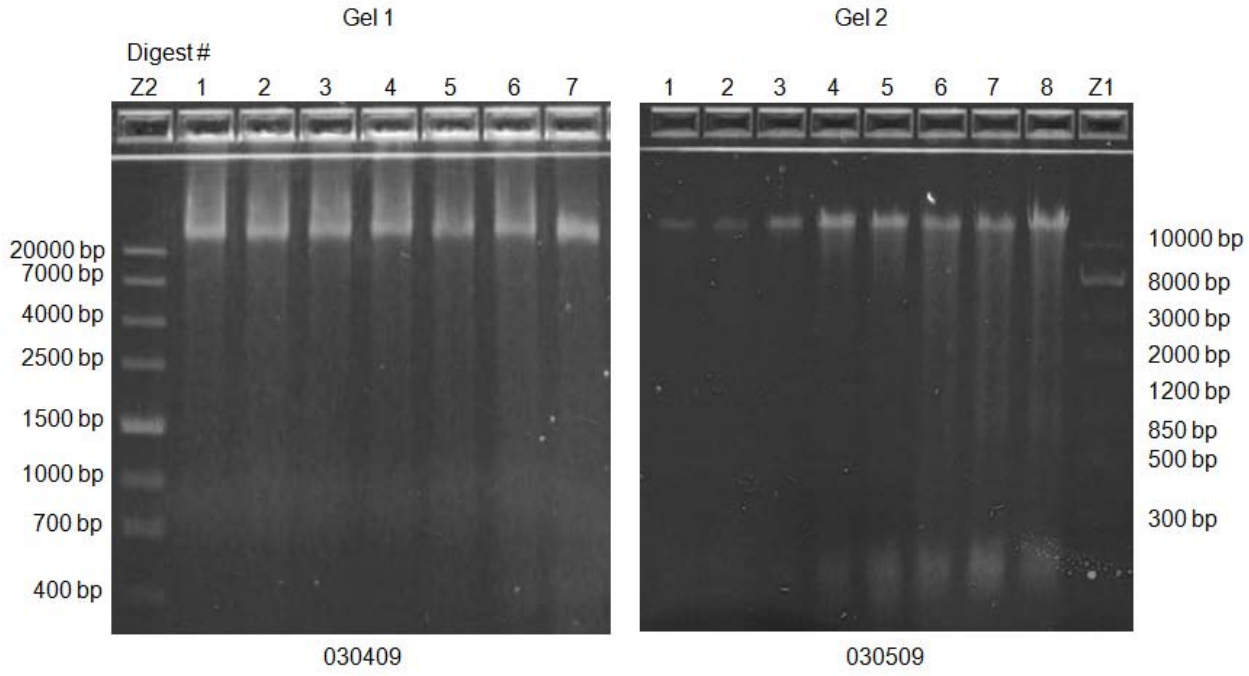

Fig. 6. Agarose gel electrophoretic analysis to assess the DNA (extract 021609) enzymatic digestion with DNase I. Gel 1 (030409) – Approximately 1 µg of DNA from Specimen #5 digested using manganese digest buffer and 1 µg – 10 pg DNase I (digest #1 – 7). Gel 2 (030509) – Approximately 600 ng blended DNA from Specimens #4, #5 and #7 post Microcon™ clean-up digested using magnesium digest buffer and 100 ng – 1 pg DNase I (digest #1 – 7) and 0 ng DNase I in # 8. Two microliters of each digest was loaded into each lane as noted above. Two microliters of ZipRuler™ Express DNA Ladder 1 and 2 (0.5 ug/µL) were loaded. The 1.2% Invitrogen E-Gel was electrophoresed for 30 minutes.

Laboratory Controlled Tissue Degradation

Primer sets that were shown to reproducibly generate fragment loss patterns when used to amplify enzymatically digested DNA were used to assess DNA extracted from tissue samples degraded in the laboratory under controlled temperature conditions. Incubating tissue samples at constant temperature eliminated the variability that usually must be corrected for by transforming the data with degree/day and degree/hour calculations. Additionally, testing samples incubated for varying lengths of time at various controlled temperatures provided data that could be used to elucidate the relationship between DNA degradation, temperature and time.

Field Controlled Specimen Degradation

Primer sets that produced reproducible fragment patterns with DNA from tissues sample incubated at controlled temperatures were used to test DNA extracted from tissue samples incubated under field conditions. These tissue specimens provided a set of samples that were identical to the laboratory controlled tissue samples (same quantity of tissue, incubation containers and incubation periods) with the exception that they were not maintained under constant temperature. Therefore, unlike the data from the samples incubated in the laboratory, field specimen data would require a degree/day or degree/hour correction to account for variability in temperature. Individual data points obtained using the field controlled specimens were compared to the trend lines obtained using the laboratory samples.

Intact Animal Field Specimen Degradation

As a final evaluation step, primer sets that demonstrated a degradation pattern from samples incubated under the field controlled conditions that was an acceptable fit to trend line data obtained from samples incubated in the laboratory were used to evaluate samples collected from an intact animal placed in uncontrolled field conditions. Unlike the field controlled conditions where sterile tissue samples of a known size were incubated in sealed polypropylene tubes, the uncontrolled field tissue samples were collected from an intact, unsterile animal that was placed on the ground, in a cage (to prevent large scavenger disarticulation with no protection from insect succession or environmental insults. It was hoped that this sample type, with the exception of the cage, would most closely parallel the sample type for which the assay was being developed. As with the field controlled specimens, individual data points transformed using the degree/day calculations and degree/hour calculations were compared to the trend lines obtained using the laboratory samples.

Amplicon Evaluation

Randomly Amplified Polymorphic DNA Analysis

Randomly amplified polymorphic DNA analysis was the initial process evaluated for this project. RAPD analysis, unlike directed PCR amplification, uses short primers and low annealing temperatures to promote random binding. Subsequent PCR amplification then replicated the randomly primed fragments. For this study, random decamers and a 34°C annealing temperature were used.

Initial investigations of RAPD analysis used approximately 80 – 100 ng of

"undegraded" reference DNA extracted from Specimen #1 and a water control, each amplified with RAPD primers 1-9. Profiles obtained using primers p1, p5, p7, p8 and p9 were weak, and no identifiable patterns were obtained using primers p2, p3, p4 and p6 (Fig. 7).

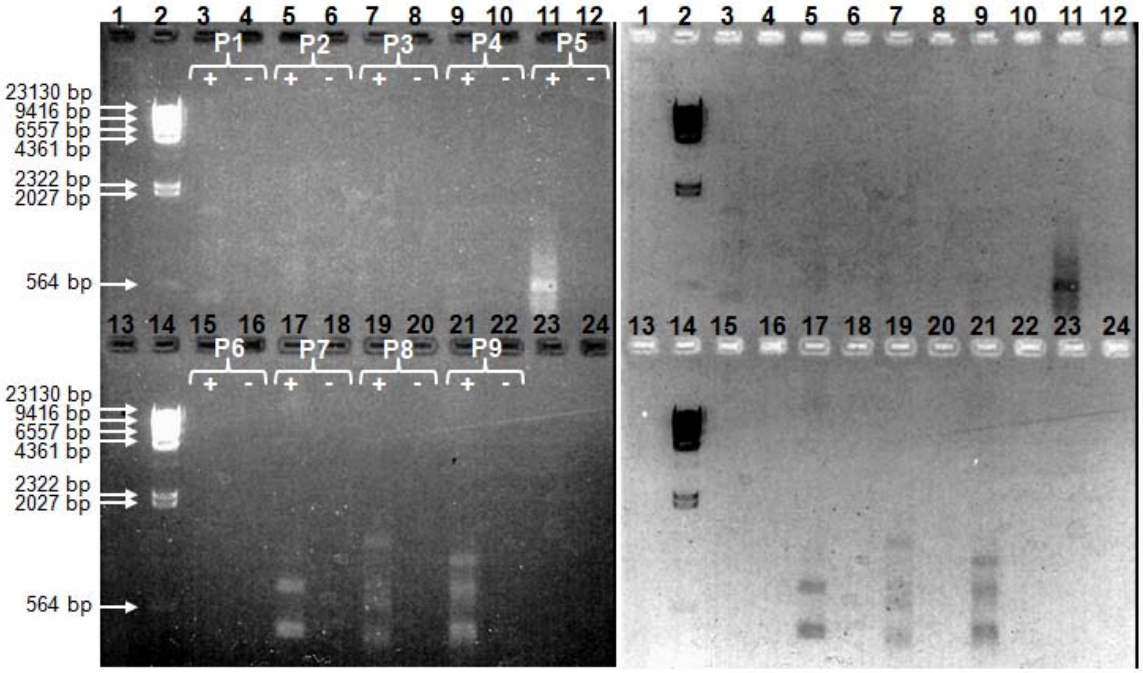

Fig. 7. Electrophoretic analysis of Specimen # 2 amplified with RAPD primers P1 – P9. RAPD Primers P1 – P9 were evaluated using approximately 80 ng of DNA extracted from the control blood samples collected from Specimen 2 (+) and water (-). Ten microliters of each amplification set was loaded in wells 3 – 12 and 15 – 22 as noted above. Two microliters of λ *Hin*d III ladder (0.5 µg/µL) was loaded in lanes 2 and 14. The 1.2% gel was electrophoresed at 200 V for 1 hour in 1X TBE. Both positive (left) and negative (right) images are presented to enhance the visibility of low level amplification in lanes 5, 7 and 9.

As was noted in the discussion of cell lysis, DNA purification and quantification above, it was later determined that the issues with RAPD analysis amplification were likely due to DNA degradation that occurred during tissue lysis. Once the lysis issue was resolved, RAPD amplification was repeated with approximately 30 ng of DNA from Specimen #7. The profiles produced indicated that the RAPD primers successfully amplified DNA that

ranges in size from approximately 100 bp to 1500 bp (Fig. 8).

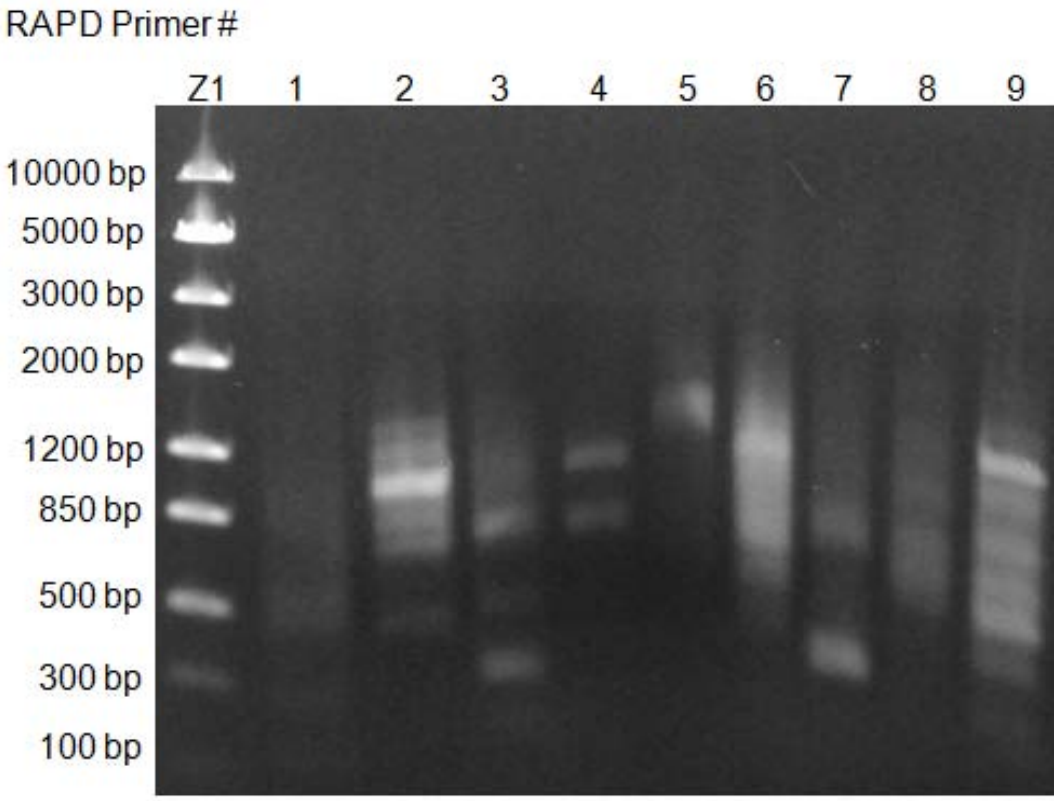

Fig. 8. Electrophoretic analysis of Specimen # 7 amplified with RAPD primers P1 – P9 and GCB 5. RAPD Primers P1 – P9 and GCB 5 were evaluated using approximately 30 ng of DNA extracted from Specimen #7 (ext 040209). Five microliters of each amplification were loaded into each lane as noted above. Five microliters of ZipRuler™ Express DNA Ladder 1 (0.5 µg/µL) were loaded in lane 1. The 1.2% agarose Invitrogen E-Gel® was electrophoresed for 30 minutes.

However, the resolution of the 1.2% agarose gel was not sufficient to differentiate individual profile bands unless they were separated by at least 50 bp. These RAPD samples were re-analyzed using 8% N-PAGE analysis and under these conditions patterns were obtained with sufficient resolution to evaluate the reproducibility of individual profiles (Fig. 9).

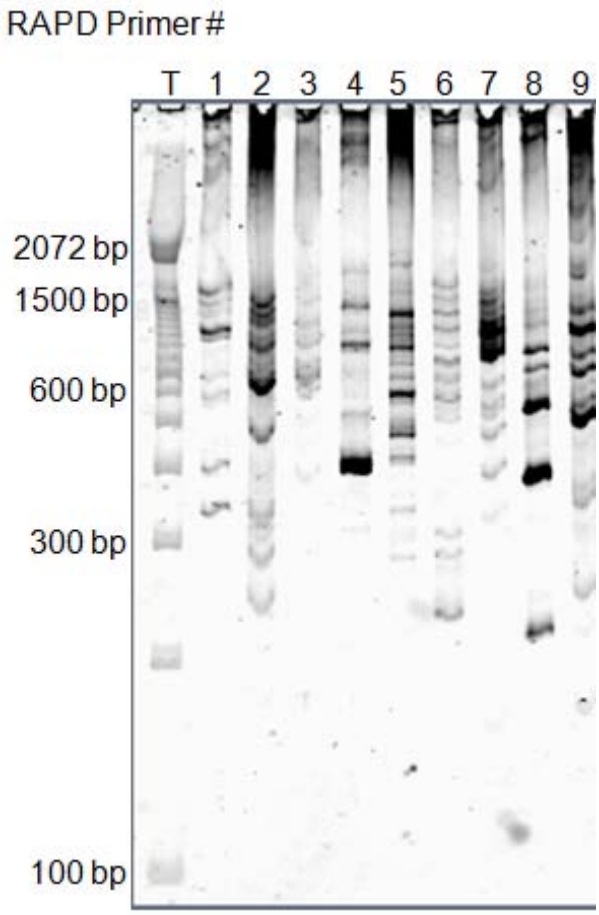

Fig. 9. Electrophoretic analysis of Specimen # 7 amplified with RAPD primers P1 – P9. RAPD Primers P1 – P9 were evaluated using approximately 30 ng of DNA extracted from Specimen #7 (ext 040209). Two microliters of each amplification was loaded into each lane as noted above. Two microliters of Trackit™ 100 Ladder (50 ng/µL) was loaded into the lane at the far left. The 8% N-PAGE analysis was performed at 400 volts for 85 minutes.

RAPD primers p2, p6 and p9 were evaluated for inter specimen polymorphism by amplifying them with approximately 30 ng of DNA from Specimens #3-7 (Fig. 10). Specimen #4 failed to produce an interpretable pattern with RAPD primers p2, p4 or p9. Specimen #3 failed to produce interpretable patterns with RAPD primers p2 and p6 but did produce a profile with p9. Based on the relative uniformity of the intra sample profiles, p9 was selected for further analysis.

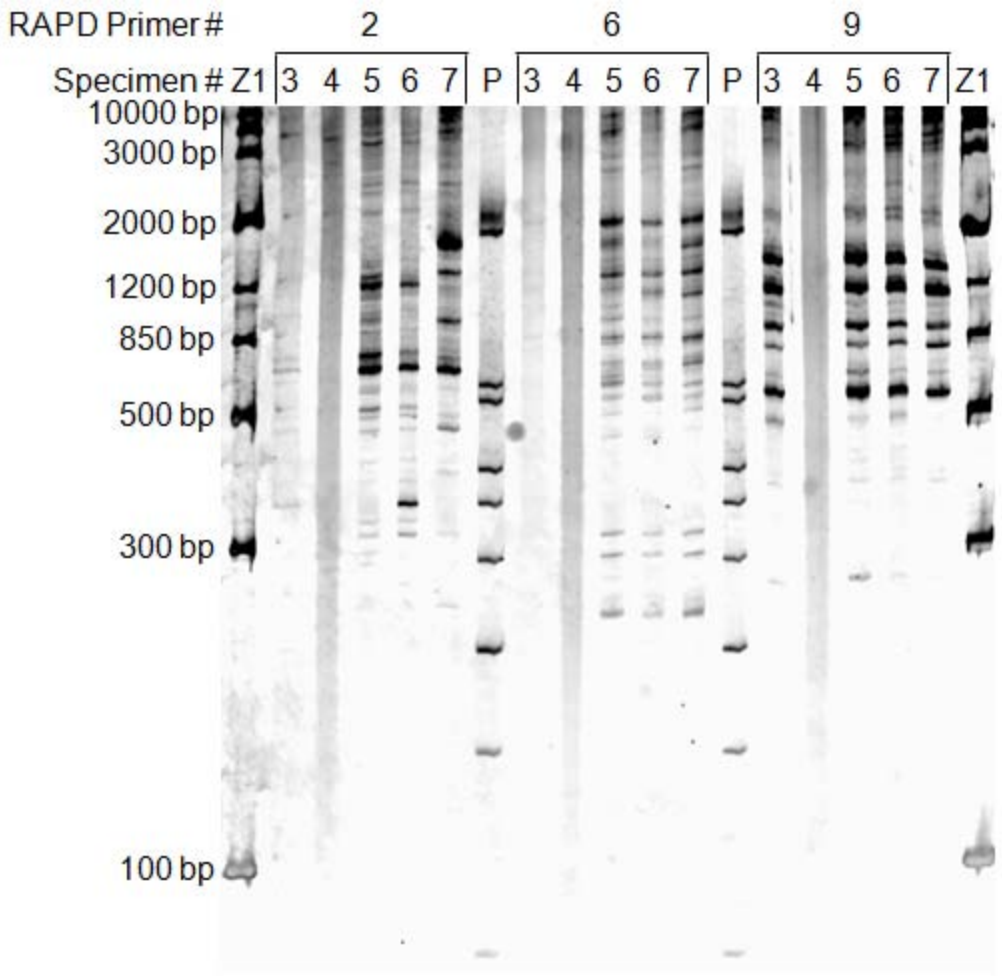

Fig. 10. Electrophoretic analysis of Specimens 3-7 amplified with RAPD primers P2, P6 and P9. RAPD Primers P2, P6 and P9 were evaluated using approximately 80 ng of DNA extracted from Specimens 3-7 (ext 040209). Two microliters of each amplification was loaded into each lane as noted above. Two microliters of ZipRuler™ Express DNA Ladder 1 (50 ng/µL) was loaded into lanes 1 and 19 and two microliters of pBR322 *Hin*f I ladder (25 ng/µL) was loaded into lanes 7 and 13. The 8% N-PAGE analysis was performed at 400 volts for 85 minutes.

The target DNA sensitivity of RAPD primer p9 was evaluated using dilutions of DNA from Specimen #7 that ranged from 30 ng to 0.029 ng of total target DNA. Although RAPD primer p9 successfully amplified DNA in the 30 ng range during earlier evaluation stages, repeated attempts to amplify DNA dilutions starting with 30 ng as well as subsequent attempts to amplify DNA extracted from tissue degraded under controlled conditions in the laboratory failed to produce interpretable patterns (data not

shown). Based on the sensitivity issues and the uncontrollable nature of the profile a determined decision was made to discontinue evaluation of the RAPD analysis as an assay for time since death. RAPD analysis provides several advantages over traditional directed PCR amplification. The random binding of the primers eliminated the need for species specific sequence data when developing the assay. The fact that the RAPD fragment sizes were only limited by the efficiency of the PCR extension step, and the potential to develop future directed primers from RAPD patterns (62, 171, 205) all made RAPD analysis an appealing option for inclusion in this study. However, liabilities such as the inability to moderate profile intensity by adjusting reaction components, the general complexity and difficulty in scoring the RAPD patterns obtained in this study and the generally recognized difficulty in standardizing RAPD analysis across various laboratories (189) outweighed the advantages for this project.

Group-Specific Component

The vitamin D-binding protein, sometimes called group-specific component (GC) is a 458 amino acid serum albumin protein that is clinically significant in that it is involved in the binding of free actin, fatty acids and the metabolites of vitamin D (258). In addition to its clinical significance, GC has also long been used as a forensic amplicon. As early as the 1960's differentiation of different isoenzyme groupings of GC has been used for paternity testing (77). Later applications have included the development, and implementation in forensic laboratories, of a reverse-dot-blot genetic assay designed to differentiate GC genotypes (61); its application in large batch typing

of GC related single nucleotide polymorphism (22); and for assessing time since death(186).

Initial investigations into using the GC gene as a locus for directed amplification involved designing primers based on published *Sus scrofa* DNA sequence (Fig.11).

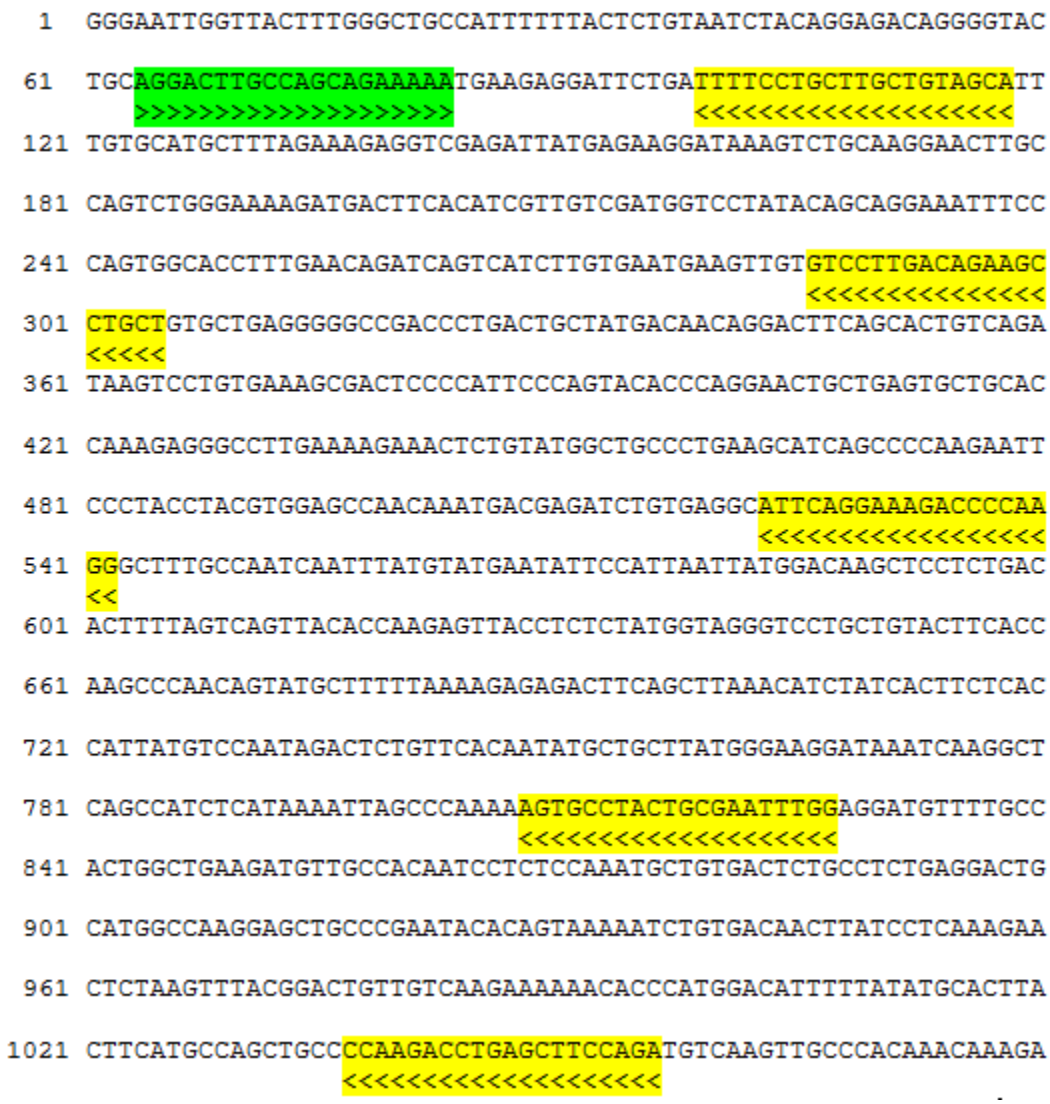

Fig. 11. Sus scrofa clone Clu_171269.scr.msk.p1.Contig1, mRNA sequence (125). Pig group-specific component (vitamin D binding protein) homolog sequence. The portion of the sequence highlighted in green is the anchor primer (GCA1) and carries a 5'- fluorescein (FL) label. The portions of the sequence highlighted in yellow are the fragment primers (GCB1-5) with the amplicon produced using GCB5 being the shortest, and the amplicon produced using GCB1 being the longest. GCB sequences are complementary to the yellow highlighted sequence shown.

Expected fragment sizes were ~55 bp, ~242 bp, ~479 bp, ~764 bp and ~993 bp. However, while optimizing annealing conditions it became apparent that this directed amplicon would not be acceptable (Fig. 12).

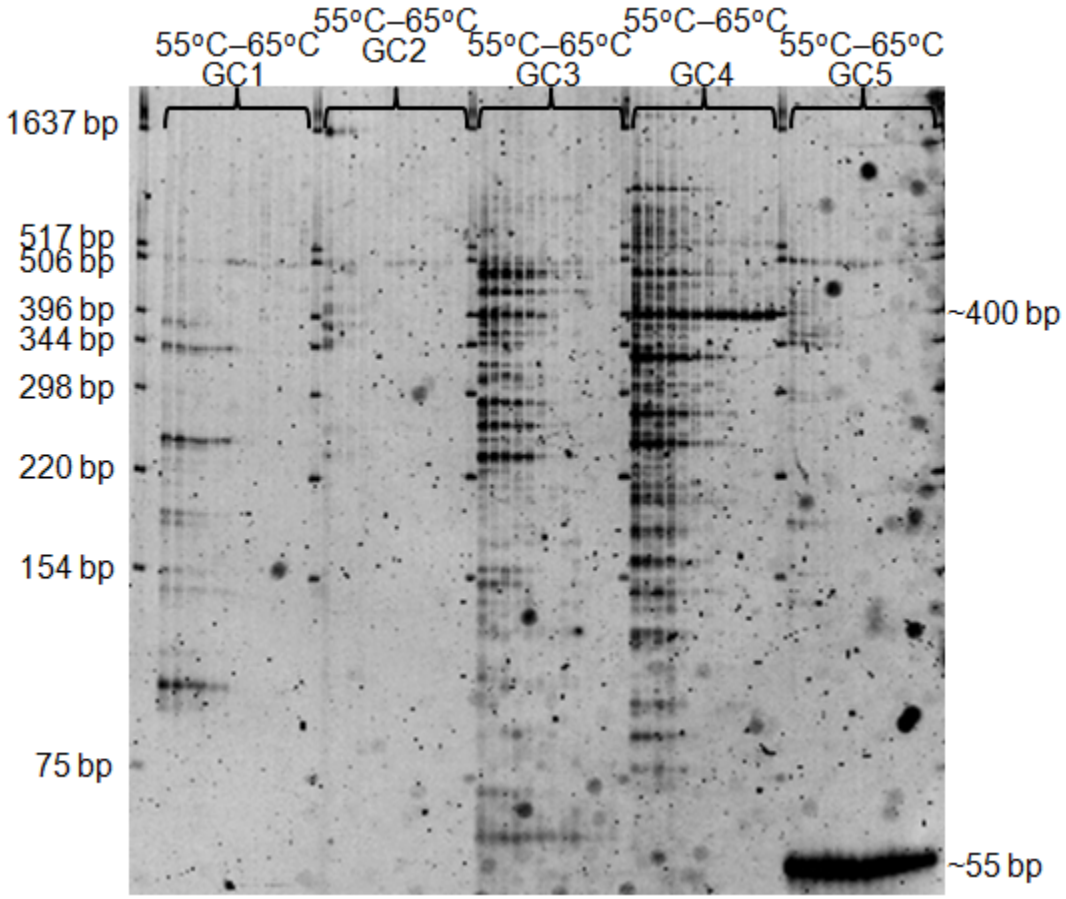

Fig. 12. Electrophoresis of temperature gradient amplification of group component amplicons GC1, GC2, GC3, GC4 and GC5. Amplification of 3 ng of Specimen #4 DNA using a temperature gradient from 55°C – 65°C. One microliter of each amplicon was loaded into each lane as noted above via membrane comb. One microliter of pBR322 *Hin*f I ladder (25 ng/µL) was loaded in lanes 1, 14, 27, 40, 53 and 66. The 8% N-PAGE analysis was performed at 400 volts for 85 minutes.

While the ~55 bp fragment (primer GC5) was reproducible with each annealing temperature tested, the primer set expected to produce the ~242 bp fragment (primer GC4) produced a fragment in the 400 bp range. Primers GC3, GC2 and GC1 failed to generate a reproducible profile. The shift in fragment size of the fragment obtained

using primer GC4 and lack of larger fragments is likely due to a heretofore unpublished intron located between primer GC5 and GC4. Given that the primers were designed using published cDNA sequence this is not entirely unexpected. This approach was necessary given the desire to incorporate the GC locus and the limited published data related to the porcine GC sequence. Based on the developmental data, the certainty that further development of the GC locus would require sequencing, and the presence of other loci more suitable for directed amplification, it was decided to discontinue studies with the GC primer set. However, in order to decrease the likelihood of encountering other unpublished intron sequences, the decision was made to limit subsequent amplicons to those that had been or were closely associated with published amplicons.

Mitochondrial Cytochrome b

Cytochrome b is the catalytic transmembrane subunit of the cytochrome b1 complex (complex III) and is an essential element of the electron transport chain in mitochondrial oxidative phosphorylation. Although its functional domains tend to be highly conserved between different species (203), its transmembrane domains have relatively fast rates of evolution (112) making the related DNA coding sequences useful as amplicons for studying evolutionary development. Forensic investigators have capitalized on this by developing DNA based speciation assays for forensic applications (131, 249). Cytochrome b is also widely studied in the medical field due to its clinical significance related to cellular respiratory disorders in humans and animals (28). Since it is the only cytochrome coded for by mitochondrial DNA there are multiple copies of

the gene in every cell. The combination of phylogenetic, forensic and clinical significance combined with the presence of multiple copies of the target amplicon per cell made the cytochrome b gene a strong candidate for consideration as an amplicon to assess degradation.

Initial investigations into using the cytochrome b gene (CB5) as a locus for directed amplification involved designing primers based on published *Sus scrofa* DNA sequence (Fig.13).

```
   1 ATGACCAACATCCGAAAATCACACCCACTAATAAAAATTATCAACAACGCATTCATTGAC

  61 CTCCCAGCCCCCTCAAACATCTCATCATGATGAAACTTCGGTTCCCTCTTAGGCATCTGC

 121 CTAATCTTGCAAATCCTAACAGGCCTGTTCTTAGCAATACATTACACATCAGACACAACA

 181 ACAGCTTTCTCATCAGTTACACACATCTGTCGAGACGTAAATTACGGATGAGTTATTCGC

 241 TACCTACATGCAAACGGAGCATCCATGTTCTTTATTTGCCTATTCATCCACGTAGGCCGA

 301 GGCCTATACTACGGATCCTATATATTCCTAGAAACATGAAACATTGGAGTAGTCCTACTA

 361 TTTACCGTTATAGCAACAGCCTTCATAGGCTACGTCCTGCCCTGAGGACAAATATCATTC
                                   >>>>>>>>>>>>>>>>>>>>

 421 TGAGGAGCTACGGTCATCACAAATCTACTATCAGCTATCCCTTATATCGGAACAGACCTC

 481 GTAGAATGAATCTGAGGGGGCTTTTCCGTCGACAAAGCAACCCTCACACGATTCTTCGCC

 541 TTTCACTTTATCCTGCCATTCATCATTACCGCCCTCGCAGCCGTACATCTCCTATTCCTG
                                                               >

 601 CAGGAAACCGGATCCAACAACCCTACCGGAATCTCATCAGACATAGACAAAATTCCATTT
     >>>>>>>>>>>>>>>>>

 661 CACCCATACTACACTATTAAAGACATTCTAGGGGCCTTATTTATAATACTAATCCTACTA

 721 ATCCTTGTACTATTCTCACCAGACCTACTAGGAGACCCAGACAACTACACCCCAGCAAAC

 781 CCACTAAACACCCCACCCCATATTAAACCAGAATGATATTTCTTATTCGCCTACGCTATC
         >>>>>>>>>>>>>>>>>>>>

 841 CTACGTTCAATTCCTAATAAACTAGGTGGAGTGCTAGCTCTAATAGCCTCCATCCTAATC

 901 CTAATTTTAATGCCCATACTACACACATCCAAACAACGAAGCATAATATTTCGACCACTA

 961 AGTCAATGCCTATTCTGAATACTAGTAGCAGACCTCATTACACTAACATGAATTGGAGGA

1021 CAACCCGTAGAACACCCATTCATCATCATCGGCCAACTAGCCTCCATCTTATATTTCCTA
     <<<<<<<<<<<<<<<<<<<<
```

Fig. 13. Sus scrofa isolate MS2 cytochrome b (cytb) gene, complete cds; mitochondrial gene for mitochondrial product (131). Pig mitochondrial cytochrome b sequence. The portion of the sequence highlighted in green is the anchor primer (CB R). The portions of the sequence highlighted in yellow are the fragment primers (CB L1 – L3) with the amplicon obtained from CB L3 being the shortest and the amplicon from CB L1 being the longest. The CB R sequence is complementary to the green highlighted sequence shown.

Expected fragment sizes were CB L1 ~645 bp, CB L2~440 bp and CB L3 ~255 bp. The initial intent was to incorporate the GC5 ~55 bp fragment into the assay as a control and to provide a fourth data point with an approximate 200 bp spread. However, the ~55 bp fragment amplification was dropped as it proved difficult to balance with other loci (data not shown). Temperature gradient amplification data for the CB L1 – L 3 primer sets showed high specificity across all temperatures tested (Fig. 14) with significant signal drop off after 67°C.

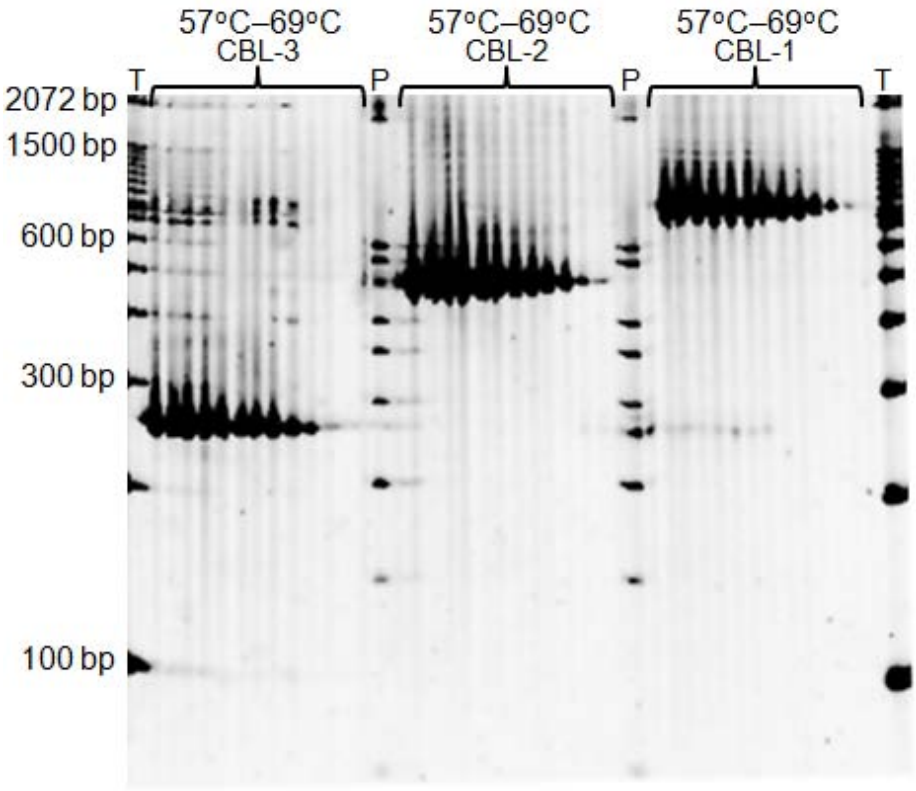

Fig. 14. Electrophoresis of temperature gradient amplification of cytochrome B mitochondrial amplicons CB L1, CB L2 and CB L3. Amplification of 3 ng of Specimen #7 using an amplification temperature gradient from 57°C – 69°C. One microliter of each amplicon was loaded into each land as noted above via membrane comb. One microliter of Trackit™ 100 Ladder (50 ng/µL) was loaded into lanes 1 and 39. One microliter of pBR322 *Hin*f I ladder (25 ng/µL) was loaded in lanes 14 and 27. The 8% N-PAGE analysis was performed at 400 volts for 85 minutes.

Although, based on these data, any temperature between 55°C and 66°C would have

provided adequate specificity with the lower temperatures providing a very strong signal, a 64^{o}C annealing temperature was selected for subsequent amplifications. It was felt that an annealing temperature towards the higher end of the temperature gradient would be more likely to reduce nonspecific amplification products not evident during development, yet provide adequate signal.

DNA target gradient amplification data for the CB L1 – L3 primers sets demonstrated very high sensitivity (Fig. 15) with all sample dilutions.

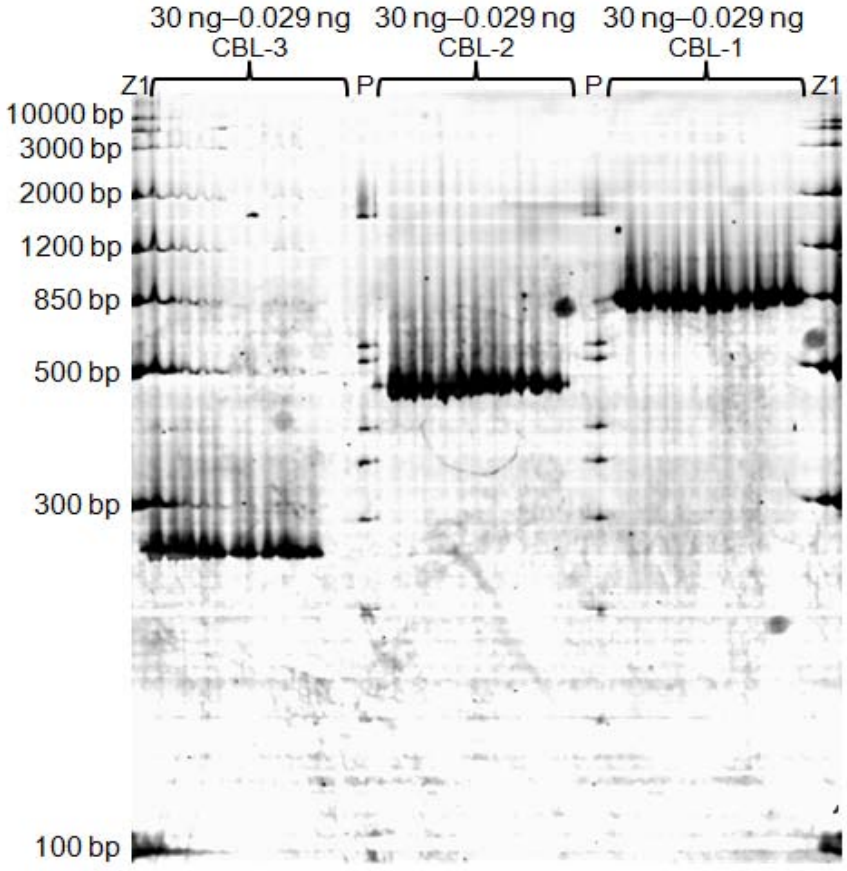

Fig. 15. Electrophoresis of a DNA target gradient amplification of cytochrome B mitochondrial amplicons CB L1, CB L2 and CB L3. Amplification of from 30 ng – 0.029 ng of (each step represents a 0.5 X decrease) Specimen #7. One microliter of each amplicon was loaded into each lane as noted above via membrane comb. One microliter of ZipRuler™ Express DNA Ladder 1 (50 ng/µL) was loaded into lanes 1 and 39. One microliter of pBR322 *Hin*f I ladder (25 ng/µL) was loaded into lanes 14 and 27. The 8% N-PAGE analysis was performed at 400 volts for 85 minutes.

However, the lack of an appreciable signal difference with total target ranges from 30 ng – 0.029 ng indicated the possibility that, regardless of the measurable quantity of DNA, the presence of multiple copies of the mitochondrial genome may result in the saturation of the amplification reaction. Initially, this caused concern regarding the viability of this locus; however this primer set was advanced in the hopes that it might provide valuable information regarding longer term sample degradation.

DNase I digested DNA amplified with primer sets CB L1 – L3 produced a degradation pattern indicating a loss of the larger amplicons (CB L1 first then CB5 L then CB L3) in only 20 minutes (Fig. 16).

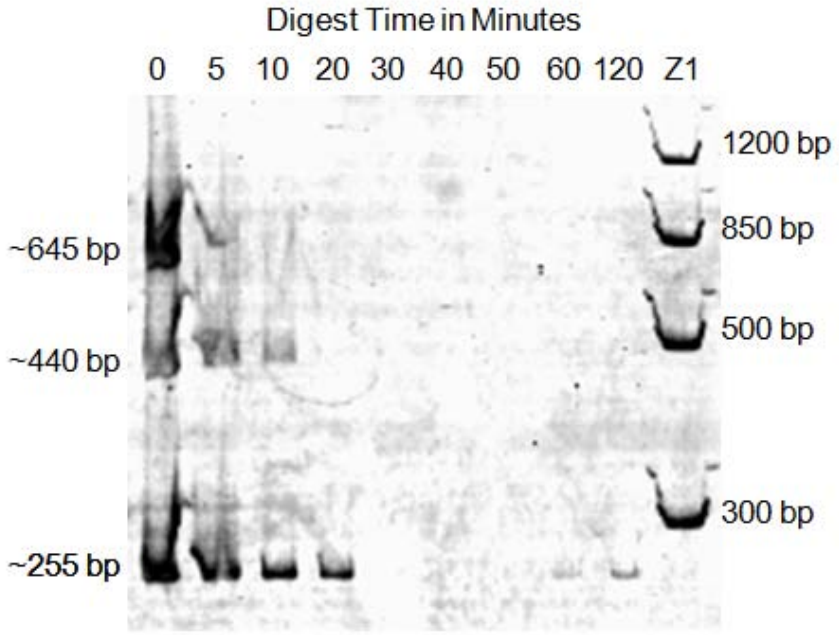

Fig. 16. Electrophoresis of DNase I digested DNA amplified with primer sets CB L-1, CB L-2 and CB L-3. Approximately 0.5 ug total DNA from Specimen #5 was digested in a 20 µL digest reaction (0.2 ng/µL DNase I) for the indicated period of time. Digested DNA was amplified with each primer set and one microliter of each amplicon was combined into a single load and loaded in the appropriate well. One microliter of ZipRuler™ Express DNA Ladder 1 (50 ng/µL) was loaded into lane 1. The 8% N-PAGE analysis was performed at 400 volts for 80 minutes.

Based on the developmental data, it was decided to continue assessing this primer set

with DNA samples degraded under temperature controlled conditions.

CB primer sets were then used to assess DNA extracted from tissue samples incubated at room temperature (~23°C) for varying lengths of time (Fig. 17).

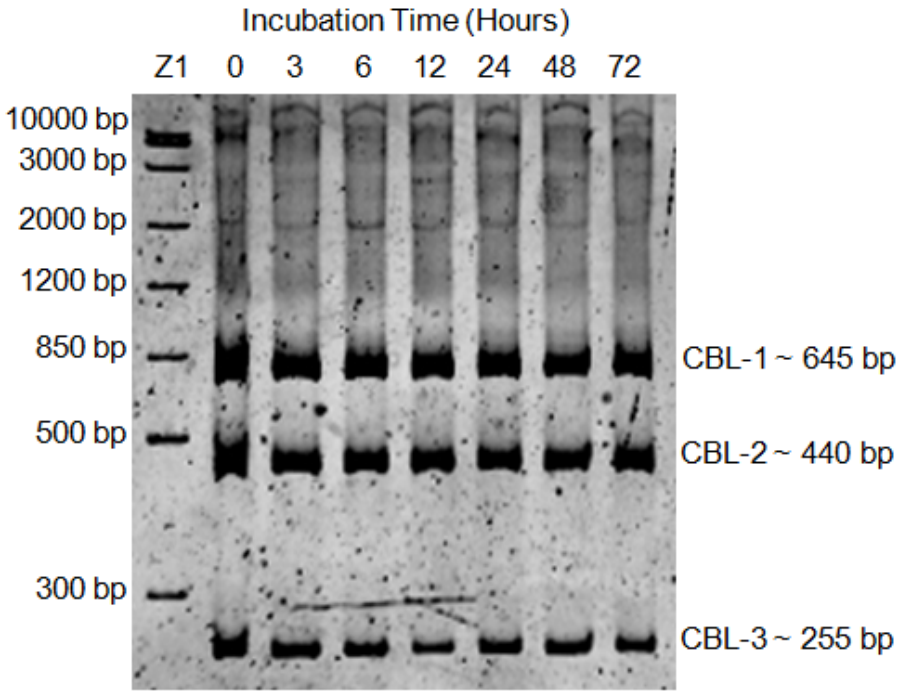

Fig. 17. Electrophoresis of DNA from laboratory controlled tissue degradation amplified with primer sets CB L1 – L3. One hundred milligram cuttings from Specimen #4 (D1 – D7), were incubated at room temperature (~23°C) for 0 – 72 hours. Four nanograms of each DNA extract was amplified separately with primer sets for amplicons CB L-1, CB L-2 and CB L-3. One microliter of each amplicon from each digest was combined into a single load, mixed with 5X loading dye and loaded into each lane. One microliter of ZipRuler™ Express DNA Ladder 1 (50 ng/µL) was loaded into lane 1. The 8% N-PAGE analysis was performed at 400 volts for 80 minutes.

As with the DNA target gradient amplification data, the lack of an appreciable signal difference with incubated over a total of 72 hours indicates that the mitochondrial DNA degradation process within tissue does not duplicate that seen in the DNase I treated DNA. This same pattern was seen with samples amplified with 20 ng – 0.2 ng total DNA, incubated at ~23°C and ~37°C, for 0 – 72 hours (data not shown).

As was noted above, the lack of variability of signal for samples amplified with

such widely varying total DNA targets and incubation temperatures is likely due to amplification reaction saturation. This is not entirely surprising since it is because there are multiple copies of the mitochondrial genome in each cell and the possibility that the additional membrane may impart additional protection from degradation that makes mitochondrial sequencing such a useful tool for the identification of degraded human remains (21). These attributes would potentially make the CB L1 – L3 primer sets suitable for assessing DNA degradation in tissues that have undergone extensive long term degradation. However, the lack of variability with samples degraded for shorter periods of time made them unsuitable for this project.

Nuclear Cytochrome b5

Cytochrome b5A (sometimes referred to as microsomal cytochrome b) is a trans-membrane protein of the endoplasmic reticulum (ER) that functions as an electron carrier for enzymes in the hemoglobin pathway. The N-terminal domain of the protein self-inserts into the ER membrane (32) and is retained by structural elements in the trans-membrane and C-terminal domains (104). Although the functional domains of CB5 show some conservation of amino acid sequence across species, it does not demonstrate the same level of cross-species conservation as mitochondrial CB and has not been used as extensively in phylogenetic studies. Likewise, while CB5 has clinical significance related to a specific hemoglobin pathway disorder, the disorder itself is relatively rare and has not been studied to the same extent as mitochondrial CB related disorder (114). For these reasons CB5 initially appeared less suitable candidate locus for investigation. However, there were three primary motivators for assessing the CB5

locus. First, forensic investigators had assessed the enzymatic activity as it related to time since death (271). Second, CB5 is coded for by nuclear DNA limiting the number of target copies per cell and potentially the saturation issues seen with mitochondrial CB. The significance of *Sus scrofa* as a food animal meant sequence data were available (24).

Initial investigations into using the CB5 gene as a locus for directed amplification involved designing primers based on published *Sus scrofa* DNA sequence (Fig.18).

```
  1 AAACATTCTCAGAAGCCAATGGAAGAAAAGACTGCTCTGGTCCAGGGAGAAAGAAGCTAC
                        >>>>>>>>>>>>>>>>>>>>>
 61 CATTAACTGCCTTGATTGACAGAATACTTCACTGGAAAATAATTTCAGTATACCTGTTTC
                                                          <<<<<
121 CTTTTCCTCCTGCATTAGTCATAAAACAAATCAAAAAGCACTGTTCTATTCTTTCTACTC
    <<<<<<<<<<<<<<<
181 CTCAACTTTTAGAGTGTGCCTTTTTATTCATCAGCTTTGTTTTGATGTTCCATCACTACA

241 TCATTTGCTTAGTGTGGGCACAATCTTTTAAAACCTATCACATTTGCCTGTCTCTTTGGT
          <<<<<<<<<<<<<<<<<<<<
301 GTATAATTGTCTGTAACGTTTGAAATCTGATTATTTGGCAGTCATTTAATATGCTGATCA

361 CTCAGACCTGCGTTGTCTGTCTCGTGCGAGGAGGAGCATCCTTGAGTCTCTTACTCTGCT

421 GTTTCATCTAATTGAATAATCAGGTACTACATGTTTCCAATGTAGTTTTTCCCCCCAAGG
                                                          <<<<<<
481 GAAATATGAAAAGCCCAGAAATAATAGCTTAAAGATTTCTAATAGTTGTTCTACTTGAAA
    <<<<<<<<<<<<<<<<
541 AGTTGAATAGATGATAAAAAGGAAAAATGCCCTATAGGACAGAGAAAAGAGACTCCATCT

601 CTTTGATTAAAAAAACACTAGCAACATCAACAAAAGCCTGTGAACCATGAGAGAACATTA

661 CCACTGTCCCTTCTCTCAGCTTAAAAGATGTCATTCCAAAGAGGTTCTCGGTTACAAAGG

721 TTCTAAAGTTTTACAGATTCCTCCTTCAGAGGTGAAAACTGTTTATGTGCTCCTGTAAGG

781 AAATGCTGATTCTCTTAATTTGAAAGACATTGGCACATTTGGAATCTGATTTTTGAAGAA

841 ATTTAGCTTCTGGTGATGGGCCATAAGGAACTCTGGTGTGGCTCCAGTGGACTGACTCAT

901 CATCTGTCTTCATTTTTCTCAGCCTCATGCTTTTTTTCTTTAAATATGGAAACTTGAGAG

961 ATGATTTTATAGAGTTGAAGTACTTCATAGTTAGCAATGATTGTCCATTGGCGTGCTAGA
                                                  <<<<<<<<<<<<<<<<<<<<
```

Fig. 18. *Sus scrofa* cytochrome b5 type A (microsomal) (CYB5A), mRNA (24). Pig cytochrome b5A sequence. The sequence highlighted in green is the anchor primer (CB5 L). The sequences highlighted in yellow are the fragment primers (CB5 R1-R4) with the amplicon obtained using CB5 R1 being the shortest and the amplicon obtained using CB5 R4 being the longest. CB5 R sequences are complementary to the yellow highlighted sequence shown.

Expected fragment sizes were CB5 R1 ~116 bp, CB5 R2 ~247 bp and CB5 R3 ~477 bp and CB5 R4 ~999 bp. Amplified fragments obtained using primer sets CB5 R1 – R3 produced amplicons that sized very close to, or identical to, the expected amplicon size. However, primer set CB5 R4 produced an amplicon that sized approximately 300 bp larger than the expected size of ~999 bp. As was seen with the GC amplification products, this was likely due to the presence of an unpublished intron. Although the CB5 R4 fragment was significantly larger than expected, it was reproducible and the decision was made to include it in the assay and evaluate it further. As with the mitochondrial CB locus, GC5 was initially considered as another data point but was eventually dropped.

Temperature gradient amplification data for primer sets CB5 R1 – R4 demonstrated the highest levels of specificity around 63^{o}C with a dramatic drop off of signal for CB5 R1 above 64^{o}C (Fig. 19).

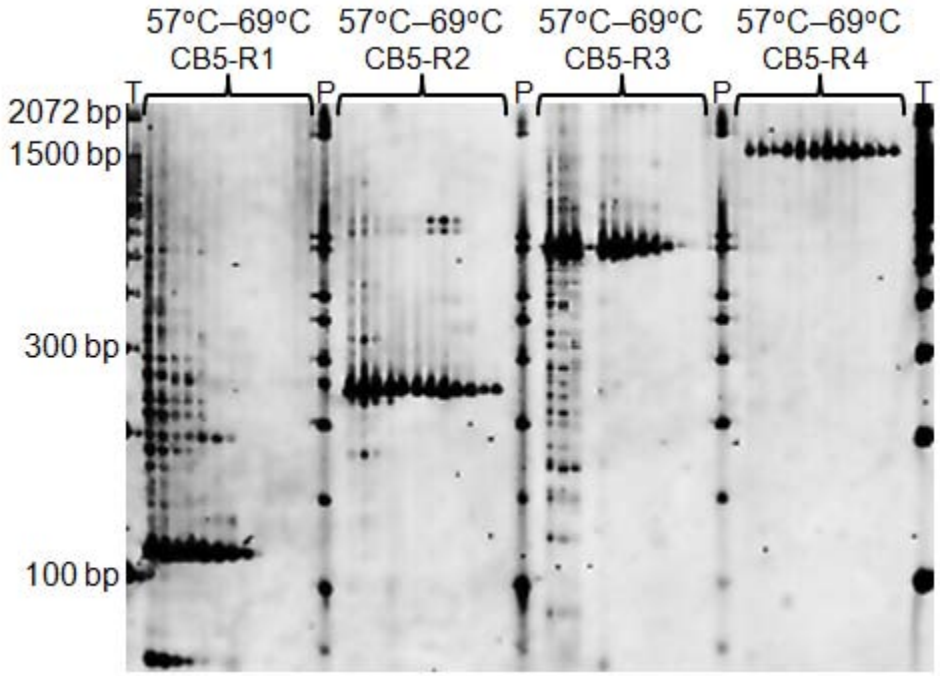

Fig. 19. Electrophoresis of temperature gradient amplification of cytochrome b5 amplicons CB5-R1 – CB5-R4. Amplification of 3 ng of Specimen #7 DNA using an

amplification temperature gradient in 1ºC increments from 57°C – 69°C. One microliter of each amplicon was loaded into each lane as noted above via membrane comb. One microliter of Trackit™ 100 Ladder (50 ng/µL) was loaded into lanes 1 and 53. One microliter of a 0.25 ng pBR322 *Hin*f I ladder was loaded in lanes 14, 27 and 40. The 8% N-PAGE analysis was performed at 400 volts for 85 minutes.

Although close to the theoretical high limit of CB5 RR1, 64°C was selected as the optimal annealing temperature. This temperature provided the best balance of specificity and signal with the largest two primer sets (CB5 R3 and R4) and adequate signal and specificity with the smaller primer sets (CB5 R1 and R2).

DNA target gradient amplification data for the CB5 R1 – R4 primer sets demonstrated a loss of signal for CB5 R4 below approximately 1.25 ng total DNA. Primer sets CB5 R1 – R3 successfully amplified DNA down to 0.625 ng total DNA (Fig. 20). Subsequent amplifications with this set of primers target 3 ng or greater total DNA.

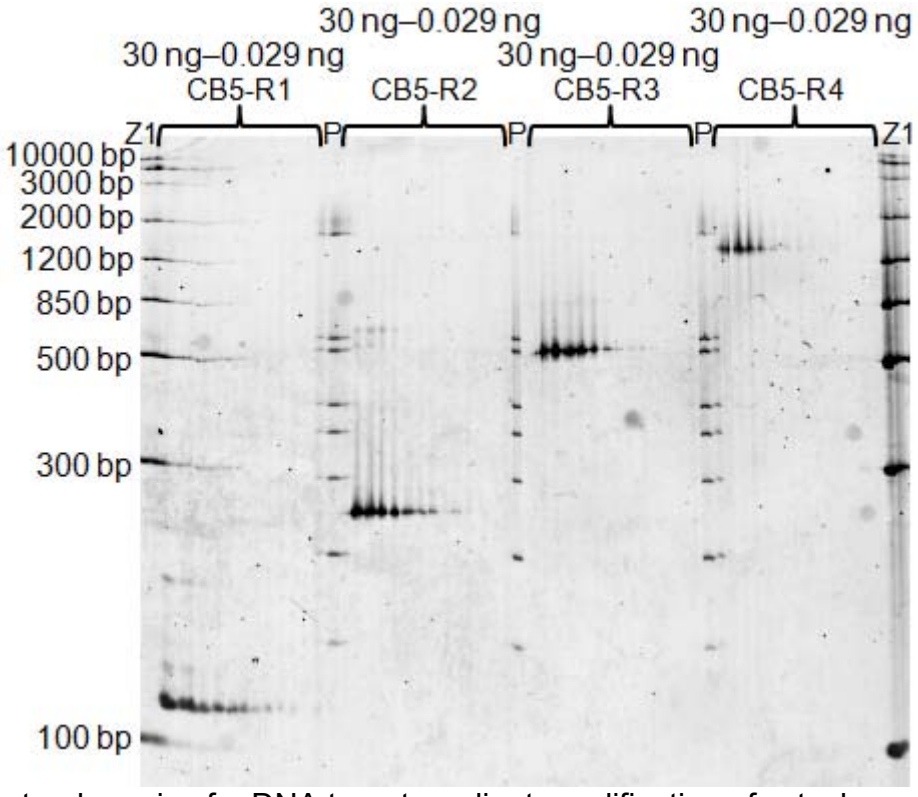

Fig. 20. Electrophoresis of a DNA target gradient amplification of cytochrome b5 amplicons CB5-R1 – CB5-R4. Amplification of from 30 ng – 0.029 ng (each step

represents a 0.5 X decrease) of Specimen #7 DNA. One microliter of each amplicon was loaded into each lane as noted above via membrane comb. One microliter of ZipRuler™ Express DNA Ladder 1 (0.50 ng/µL) was loaded into lanes 1 and 39. One microliter of pBR322 *Hin*f I ladder was loaded into lanes 14 and 27. The 8% N-PAGE analysis was performed at 400 volts for 85 minutes.

Unlike the pattern seen with the mitochondrial CB primer sets, where all primer sets produced detectable amplicons for all digests, DNase I digested DNA amplified with primer sets CB5 R1 – R4 produced a degradation pattern indicating a loss of amplicons from largest to smallest (CB5 R4 first then CB5 R3 etc.) (Fig. 21).

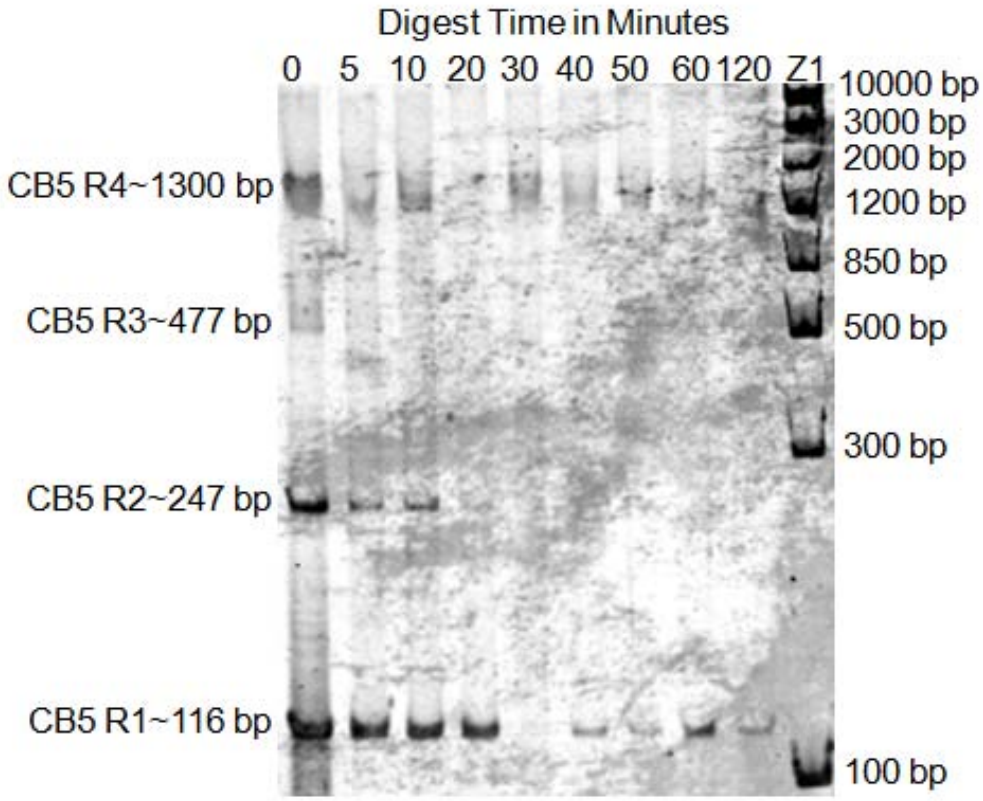

Fig. 21. Electrophoresis of DNase I digested DNA amplified with primer sets CB5 R1, CB5 R2, CB5 R3 and CB5 R4. Approximately 0.5 µg total DNA from Specimen #5 was digested in a 20 µL reaction (0.2 ng/µL DNase I) for the indicated period of time. Digested DNA was amplified with each primer set. One microliter of each reaction was combined into a single load and loaded in the appropriate well. One microliter of ZipRuler™ Express DNA Ladder 1 (50 ng/µL) was loaded into lane 1. The 8% N-PAGE analysis was performed at 400 volts for 80 minutes.

This pattern of amplicon loss, from largest to smallest, is consistent with what is understood about DNA degradation and what was has been demonstrated with RT-PCR based methods (235). Based upon this developmental data, it was decided to continue assessing this primer set with DNA samples extracted from tissue specimens degraded under controlled conditions.

Sterile tissue samples, weighing 0.1 g, were incubated in duplicate sets in sealed polypropylene tubes at 13^{o}C, 23^{o}C and 37^{o}C for 0 – 72 hours. Once extracted, DNA from the specimen extracts was amplified using the CB5 primer set. Unlike the profile obtained using the mitochondrial CB primer set, the pattern obtained using the CB5 primer set showed a significant shift in the profile intensity relative to time. Specifically, the pattern was consistent with the time-dependent loss of the largest amplicon followed by the next largest amplicon and so on. Although not identical, this change in the profile was consistent with the change profile seen with the enzymatically degraded DNA. This indicates that the fragmentation of purified DNA caused by enzymatic digestion in a test tube is not radically different than the fragmentation caused by cellular autolysis. Additionally, as the temperature of incubation increased the shift in the profile intensity (with fragments disappearing in the order from largest to smallest over time) appeared to accelerate, regardless of the quantity of DNA amplified (Fig. 22).

A visual inspection of the N-PAGE results indicates that, when other environmental factors are kept constant, amplicon signal decay relative to time occurs in a predictable pattern from the largest to the smallest amplicon. While these results (visual) tend to support the idea that DNA degradation is occurring in a predictable manner and can be used as an indicator of post mortem interval, result in this form do

not yet reflect a quantitative approach and thus are not yet suitable for comparisons across experiments that vary time and temperature.

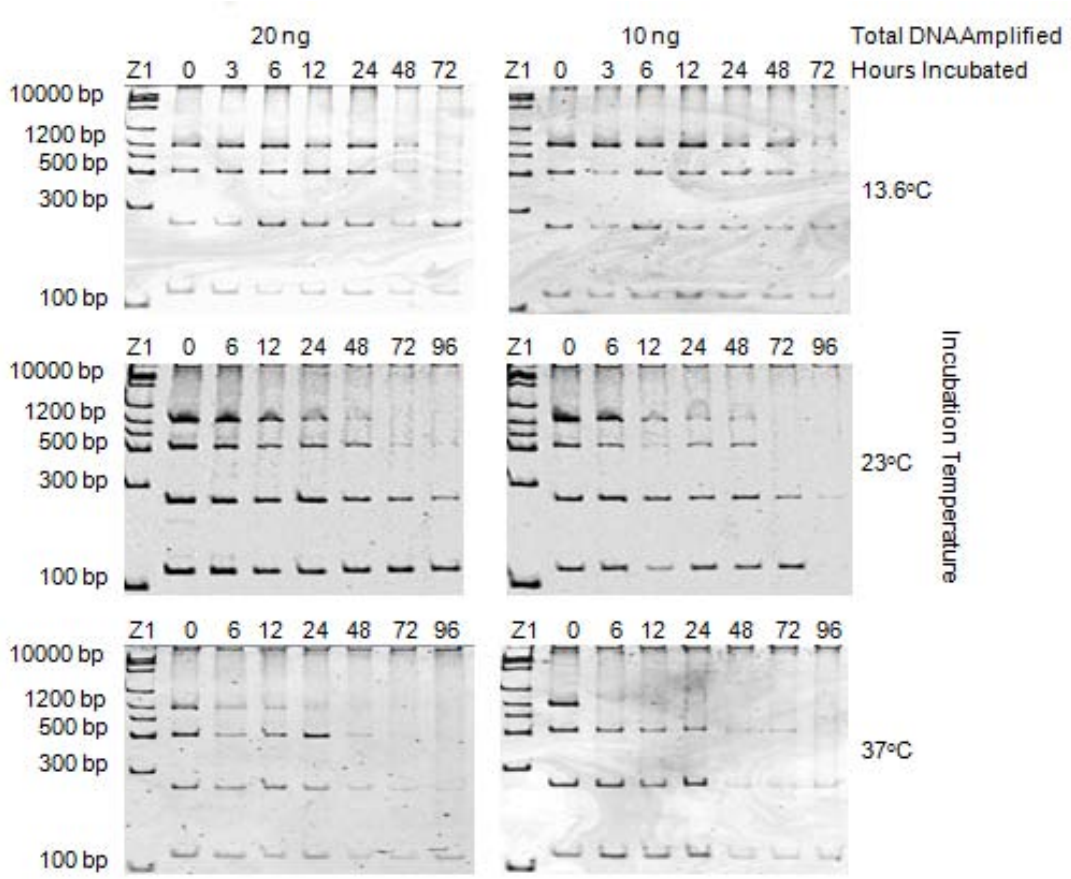

Fig. 22. Electrophoresis of DNA from laboratory controlled tissue degradation samples amplified with primer sets CB5 R1 – R5. One hundred milligram cuttings from Specimen #4 were incubated at room temperature 12°C, 23°C, and 37°C for 0 – 72 or 0 -96 hours. Each DNA extract was amplified targeting 20 ng and 10 ng total DNA (separately) with primer sets for amplicons CB5 R1 – R5. One microliter of each reaction was combined into a single load sample and this was mixed with 5X loading dye and loaded in the designated lane. One microliter of ZipRuler™ Express DNA Ladder 1 (50 ng/µL) was loaded in land 1. The 8% N-PAGE analysis was performed at 400 volts for 80 minutes.

In order to better understand the dynamics of the profile decay a method was used to quantify the signal of the amplicon. Once quantified, a variety of approaches could be used to assess the amplicon signal data.

Upon completion of N-PAGE analysis, individual lanes were tracked, specific amplicon bands identified and signal quantified using the Bio-Rad Laboratories' Quantity One® software (v4.65). Signal values in Relative Fluorescent Units (RFU) were compiled in Microsoft Office Excel® 2007. The Quantity One® software was then used to determine and remove gel background noise (Fig. 23). Once compiled and corrected, the individual amplicon signals were used to determine if this approach could be used to assess the relative level of DNA degradation.

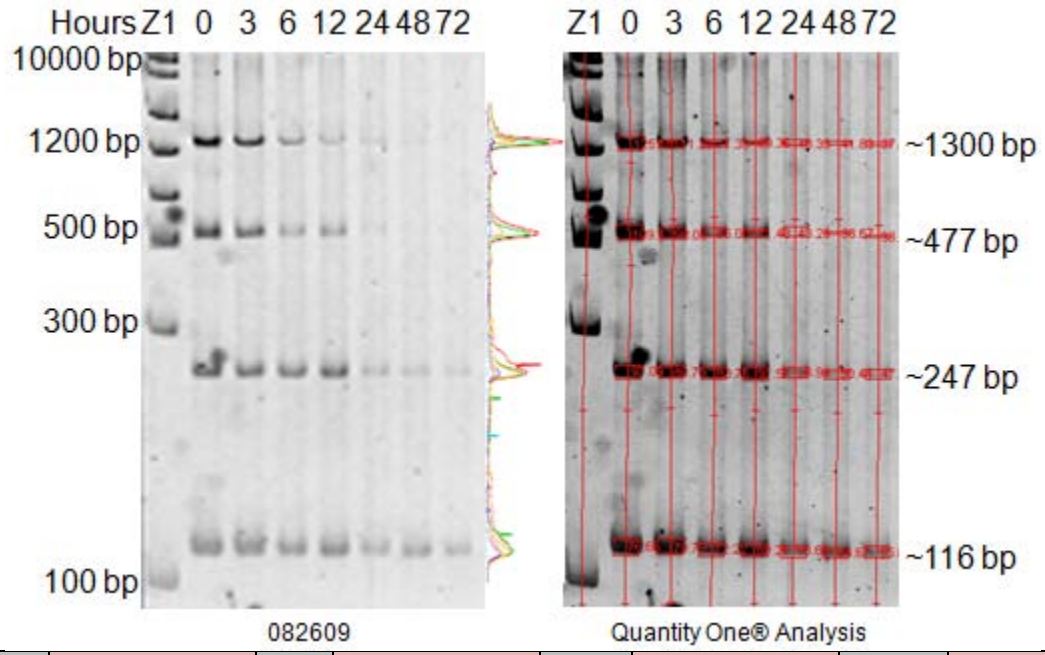

Hours	Signal 116 bp	Corrected Amplicon Signal 116 bp	Signal 247 bp	Corrected Amplicon Signal 247 bp	Signal 477 bp	Corrected Amplicon Signal 477 bp	Signal 1300 bp	Corrected Amplicon Signal 1300 bp
0	79	44	102	68	109	75	135	100
3	77	43	80	46	90	55	96	62
6	71	37	84	50	61	26	66	32
12	78	44	91	56	67	33	56	21
24	58	24	53	19	43	9	46	12
48	62	28	51	16	0	0	41	6
72	54	19	47	13	0	0	0	0

Fig. 23. Bio-Rad Laboratories' Quantity One® analysis of N-PAGE electrophoresis gel. The gel on the left is the N-PAGE analysis data from samples electrophoresed on

08/26/09. The gel on the right shows amplicons bracketed and quantified by the Quantity One® software with values shown in the gray table columns. Values in the pink columns represent the signal quantification with a background correction of 35 RFU.

Data assessment began with a simple graph of the individual amplicon signals as a function of incubation time. To determine the effect of gel background on the pattern, uncorrected amplicon signals were often graphed and compared to graphs of the same data which had been subjected to the background correction. As seen in Fig. 24 background correction had an effect on the data for amplicon values. In particular it "smoothed out" the curves at later time points where RFU values were low.

Once background corrected amplicon signal values were obtained, an accumulated degree/hour and degree/day calculation was applied to the time interval that had elapsed during collection (equivalent to post mortem interval). Accumulated Degree/Hours (ADH) and Accumulated Degree/Days (ADD) are used to compensate for the constant variability in temperature that effects a body in an uncontrolled environment (257). The ADH is defined as the sum of the hourly temperature minus the minimum threshold (80). The ADD is defined as the average of the sum of the maximum daily temperature plus the minimum temperature minus the minimum threshold (166). In the calculation of accumulated degree/hours and degree/days, both 0ºC and 4ºC minimum thresholds were assessed (Fig. 25). The minimum threshold is the base temperature at which degradation ceases (140). While the amplicon data remains unchanged, the change in the X-axis corresponding to a decrease in degree hours may be relevant to real world PMI calculations.

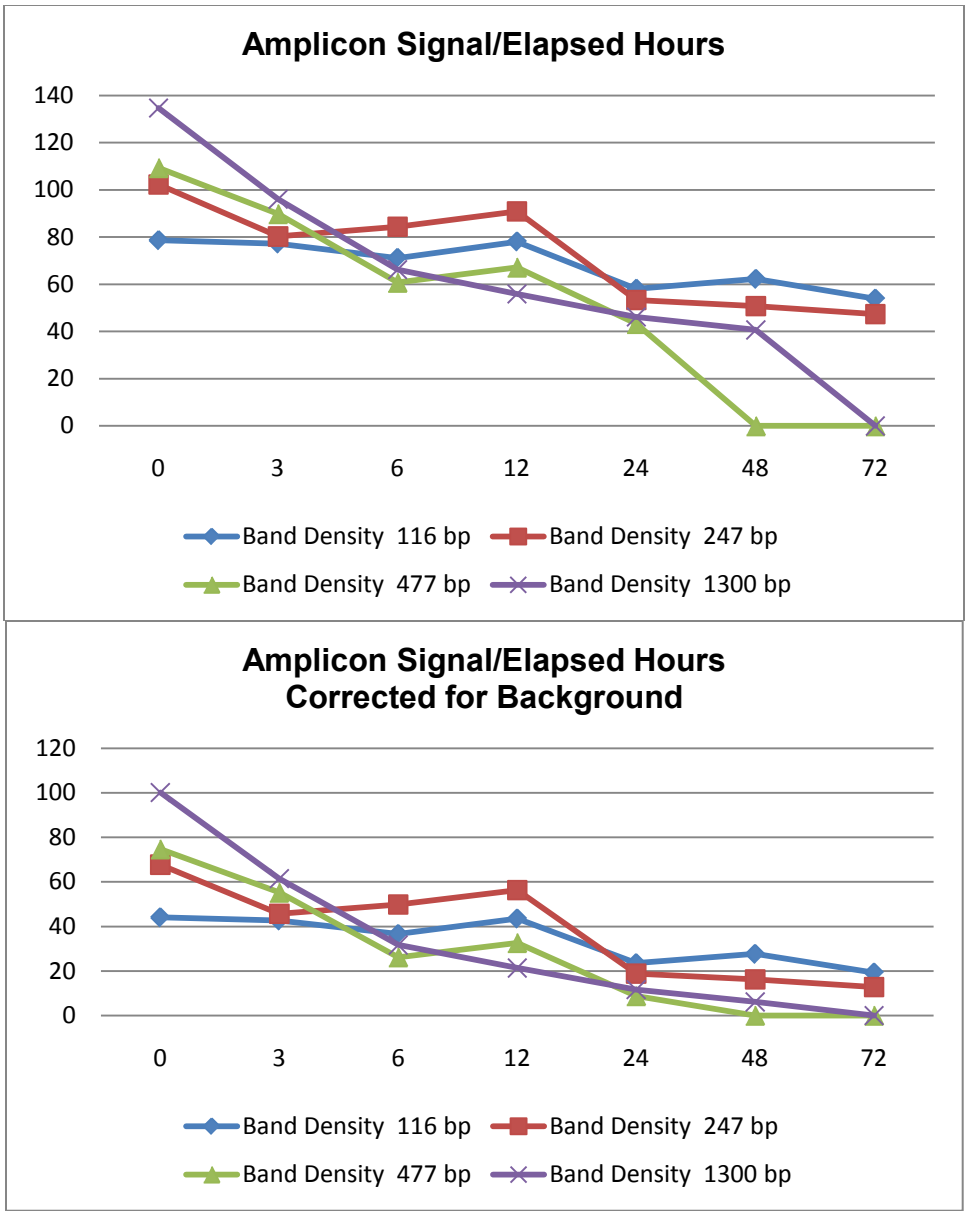

Fig. 24. Amplicon signal relative to elapsed hours. The top graph shows the decay in individual amplicon signal over 72 hours for data obtained on gel 08/26/09. The lower graph shows the same data corrected for background.

As noted in the visual inspection of the signal data, the total sample amplicon signal (sum of all lane amplicon signals) decreased as degree/hours increased. Additionally, individual amplicon signals decreased with larger amplicons (1300bp and 477 bp) showing the greatest decrease (Fig. 26).

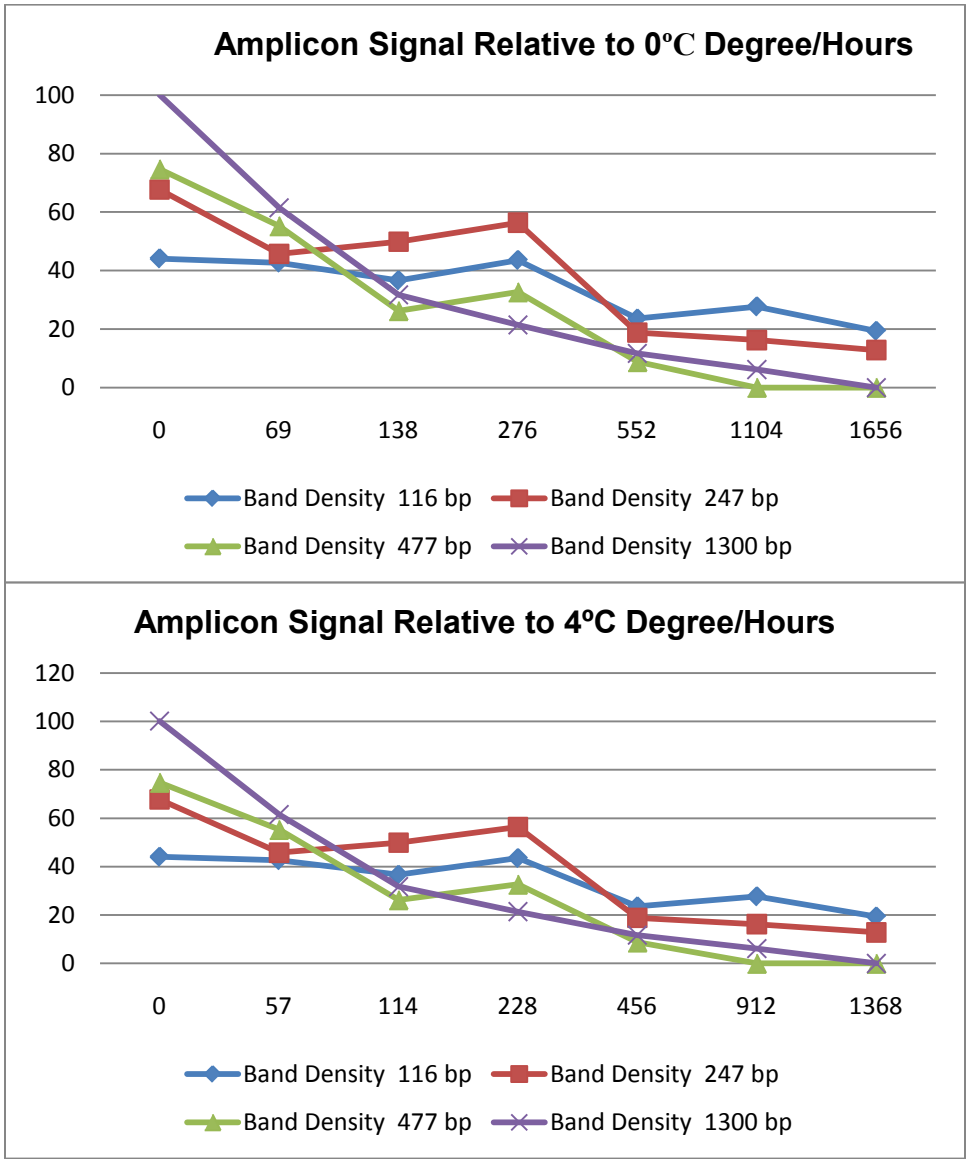

Fig. 25. Amplicon signal relative to degree/hours. The top graph shows the decay in individual amplicon signal relative to degree/hours assuming no minimum threshold for data obtained on gel 08/26/09. The lower graph illustrates the same data using a minimum threshold of 4ºC. The data points are the same, only the degree/hour values along the X-axis shift. Similar shifts were seen when calculating using degree day variants (data not shown).

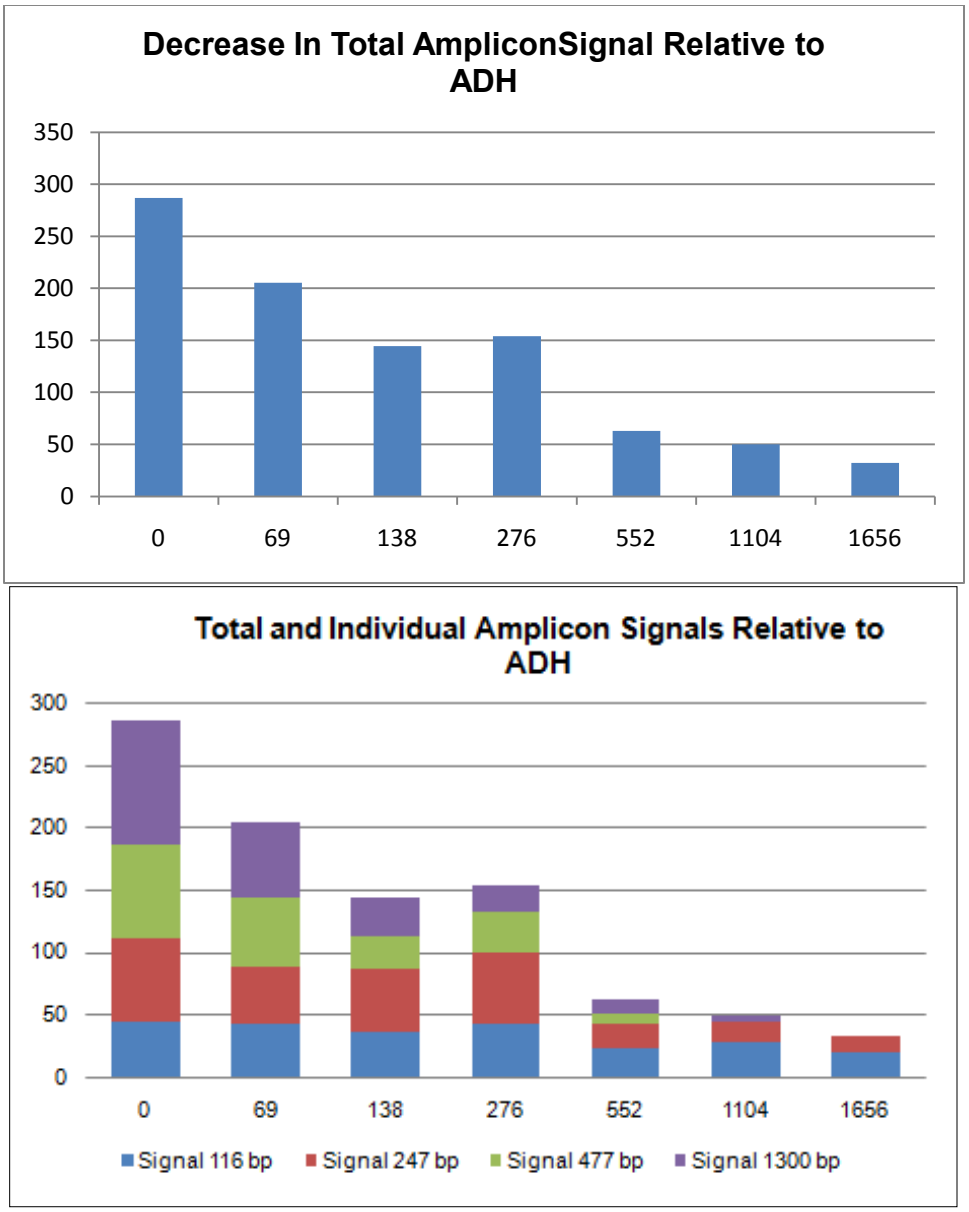

Fig. 26. Decrease in total sample signals. The top graph shows the decay in total sample signal relative to elapsed degree/hours for data obtained on gel 08/26/09. The lower graph shows a break out of the same data by individual amplicon signals with the total signal value along the X-axis.

During the course of this project, multiple approaches were attempted to ameliorate variability introduced during the testing. These included, but were not limited to, varying the amplification set-up procedures, varying quantification processes, varying load quantity, modifying pre-electrophoresis conditions and evaluating different

post-electrophoresis staining techniques. Regardless of the approach, some level of intensity variability, not attributable to amplicon signal decay remains.

In order to correct for this "uncontrollable" variability, it became necessary to develop a process to normalize amplicon signal data across all lanes. One approach assessed involved converting individual amplicon signal values from an RFU value to the proportion of the total RFU value for all amplicon values in the lane (Table 3).

TABLE 3. Normalization of amplicon signal. Individual amplicon signal was normalized by conversion to a fraction of the sum of the lane signal for data obtained on gel 08/26/09.

D/H	Signal 116 bp	Signal 247 bp	Signal 477 bp	Signal 1300 bp	Sum	116 bp Proportion of Lane Signal	247 bp Proportion of Lane Signal	477 bp Proportion of Lane Signal	1300 bp Proportion of Lane Signal
0	44	68	75	100	287	0.15	0.24	0.26	0.35
69	43	46	55	62	206	0.21	0.22	0.27	0.30
138	37	50	26	32	145	0.26	0.34	0.18	0.22
276	44	56	33	21	154	0.29	0.36	0.21	0.14
552	24	19	9	12	64	0.38	0.30	0.14	0.19
1104	28	16	0	6	50	0.56	0.32	0.00	0.12
1656	19	13	0	0	32	0.59	0.41	0.00	0.00

The sum of the transformed amplicon values within a lane, this totaled one. Data points for the transformed data were then graphed to determine which amplicons, if any, exhibited a predictable shift in the proportion of the total signal. The plot of the proportional signals (Fig. 27) shows that as was expected the 477 bp and 1300 bp amplicon proportional signals decreased as degree/hours increased, while the proportional signal of the 116 bp amplicon increased. Relative to those changes, the proportional signal of the 247 bp amplicon remained relatively unchanged relative to degree/hours (lower graph Fig. 27). These shifts are more apparent when the data from only two amplicons is included per graph (Fig. 28). It is important to remember that as

degree/hours increased the total amplicon signal decreased and that the increase in the 116 bp amplicon was only in proportion to the other amplicons making up the total signal. This is not unexpected since mathematically, as the contribution of the two large amplicon's signals decrease, the proportional contribution of the smaller amplicon's signals to the total increases even if the absolute signal for these amplicons decreases somewhat.

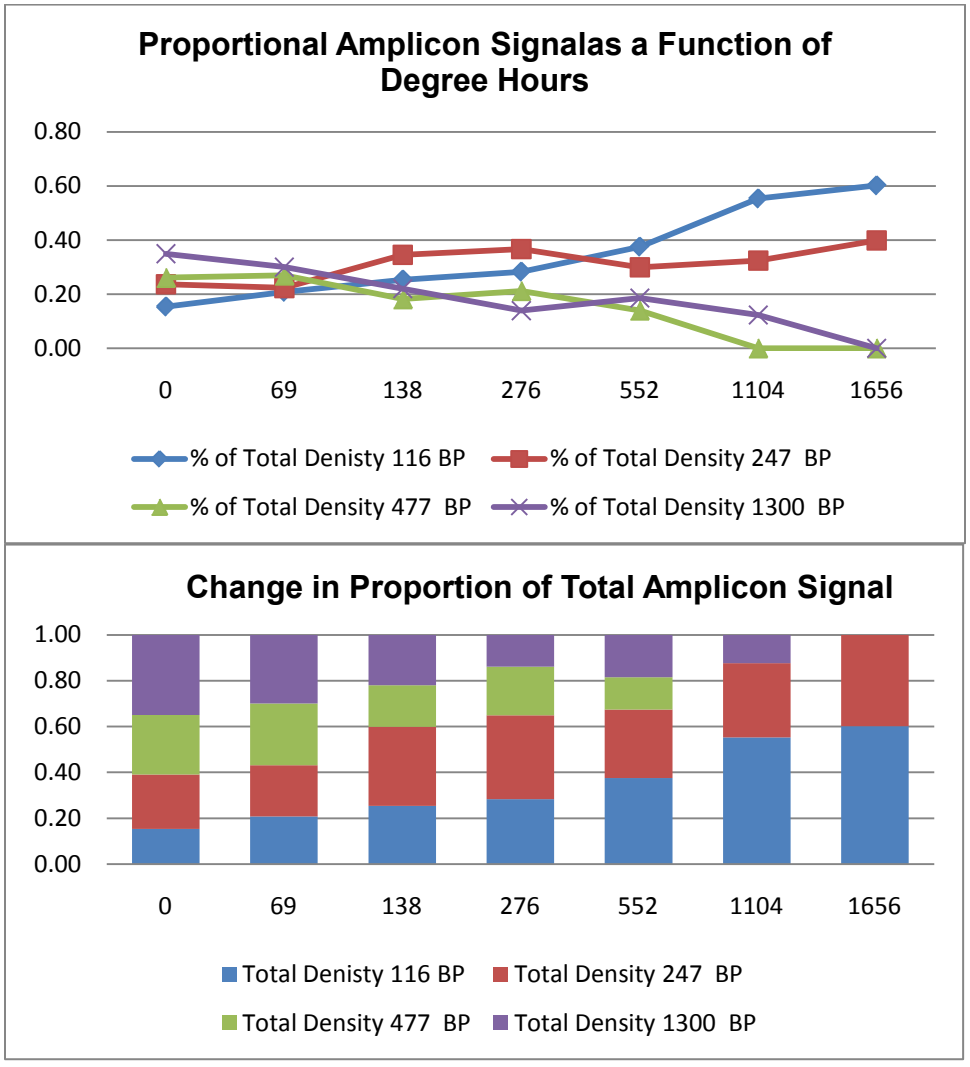

Fig. 27. Change in proportion of total amplicon signal as a function of degree/hours. To correct for variability in sample quantification/amplification, amplicon signals were calculated as a proportion of the total sample signal. The upper graph shows the change, relative to degree/hours, of the individual sample signals relative to the total lane signal for data obtained on gel 08/26/09. The lower graph shows the same data in

a slightly different format. The increase is as a proportion of the total sample signal which actually decreases as shown in the upper graph of Fig. 25.

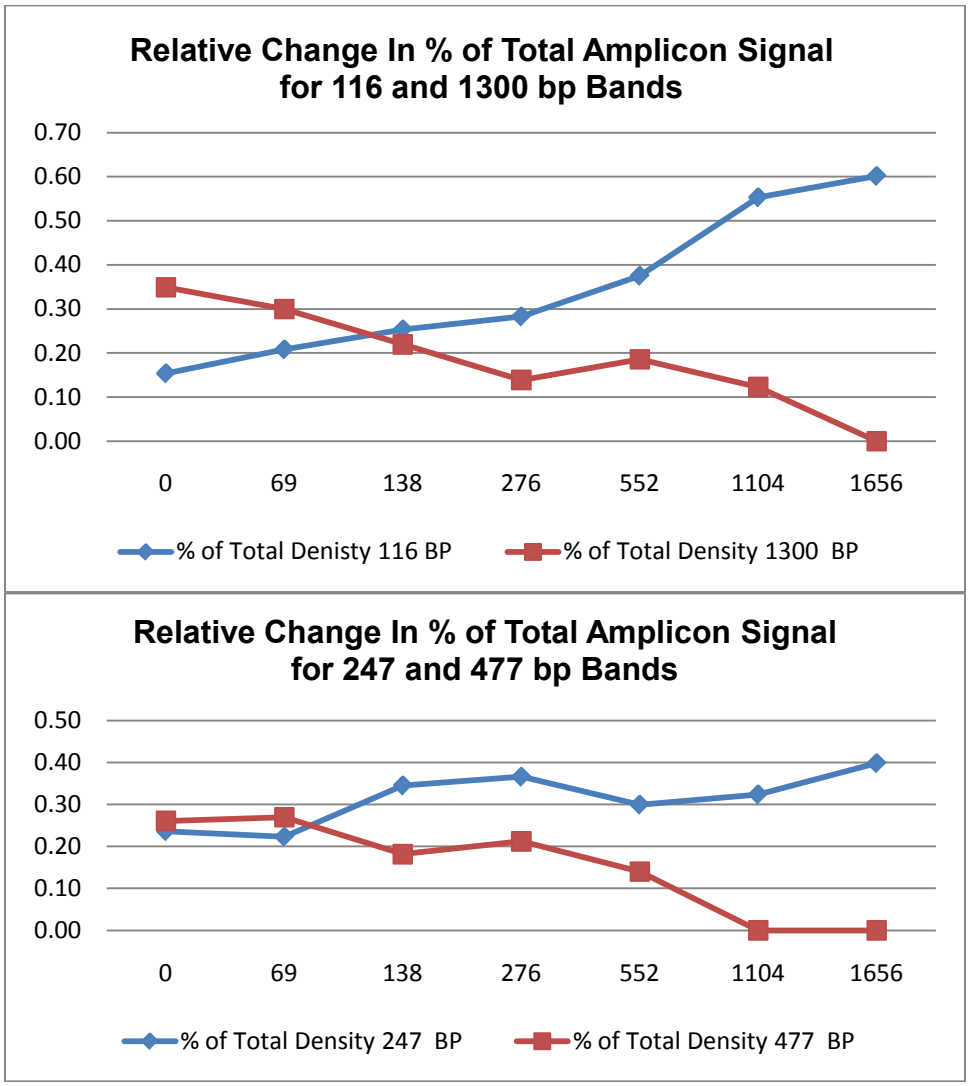

Fig. 28. Relative change in proportion of total amplicon signal. The upper graph from Fig. 26 has been broken out to more clearly illustrate the change in the proportion of the total sample signal. The upper graph shows the change, relative to degree/hours, of the signal values for the 116 and 1300 bp amplicons. The lower graph shows changes for the 247 bp and 477 bp amplicons for the same period. As noted in Fig. 26 the regardless of the direction of the proportional signal, the actual measured amplicon signals decrease as degree/hours increase.

This approach appeared to work as it corrected for differential amplification success between samples. However, this approach also proved to be confusing since even

though all absolute amplicon values clearly decreased relative to time, the corrected values for the smaller amplicons increased. To eliminate this issue other options for normalizing the data were explored.

As noted above, while the proportional signal of the 116 bp amplicon increased with incubation time, the actual amplicon signal decreased slowly, falling by about 55% over the course of the experiment. While this is a significant decrease, relative to the other amplicons it was the most stable data point (the lowest decay rate). Since the intensity of the 116 bp amplicon remained relatively constant over an extended period of time (relative to the changes in the other amplicon values), it was decided to use the 116 bp amplicon as an internal amplification control value to which all other amplicon intensities would be compared. Fig. 29 shows data where the relative amplicon signals were reported as ratios of the 116 bp amplicon signal in each lane.

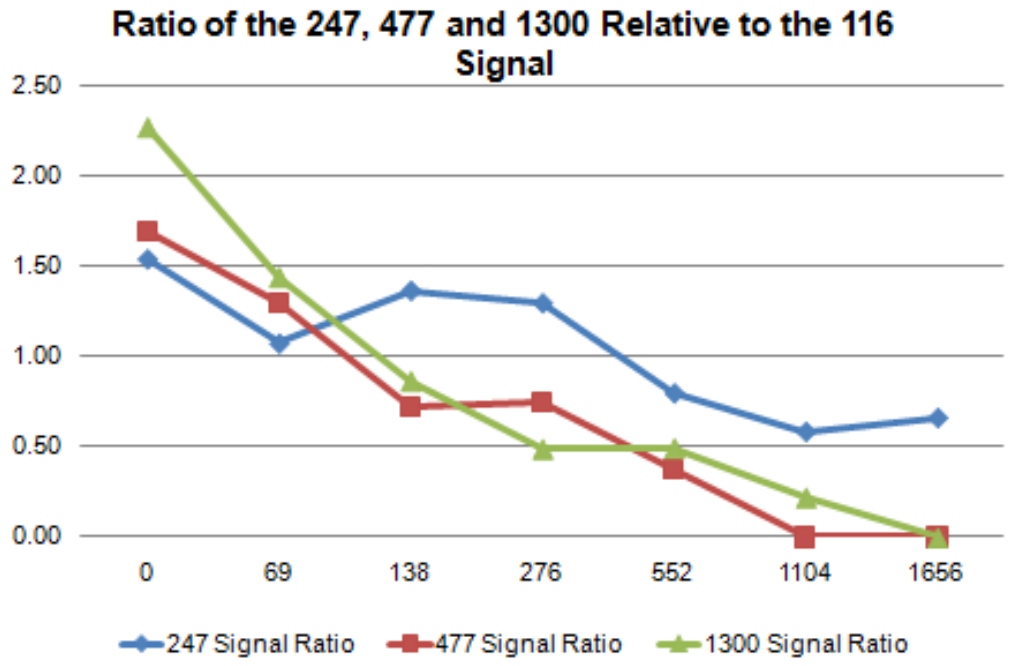

Fig. 29. Ratio of individual amplicon signals relative to the 116 bp amplicon signal. This graph shows the ratio of the 247 bp, the 477bp and the 1300 bp signals to the signal of the 116 bp amplicon within a sample lane for data obtained on gel 08/26/09.

Just as the normalization of the individual amplicon signal relative to the sample signal allowed the comparison of signal data from sample to sample within an experimental set; calculating the ratio of the amplicon signals for larger amplicons relative to the 116 bp amplicon provided a normalization of the data obtained from individual samples collected at different degree/hour points within a data set. Additionally, this more readily allowed for comparisons of data between data sets. When the raw amplicon signals were transformed in this manner, it became apparent that the 247 bp amplicon signal changes tracked very closely with those for the 116 bp amplicon. Although it is apparent that the 247 bp amplicon decays somewhat more rapidly than the 116 bp amplicon in data shown in Fig. 28, when the 247 bp amplicon values for multiple experiments was taken as a whole the difference in decay rates became less apparent, and less easily quantified (data not shown). It is possible that including the 247 bp amplicon ratio values, instead of, in addition to or averaged with the116 bp amplicon values might provide improved reproducibility to the overall signal decay pattern. However, for the purposes of this study it was felt that analysis of the 116 bp, 477 bp and 1300 bp amplicon signals provided sufficient information to address the underlying question posed for this project. Therefore, the 247 bp amplicon, though still amplified for all subsequent samples, has not been included in the data analysis reported here.

In order to compare amplicon signal decay patterns across data sets it was necessary to further normalize for variations in signal intensity. To do this, the values obtained for each of the elapsed degree/hour points of a data set were calculated as a ratio of the value obtained for the 0 degree/hour point. Therefore, the values for the 477 bp amplicon and 1300 bp amplicon at the 0 degree/hour point were each set to 1.

Subsequent data points were then normalized by calculating them as a ratio to the corresponding zero time point value. As with the previous normalization process, this normalization did not alter the actual decay profile, only the vertical scale (Fig. 30). When the 477 bp and 1300 bp amplicon signal decay curves were overlaid, it became apparent that their decay patterns were very similar (Fig. 31).

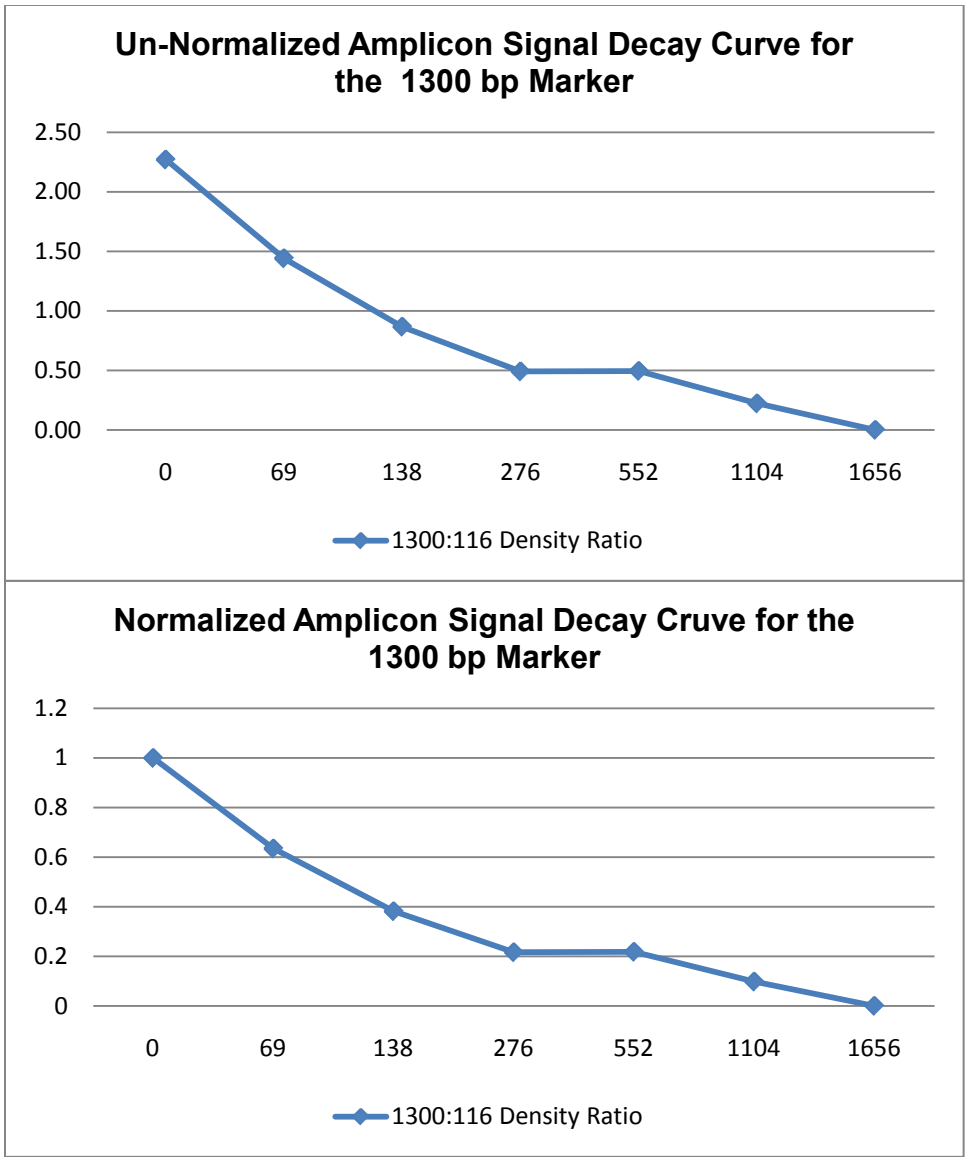

Fig. 30. Comparison of the un-normalized (top graph) and normalized (bottom graph) amplicon signal decay patterns for the 1300 bp amplicon. The top graph shows the un-normalized signal decay pattern of the 1300 bp amplicon relative to the signal pattern of

the 116 bp amplicon for data obtained on gel 08/26/09. The bottom graph shows the normalized data. The scale changed but the decay pattern remained constant.

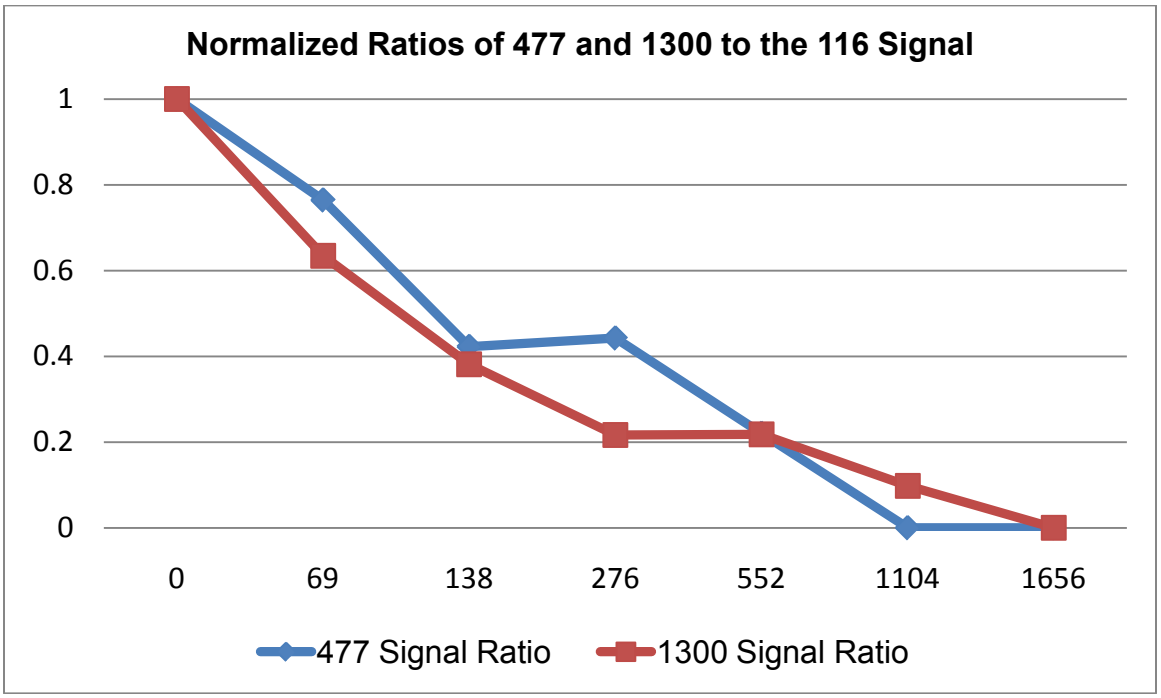

Fig. 31. Normalized ratios of the 477 bp and 1300 bp amplicon signal to the 116 bp amplicon signal. Normalized signal decay pattern of the 477bp and 1300 bp amplicons relative to the signal decay pattern of the 116 bp amplicon for data obtained on gel 08/26/09.

Once a means had been developed to minimize the effects of process variation (both within and across sample sets) by normalizing the data, it was applied to the balance of the signal data. Samples exposed to similar conditions and processing often produced consistent results with both the 477 bp and 1300 bp amplicons. The application of a logarithmic trend line was found to be helpful in comparing the data (Fig. 32 and 33). However, not all of the data sets showed this level of consistency and it was not uncommon for some sets processed in identical manners to produce dissimilar data (Fig. 34).

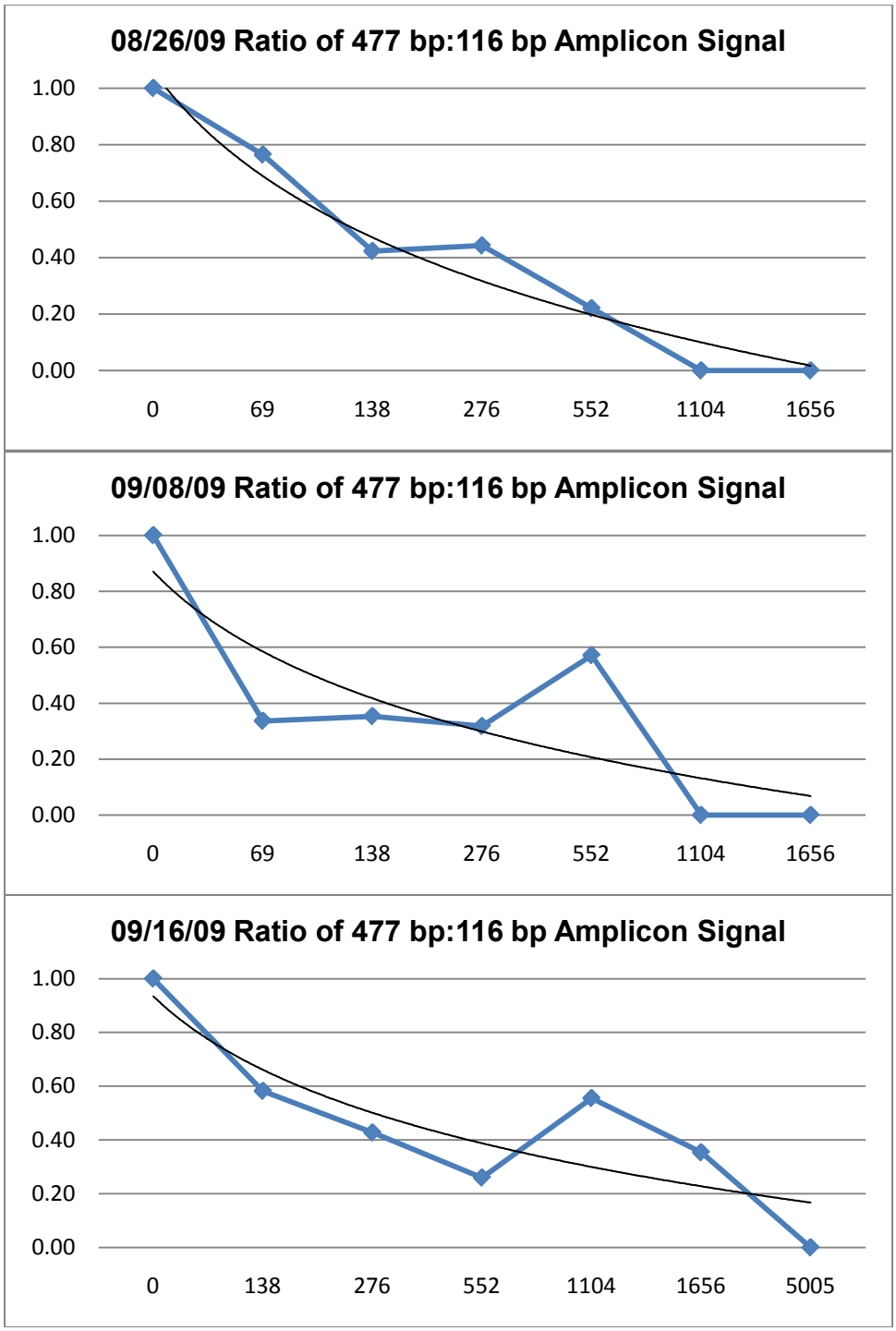

Fig. 32. Comparison of the ratio of the 477 bp:116 bp amplicon signal from 3 data sets. Ten nanograms of DNA were amplified from extracts of tissue specimens incubated at 23ºC.

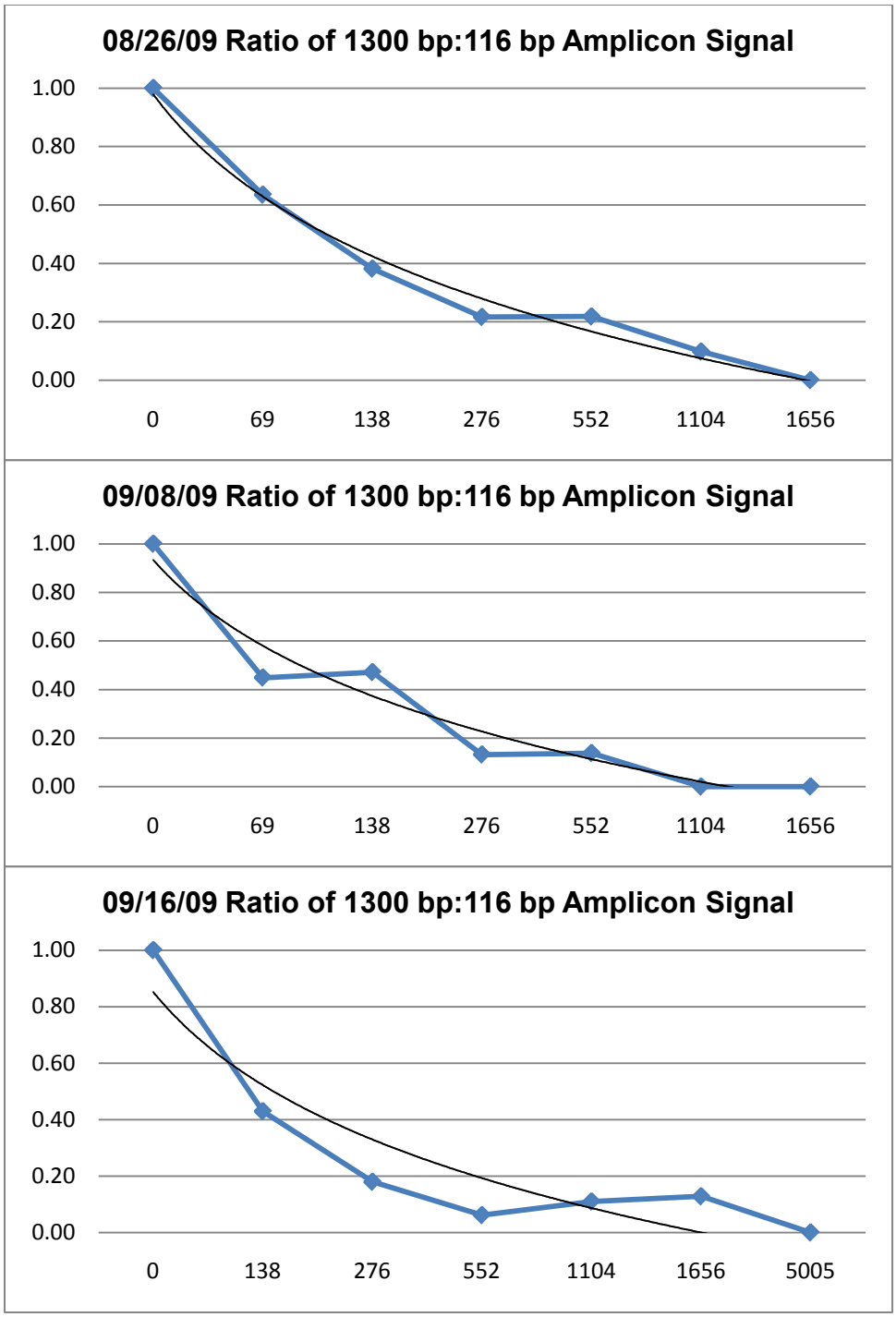

Fig. 33. Comparison of the ratio of the 1300 bp:116 bp amplicon signal from 3 data sets. Ten nanograms of DNA amplified from tissue incubated at 23ºC.

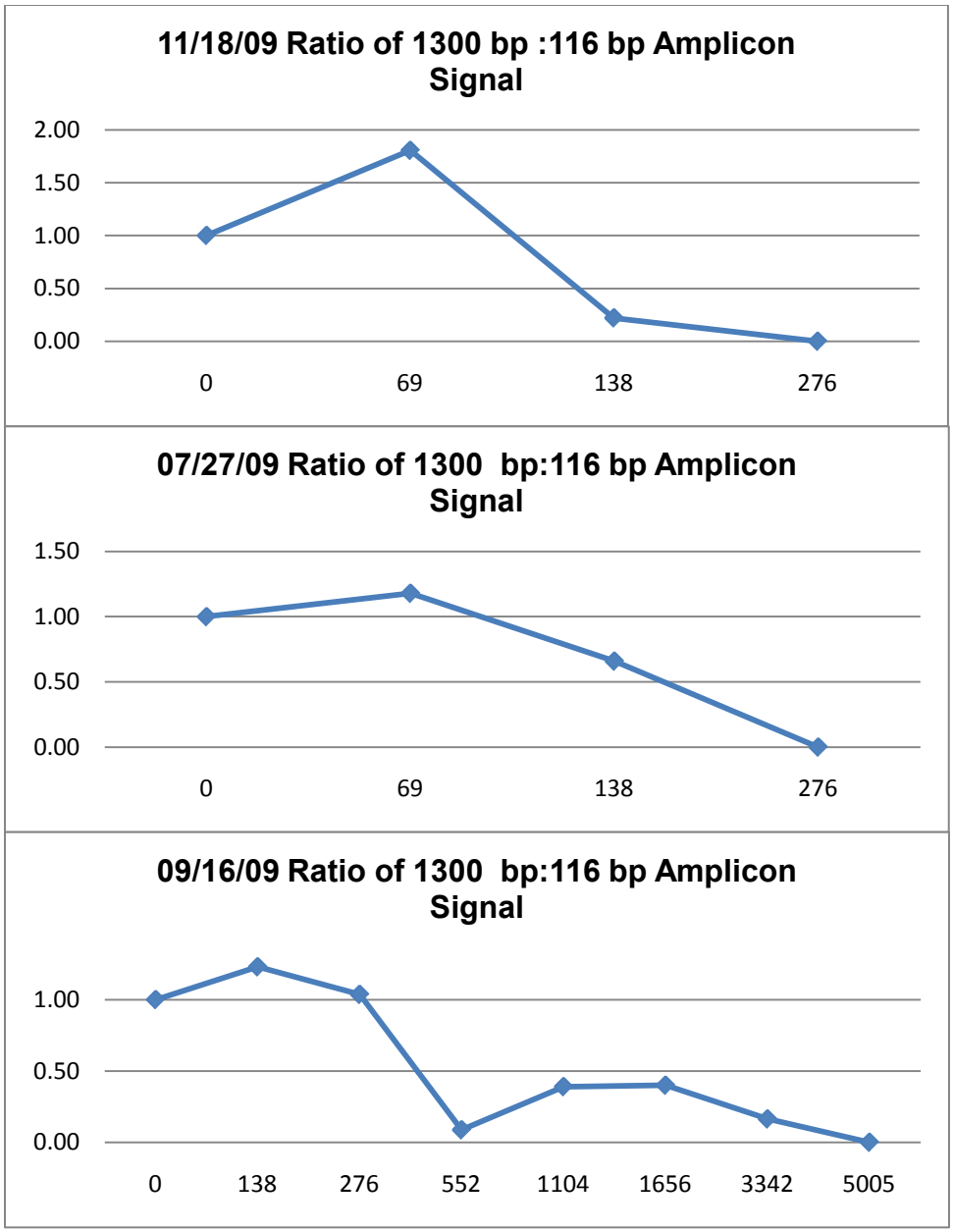

Fig. 34. Ratio of the 1300 bp:116 bp amplicon signal from 3 data sets. Ten nanograms of total DNA from tissue incubated at 13.6ºC (top graph). Twenty nanograms of DNA amplified from tissue incubated at 23ºC (middle graph). Twenty nanograms of DNA amplified from tissue incubated at 37ºC (bottom graph).

Plotting data produced by a similar treatment of all of the signal data demonstrated significant scatter (Fig. 35). A review of data from the individual sample sets exhibiting scatter indicated that one or more of a combination of factors likely

affected the data. Several sample sets were influenced by one or more data points exceeding the normalized value for the 0 degree/hour data point in that set.

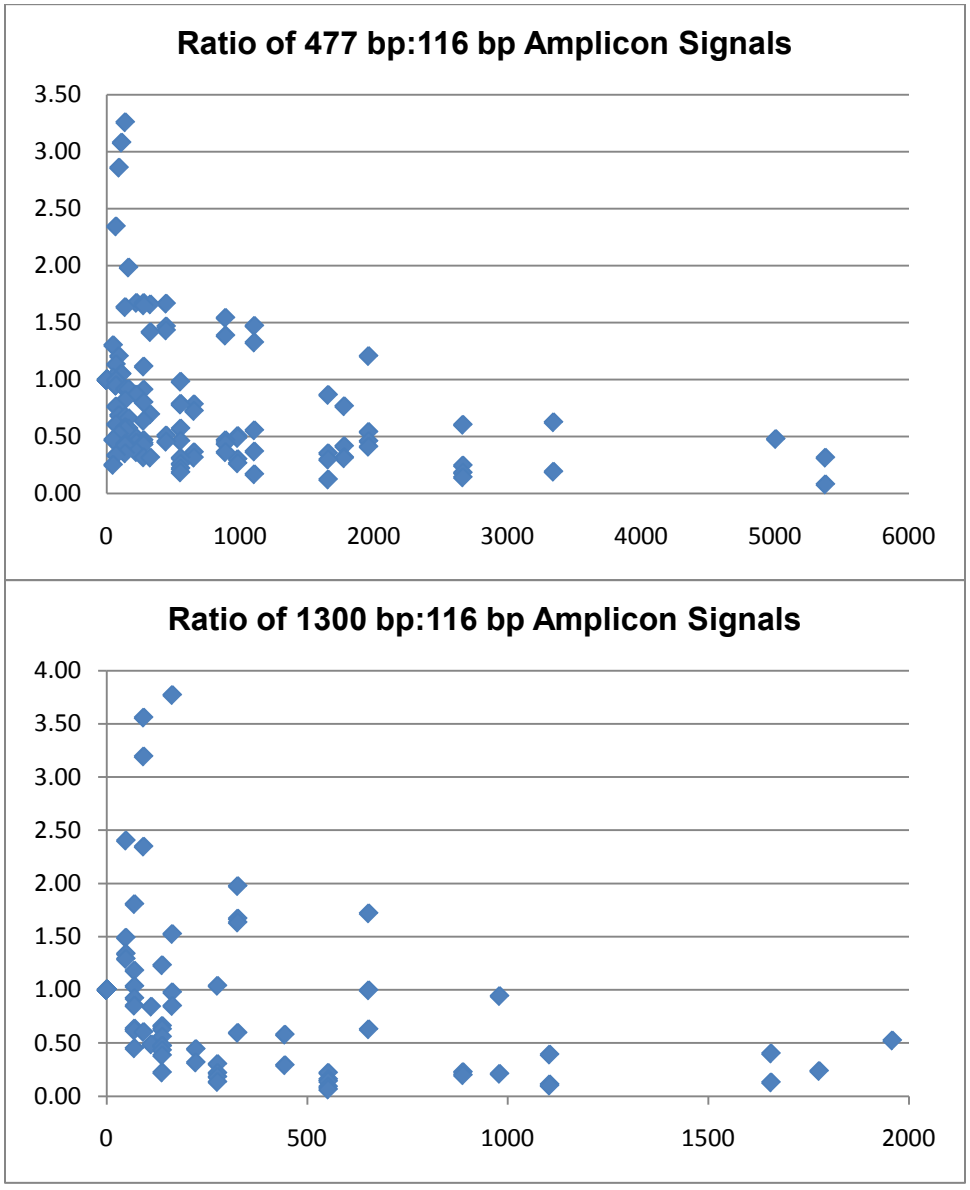

Fig. 35. Scatter plot of all of the 477 bp:116 bp and 1300 bp:116 bp amplicon signal data. Plot includes all ratio values from samples incubated at 13.6ºC, 23ºC and 37ºC and amplified using 10 or 20 ng total DNA.

In some instances, this was seen with both the 10 ng and 20 ng total DNA dilution for that set indicating that the likely contributor was a failure to adequately quantify the sample (i.e., all three graphs in Fig. 34). Signal ratio values for some data sets

appeared to decay at a faster degree/hour rate than observed with other data sets (i.e. the top and middle graphs in Fig. 34). There were several examples of samples incubated at 37ºC showing a potentially accelerated rate of signal decay indicating that there is a possibility that the rate of DNA degradation may be affected by temperature in a way that correcting for degree/hour may not sufficiently compensate for.

However, pooling and averaging select data sets suggests that may in fact be promise for this approach to provide data that would call for the development of a mathematical model that could prove suitable for assessing PMI with unknown degraded samples. For example, Fig. 36 uses averaged values from the data sets shown in Fig. 32 and 33. The logarithmic trend line was again used to provide a mathematical reference. The averaged data points closely follow the trend line indicating a relatively good fit. It is possible that processing more data sets under similar conditions would improve the data fit. However, more data sets may not be necessary. Additional focus on removing process variation may serve the same purpose by eliminating data points that fall outside the expected trend.

The totality of the data obtained using the CB5 amplicon set during the laboratory controlled portion of this project has not yet provided a clear-cut mathematical approach that could be used to quantitatively assess PMI. However, a portion of the data sets did show a straightforward trend of increasing DNA degradation with increasing degree/ hours with a logarithmic decay in the ratio of larger to smaller amplicons. The next phase of the project was to assess this primer set using tissue degraded under field conditions. To do this, three sets of sterile tissue cuttings, (two sets from Specimen #4 and one from Specimen #7) each weighing 0.1 g, were incubated in sealed

polypropylene tubes for 0-72 hours. Unlike laboratory controlled specimens, these samples were incubated outside with no measures taken to maintain a constant ambient temperature.

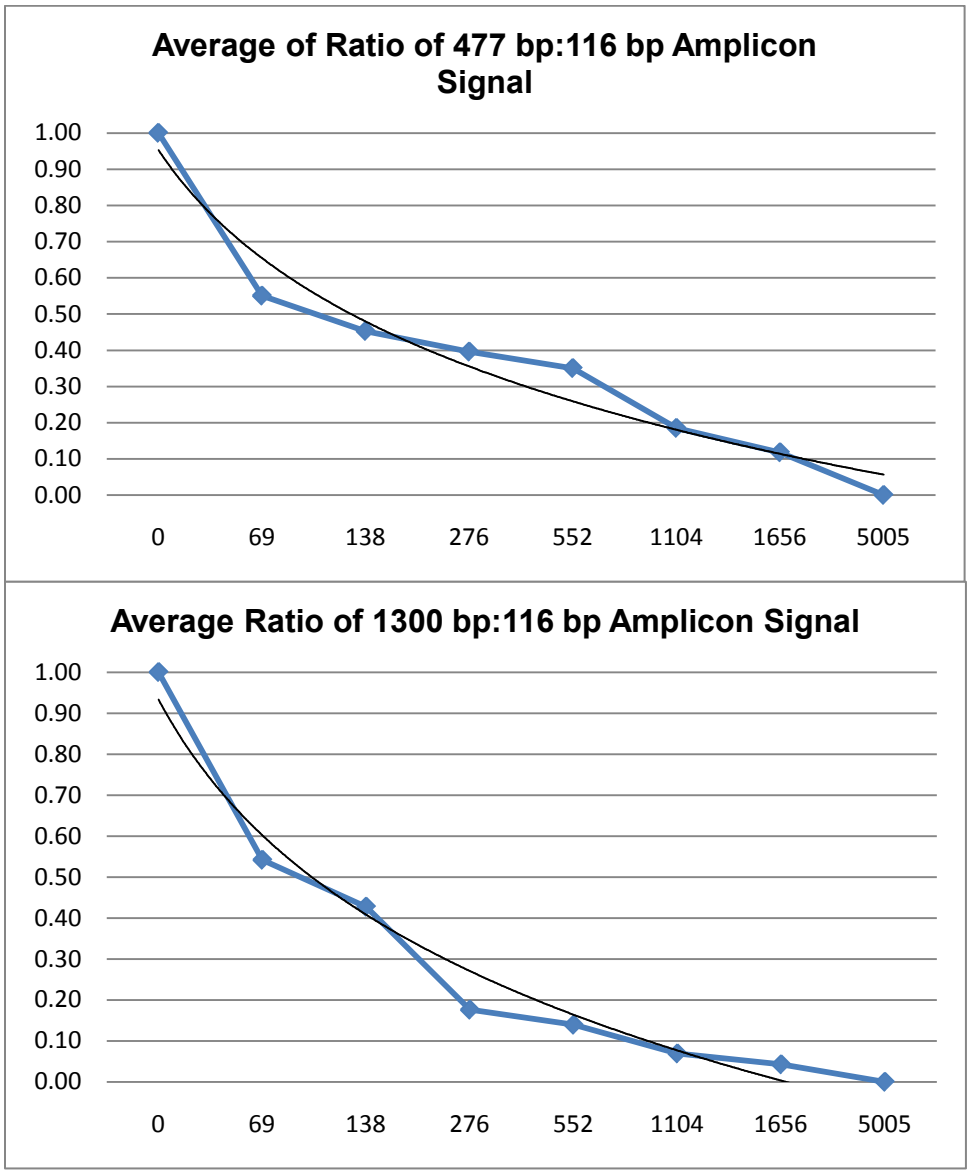

Fig. 36. Average of the ratio of the 477 bp:116 bp and 1300 bp:116 bp amplicon signal from 3 data sets. Ten nanograms of DNA amplified from tissue incubated at 23ºC.

Once processed, 20 ng total DNA from each specimen extract was amplified using the CB5 primer set. The amplicon profile from all three sets showed a shift in amplicon

intensities consistent with the profile intensity shifts seen with laboratory controlled specimens (Fig. 37). The signal values were averaged and normalized as outlined above (top graph Fig. 38).

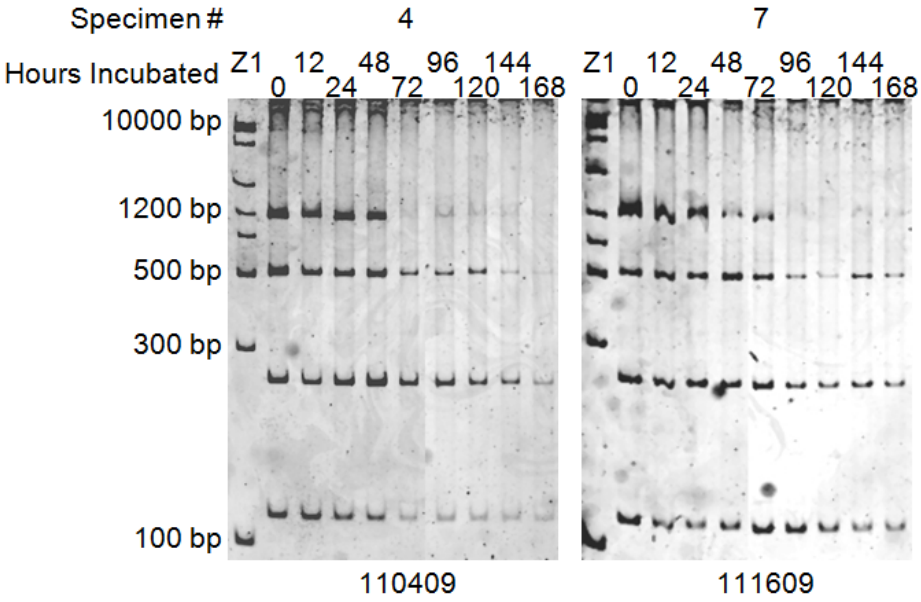

Fig. 37. Electrophoresis of DNA from field controlled tissue degradation samples amplified with primer sets CB5 R1 – R5. One hundred milligram cuttings from Specimen #4 and #7 were incubated outdoors at temperatures ranging from 11°C to 22°C (average 16°C) for 0 – 168 hours. Each DNA extract was amplified targeting 20 ng total DNA separately with primer sets for amplicons CB5 R1 – R5. One microliter of each amplicon was combined into a single load sample and mixed with 5X loading dye and loaded in the designated lane. One microliter of ZipRuler™ Express DNA Ladder 1 (50 ng/µL) was loaded into lane 1. The 8% N-PAGE analysis was performed at 400 volts for 80 minutes.

As with the laboratory controlled specimens, scatter was seen with this data. However, once removing 3 of the 9 data points, the signal decay pattern was very close to that seen with the optimal laboratory controlled specimens (lower graph Fig. 38). Trend lines were fitted as above for comparison purposes. Although this approach may seem somewhat arbitrary, data manipulation processes such as Winsorizing (limiting the influence of outliers by replacing them with the observations closest to them) and trimming (excluding a set percentage of outliers) are both accepted practices when

dealing with extreme outliers (229).

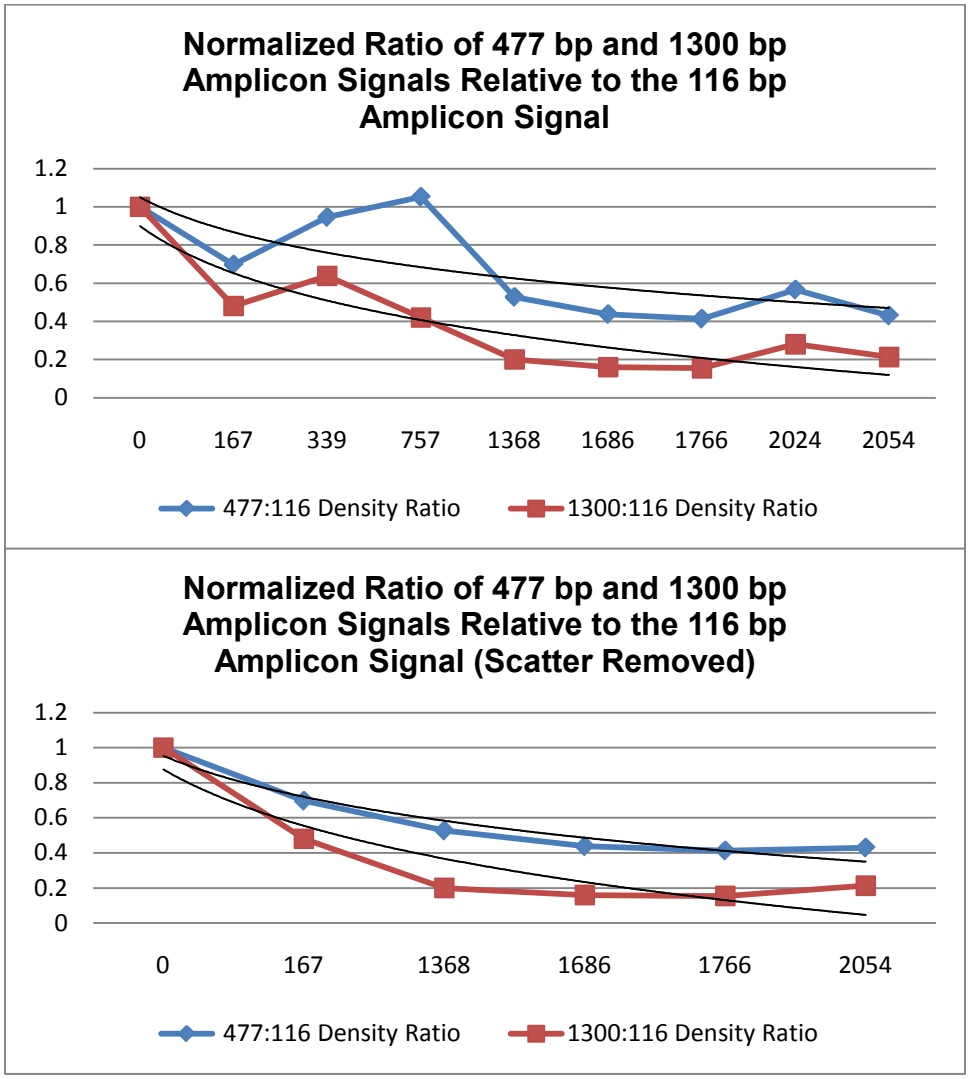

Fig. 38. Ratio of Individual amplicon signals relative to the 116 bp amplicon signal (Field Controlled Incubation). The upper graph shows the averaged ratios of the 477 bp and 1300 bp relative to the 116 bp amplicon signal from the field controlled specimens (20 ng total DNA amplified). The lower graph shows the same data with the outliers at 339, 757 and 2024 degree/hours trimmed.

The original intent of this project was to determine if DNA degradation could be used as an indicator of time since death. It was hoped that correcting for degree/days or degree/hour would allow specimens degraded under controlled field conditions to be compared to samples degraded in the laboratory under controlled conditions. As

discussed previously, trends were observed in the laboratory controlled data. However, excessive scatter made comparisons of field data to the pooled and averaged laboratory data difficult. In order to facilitate a comparison it was decided to select, plot and generate logarithmic trend lines for a single data set incubated at each laboratory controlled temperature and the averaged data from the field samples (Fig. 39).

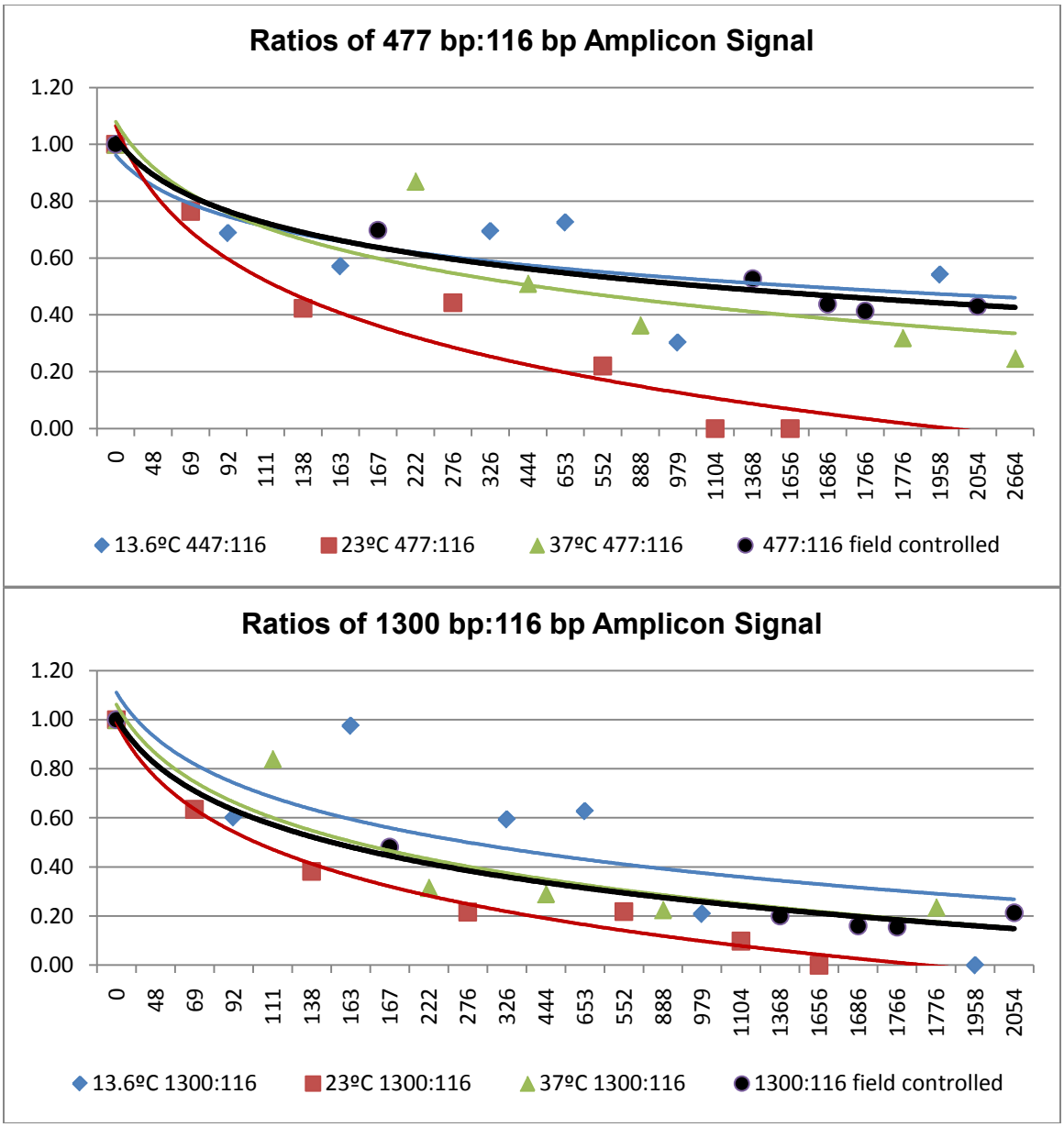

Fig. 39. Comparison of laboratory controlled specimen and field controlled specimen signal data. Logarithmic trend lines obtained for field data (black line), and laboratory control data (blue, gold and red).

In the theory, the decay of the amplicon signals plotted by degree hours should be the same for 13.6ºC, 23ºC and 37ºC and the field data sets. Encouragingly, logarithmic trend line produced for field data fit within the trend lines produced for both the 13.6ºC and 37ºC laboratory control data. However, it appears that the DNA in specimens incubated at 23ºC degraded at a faster rate than the specimens incubated under other conditions. This difference in the amplicon decay rate remains unexplained and requires additional investigation.

Based on the strength of the results obtained with the field controlled samples, the CB5 primer set was used to assess DNA extracted from samples collected from an intact animal decomposing under uncontrolled field conditions. The intact carcass (designated Specimen #1) was placed in a cage designed to prevent disarticulation by large scavengers but not limit insect succession or environmental insult. Tissue samples were collected every 24 hours from 07/24/04 – 08/28/04 and preserved as noted above. DNA extracts from specimens collected from 0 – 240 hours were amplified using the CB5 primer set and many but not all of the samples tested up to 144 hours produced measurable amplicon signal values (Fig. 40). As with the field controlled specimens, 477 bp and 1300 bp amplicon signal data produced from the intact animal field specimens was normalized and plotted (Fig. 41). Trend lines produced from this data were then compared to the laboratory data set used for the Fig. 39 comparison (Fig. 42). Unlike the field controlled specimens, the intact animal field specimens did not fall within the trend lines plotted from signal data produced from the laboratory controlled specimens. There are several possible explanations for why the intact field specimens plotted above the laboratory controlled specimens.

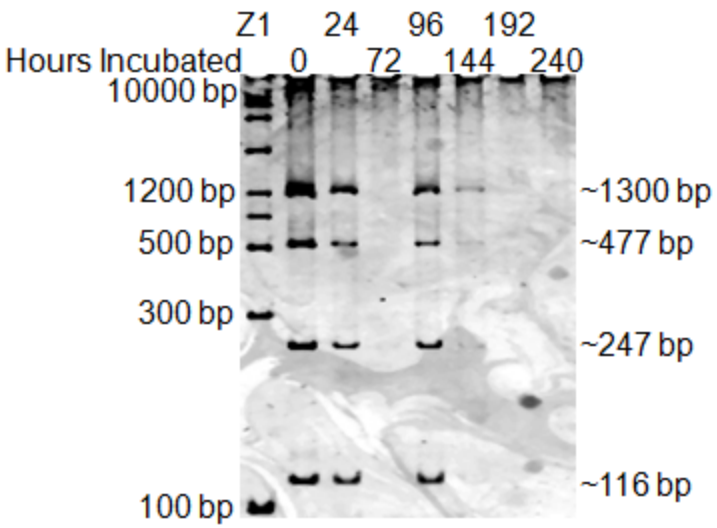

Fig. 40. Electrophoresis of DNA from field uncontrolled tissue degradation samples amplified with primer sets CB5 R1 – R5. Specimen #1 was incubated outside in temperatures ranging from 11°C to 22°C (average 16°C) for 0 – 168 hours. An eighty milligram cutting from each tissue collection was extracted. Each DNA extract was amplified targeting 20 ng total DNA separately with primer sets for amplicons CB5 R1 – R5. One microliter of each amplicon was combined into a single load sample and mixed with 5X loading dye and loaded in the designated lane. One microliter of ZipRuler™ Express DNA Ladder 1 (50 ng/µL) was loaded into lane 1. The 8% N-PAGE analysis was performed at 400 volts for 80 minutes.

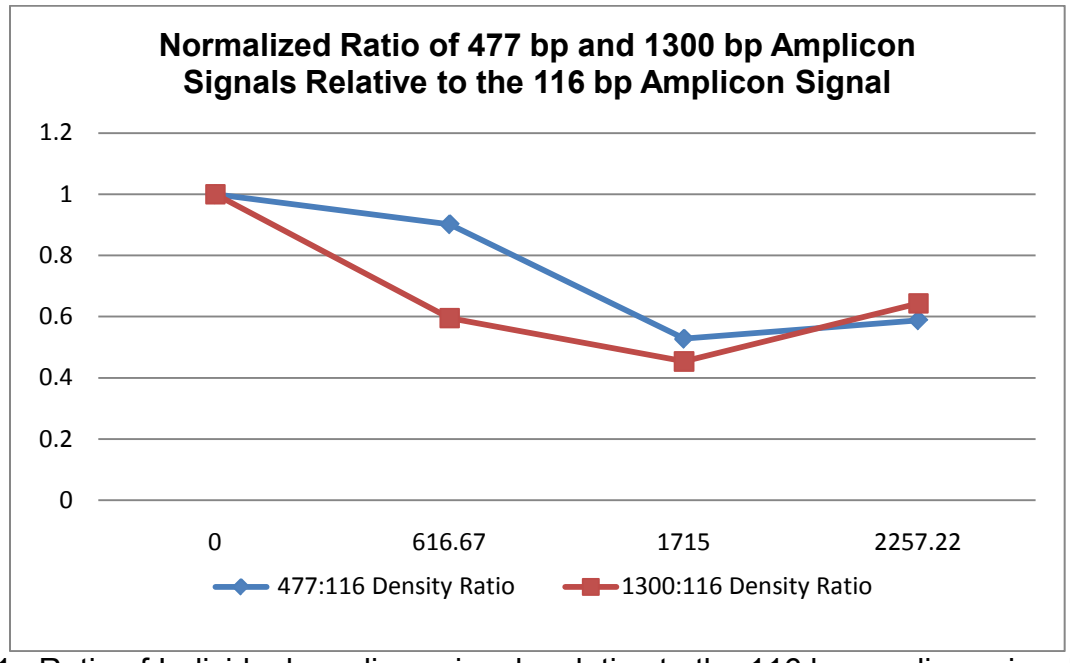

Fig. 41. Ratio of Individual amplicon signals relative to the 116 bp amplicon signal (Intact Animal Field Specimen). This graph shows the ratios of the 477 bp and 1300 bp relative to the 116 bp amplicon signal from the intact animal field specimen.

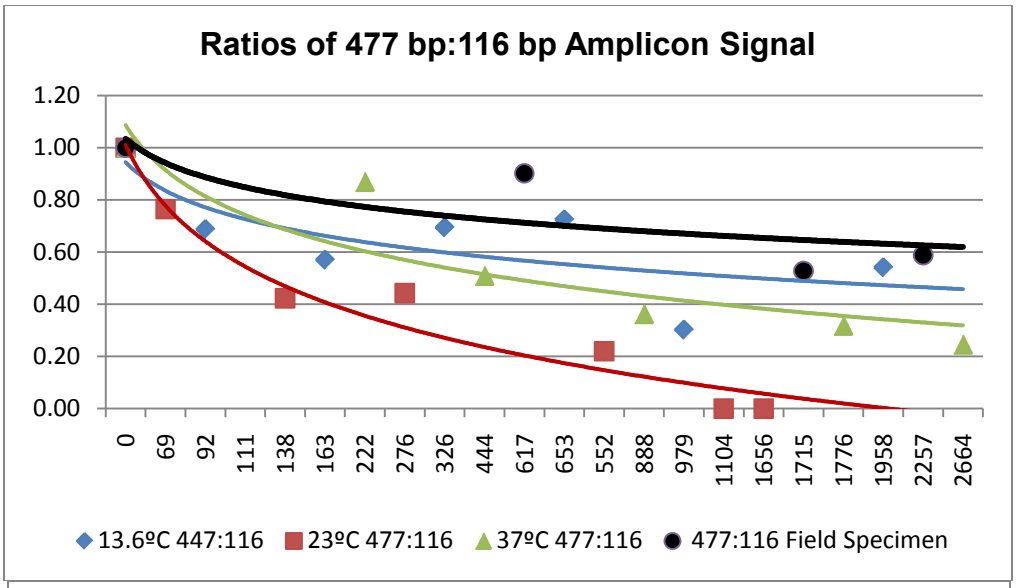

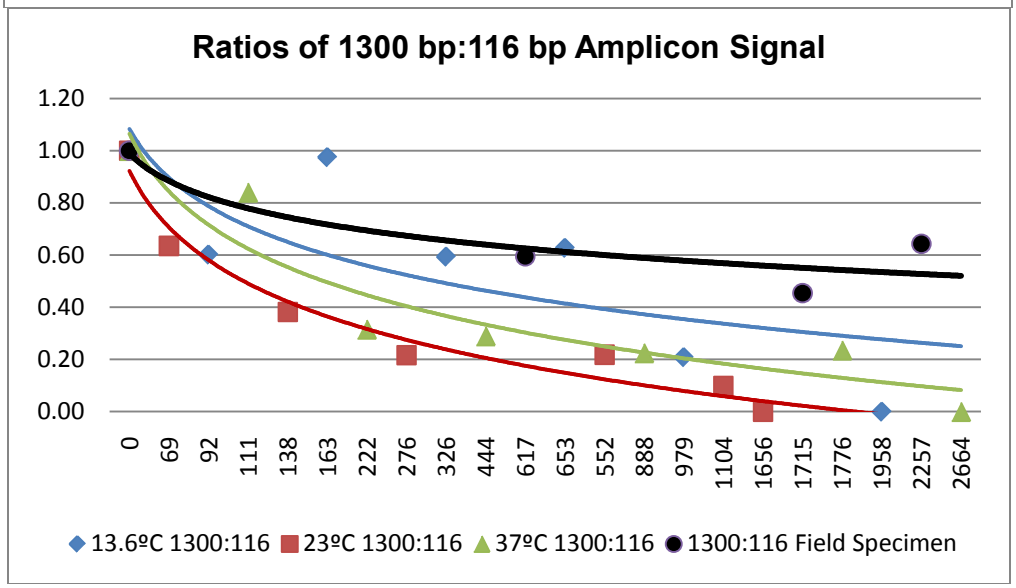

Fig. 42. Comparison of laboratory controlled specimen and intact animal field specimen signal data. Logarithmic trend lines obtained for field data (black line), and laboratory control data (blue, gold and red).

The intact field animal was exposed to the environment while the laboratory samples were sealed in polypropylene tubes. Just as exposure to the environment could have resulted in surface drying of the intact field animal resulting in the retardation of DNA degradation; sealing tissue plugs in a tube likely resulted in elevated humidity potentially leading to increase in the DNA degradation rate.

CHAPTER 4

CONCLUSIONS

Determining the time since death can provide critical information to the individuals charged with investigating that death. Depending upon the circumstances, an accurate assessment of the Post-Mortem Interval (PMI) can provide the information necessary to differentiate an ancient death from a modern death; offer clues to the identity of the victim or suspect; and establish or demolish a suspected perpetrator's alibi.

There are two common strategies or approaches for assessing PMI. The first of these approaches are the concurrence based methods. Concurrence based methodology is based on examining things associated with the deceased that occurred at a known time or can be limited to a specific period (I.e. clothes from the 1950s on a skeleton or a dated ticket stub in the pocket). There are circumstances where concurrence based methods can provide definitive information regarding the PMI (i.e. a dry body on a lawn watered one hour before discovery, stopped watch on a jumper's body, etc.). However, as this type of information is often not available, concurrence based methods often cannot provide sufficient information to narrow the PMI to within hours of the actual death. It is for this reason that so many individuals, in so many different forensic disciplines have focused on developing rate-of-change methodologies to estimate PMI. Measuring the changes associated with a process that initiates or terminates with death and proceeds at a known rate provides the potential for narrowing the PMI estimate to a range of a few hours. Presumably, a sufficiently precise method could narrow PMI estimates even more. As discussed in the Introduction, all rate-of-

change methods have limitations and are subject to influences that the forensic investigator may be unaware of. It is for these reasons that any investigator relying on a rate-of-change method for PMI estimation must acknowledge its limitations and take steps to account for potential sources of variability. It was with these issues in mind that this project was undertaken.

Summary of Findings

During the course of this project two types of polymerase chain reaction (PCR) based-assays were considered for use. Both use fragment size analysis (FSA) PCR amplification of target loci to assess DNA degradation in tissue samples. In each case, the level of DNA fragmentation is then used to estimate time since death. Both randomly amplified polymorphic DNA (RAPD) analysis and directed PCR amplification were used to estimate the level of genome degradation by measuring the shift in the amplicon profile (presence and/or intensity of individual amplicons in the control profile) as a function of time. In order to determine their suitability, prospective markers were evaluated to verify that they exhibited sufficient specificity, sensitivity, reproducibility, and degradation-based variability. The assay that was determined to best meet these criteria was used in a subsequence study specimens degraded under a variety of laboratory and field controlled and uncontrolled conditions.

RAPD analysis was initially considered the most appropriate type of analysis for consideration. It was felt that RAPD analysis' use of short non-specific primers and low annealing temperatures, used to promote random DNA binding, provided a straightforward and uncomplicated approach towards examining degraded DNA.

Random binding of the RAPD primers also eliminated the need for species specific sequence data in the early development stages of the assay. Additionally, the distribution of product amplicons from a set of primers could be driven toward a preponderance of larger or smaller fragments through temperature variation.

Nine separate RAPD primers were evaluated to determine if they met the necessary criteria outlined above. Of the nine primers assessed, six either failed to produce a sufficiently balanced or "spread" of profile bands (arbitrarily set at 200 bp for the preferred smallest amplicon to 1500 bp for the largest with relatively similar stained amplicon intensities) to advance them for further consideration. The three primers that were selected for additional evaluation produced relatively balanced profiles with an acceptable size range of profile amplicons. Profile polymorphism between individuals would not be acceptable for the purpose of this study and when tested, only two of the remaining three proved sufficiently monomorphic to make intra-specimen comparisons possible. However, one of the two did not successfully amplify all samples and was thus not advanced for final consideration. This left a single RAPD primer (p9) from the original nine that was found to produce an acceptable spread of balanced intensity bands and to exhibit good amplicon reproducibility between unrelated individuals. However, subsequent studies revealed p9 to be insufficiently sensitive, requiring a minimum of 30 ng for successful amplification. While there is no set requirement for sensitivity, most forensic assays target less than 10 ng total DNA for amplification and it was felt that the requirement for 30 ng would make a primer unviable in a forensic setting.

Thus, while RAPD analysis in principle would appear to have strong potential for

assessing degraded DNA samples, the data obtained using these nine primers revealed several limitations that would need to be overcome before this approach could be further evaluated in this capacity. In general the successful RAPD amplification, like all PCR amplification, is susceptible to the quality of the DNA extracted. Additionally, the sensitivity issues, the inability to moderate individual profile band intensity by adjusting reaction components, the general complexity of the RAPD profiles obtained and the generally recognized difficulty in standardizing RAPD analysis contributed to eliminating RAPD analysis for further consideration at this time. One final weakness of using RAPD amplicons for this purpose stems from the fact that the genomic location of individual amplicons in a RAPD location is unknown. Some may be in euchromatic regions while others could be located in heterochromatic regions. Since euchromatin and heterochromatin are degraded at different rates due to accessibility to the nucleases, this would simply add another variable into the process of interpreting results.

After it was determined that a non-specific amplification approach would not provide the data necessary for this project, it was decided to focus on directed PCR amplification of specific genes or fractions thereof. Directed PCR amplification, while requiring more focus on primer design and optimization, allowed for more control over amplicon size and intensity. It was felt that by balancing amplicon intensity, direct comparisons could be more readily and reliably made between larger and smaller amplicons.

The first directed PCR amplicon set considered was selected to amplify regions of the group-specific component (GC), a serum protein involved in the vitamin D-

pathway. GC was considered before other possible directed PCR amplicons because its analysis has been used for forensic applications in the past (61). The sequence of the gene had also already been determined for our chosen model organism, making primer design a much simplified process.

Initial GC primers were designed using published *Sus scrofa* DNA sequence. The expected amplicon sizes were ~55 bp, ~242 bp, ~479 bp, ~764 bp and ~993 bp. Following laboratory amplification, the amplicon GC5 had a measured length of ~55 bp. However, amplicons associated with primer sets GC1-4 (the larger amplicons) were not as expected. In the case of GC4, an amplicon was obtained that was significantly larger than anticipated (~400 bp). Primer sets GC 1-3 either failed to successfully amplify or produced amplicons outside the resolution range of the N-PAGE analysis system selected for this study. The GC primers were designed based upon a published cDNA, not genomic, sequence (at the time, all that was available). Although the precise reasons for the "enlarged" GC4 amplicon and the inability to assess GC1-3 amplicons were not elucidated, the most likely explanation was considered to be an unpublished large intron between the GC4 and GC3 annealing sites that shifted the amplicon sizes substantially up in molecular weight and a small intron within the GC4 amplicon. In the absence of available genomic sequence it was decided to eliminate the GC locus from consideration. Completing a sequence analysis of the larger amplicons would be necessary to allow for new primer design and this was deemed unnecessary considering the fact that other potential directed amplification loci were available. However, based on this experience it was decided to focus further directed PCR amplification efforts only on loci for which genomic DNA sequence data was available or

for which genes encoding published cDNAs had been previously determined to be intron free.

The next directed PCR amplification locus evaluated was the gene encoding mitochondrial cytochrome b protein. The cytochrome b gene product is involved in the electron transport chain in mitochondrial oxidative phosphorylation. Cytochrome B was selected because it is a mitochondrial gene that has been well characterized in multiple species. This allowed for the selection of several amplicons that had been previously applied for other applications or were known to be intron free. Additionally, the mitochondrial origin of the gene meant that there would be multiple copies of the gene in every cell, ensuring a sufficiently abundant DNA target to guarantee very high sensitivity for the assay.

Initial investigations using amplicons CB L1-3 (all located within the cytochrome b gene) yielded expected amplicon profiles in the 250-700 bp range that showed exceptional specificity with little or no production of non-specific amplicons. Additionally, the CBL 1-3 amplicon set was reproducible across unrelated animals and showed a reproducible degradation of the amplicon profile when amplified using enzymatically digested DNA. However, it failed to show the same degradation-based changes in the amplicon profile when DNA from “real world” samples was amplified (no variability across a 100-fold dilution of substrate DNA). It was felt that this was likely due either one or both of two properties of mitochondrially encoded genes. The mitochondrial genome exists as multiple copies per cell, up to 100’s or even 1000’s per cell. High numbers of initial target might act as a “pre-amplification”, resulting in actual amplification reaction saturation. Alternatively, isolation of the chromosome in the

double membrane-bound organelle might provide the DNA with a degree of protection from cellular nucleases released upon death, giving mtDNA a much slower rate of degradation when compared to the breakdown of nuclear-encoded genes. The mitochondrial amplicon set may be useful for a long term degradation study. However, the lack of change in the amplicon profile with short term degradation samples made the system unsuitable for use in this project at this time.

Cytochrome b5A is a nuclear-encoded gene and, like the mitochondrial cytochrome B gene, encodes a trans-membrane protein. However, unlike the mitochondrial cytochrome B gene, the cytochrome b5A is located in the nucleus, is not as well preserved across species and has not been studied to the same extent as its mitochondrial counterpart. As a point of further interest, the CB5 gene product had been previously studied as a protein marker for assessing time since death. Most importantly, due to its involvement in the 16-androstene steroid pathway, the gene sequence in *Sus scrofa,* a primary food animal, was available (24).

Initial experiments using the CB5 R1-4 amplicon primer sets produced specific, reproducible amplicons ranging in amplicon size from CB5 R1 with a size of approximately 116 bp, to CB5 R2 with a size of 247 bp, CB5 R3 with a product of 477 bp and CB5 R4 with an expected amplicon of 999 bp. However, in the case of CB5 R4, amplification yielded an amplicon that reproducibly sized approximately 300- bp larger than the expected size, about 1300 bp. As was seen with the GC amplification products this was likely due to the presence of an unpublished intron. Although we had focused on amplicons within published sequence that had been developed for other applications, no amplified fragments had been developed in this particular amplicon

range. Still, the amplification products with each primer set showed high specificity and the amplicon set as a whole demonstrated good sensitivity down to 3 ng total input DNA. Finally amplifications with the primer set yielded a reproducible amplicon profile that exhibited degradation-based variability (loss of amplicon products with increased DNA degradation) using DNA from both enzymatically digested DNA samples and control incubated tissue samples. Based on these factors the CB5 R1-4 amplicon set was utilized to assess DNA degradation levels in samples for the balance of this project.

Data Transformations

In order to compare amplicon data profiles from one amplification to another and to compare results from one data set (timed set of samples that make up a laboratory or field degradation experiment) it was necessary to carry out two manipulations of the data. The first manipulation was designed to allow for comparisons of degradation experiments where the incubations were carried out at different temperatures. In the case of field condition degradations it also addressed the variability in temperature as a function of time (variation in outdoor temperature as a function of time of day and one day to the next). For these reasons it was found to be both convenient and appropriate to complete a calculation of accumulated degree/days and/or degree/hours for each sample. This approach has been traditionally put forward as a means of assessing PMI using rate-of-change methods that rely on a measuring a process that is affected by minimum threshold temperatures above 0ºC --such as insect development (35). Although the use of a 4ºC minimum threshold (in essence using four degrees as the zero point for calculations of temperature) has also been suggested, the difference in

calculations would be minor and linear and could be easily addressed during subsequence data analysis if desired. For this reason, the data reported in this project calculated degree/hours with 0ºC correction for minimum threshold.

The next step in data analysis involved normalizing amplicon signal between both lanes (samples) in an experimental set and between samples in different experimental sets. Amplicon signal was measured as Relative Fluorescent Units (RFU) from a scan of experimental gels. It became clear at an early point in this study that there was variability in sample amplification that was not simply the result of the degree of DNA degradation in the input DNA sample. Due to this variability in sample amplification efficiency between lanes/samples it was not possible to perform a direct comparison of RFU values between samples that differed, for example, by time of degradation. Since this study absolutely required such comparisons to be made a method to normalize for inter-lane variability was needed.

Two primary factors were identified as possible explanations for this inter-sample variability. One potential explanation would be to presuppose the presence of variable amounts of PCR inhibitors in samples. This would be a particularly likely explanation with DNA isolates derived from tissue samples that had been exposed to a range of different environmental conditions. A second possibility would be based upon the method used to quantify the amount of DNA present in individual isolates. Since no RT-PCR based method for quantifying pig DNA existed, a simple absorbance method was used to determine the concentration of total DNA in each isolate. Tissue samples provide excellent conditions for microbial growth and microorganisms contain DNA, too. Therefore, although each amplification reaction contained the same amount of DNA, no

method was available to determine what proportion of this DNA originated from the tissue itself. A higher proportion of microbial DNA in the sample would have the effect of lowering the amount of input pig DNA into the amplification reaction. Therefore, for purposes of interpreting these data an assumption was made. Whatever the reason for the variation in observed amplification success, it was assumed that the effect impacted the amplification of each of the amplicons equally.

As part of the first attempt to normalize for inter-lane variability, the individual amplicon RFU values in a lane were first converted to "proportional amplicon values" by calculating their proportion of the sum of the total RFU for all amplicons in that lane (e.g. for that sample). This manipulation of the RFU data did "smooth" the results considerably, and allowed for comparisons of the results from one sample to another. However, while a plot of the proportional amplicon value vs. time of degradation gave a curve for the 1300 bp amplicon that decreased with time, the curves for the 116 and 247 amplicons increased with time of degradation. This result was as would be expected, with the larger amplicons being preferentially destroyed by the degradation process, but from a visual standpoint this presentation format was considered somewhat less than ideal. A second approach was based upon the fact that the smallest amplicon (116 bp) exhibited a relatively small decay in signal strength over the experimental times utilized. Here amplicon RFU values were converted to a proportional ratio of that amplicon's RFU value to the RFU value for the 116 amplicon. This approach provided a smoothing of the data, as had the above approach, and gave a more visually or intuitive data presentation. It should be noted that there were still a significant number of "outliers" in the data that could not be explained by a uniform inhibition of amplicon

signal/amplification that would be corrected for by either of these corrective manipulations. Once the amplicon values were converted to proportional values, it was clear that the ratios of the RFU values for the 247 and 116 amplicons paralleled each other too closely to be of much experimental value with the presently observed level of remaining experimental variation. Therefore, only the 477 bp and 1300 bp data were used for further calculations. The final manipulation of the data involved converting the 477 bp and 1300 bp ratios from the 0 degree/hours time point to a value of 1.0 and recording the corrected values from other samples in the set as a proportion of this value. This final manipulation allowed comparisons of data from one experiment to the data from a second sample set to be carried out much more readily

These treatments of the data showed promise as mechanisms of addressing specific experimentally-induced variability between samples, and many sets of samples yielded results consistent with the basic assumptions that DNA would be degraded over time and that the necessary templates to produce large amplicons with be destroyed as a higher rate than the templates for smaller amplicons. However, during the course of this study there were several data sets that, given the basic assumption that DNA degrades over time, yielded one or many data points that would have to be considered illogical. The most likely source of these outliers is process variability outlined above. Therefore, before attempting to refine this data treatment, additional effort will need to be put into improving the isolation and amplification processes.

Testing Degraded Samples

Approximately 250 samples were profiled using the CB5 R1-R4 amplicons.

These samples ranged from tissue samples incubated in sealed containers at controlled temperatures collected at specifically set times to samples collected from an intact pig incubated for 35 days in a dappled shade area with no accommodations made for environmental control. Although there was a very apparent overall trend showing a clear pattern of increasing DNA degradation as a function of an increase in postmortem degree/hours, there was still an easily noted level of scatter in the data from most sample sets and unacceptable levels in the data from other sets. When the individual data sets are examined, it is apparent that many of the data sets that exhibited the highest level of scatter were those sets where one or two extreme outliers had greatly altered the underlying trend. In many instances these outliers were derived from a sample or samples collected at degree/hour points after the 0 degree/hour point, but had proportional RFU values that exceeded the 0 degree/hour theoretical maximum. Examining concurrent and duplicate samples tended to show that much of the variability was likely associated with processing error. Despite the instances of variability, many sample sets, including those incubated in the field, exhibited profiles that appear quite consistent with a logarithmic decay of amplicons with the rate being measurably higher for the larger amplicons. At this point it is not possible to say whether or not a logarithmic decay model would successfully describe DNA degradation as a function of degree/hours. However, given the results to date it appears promising.

Concluding Remarks

There were several observations made and issues encountered that should be considered if this project, or similar projects, are undertaken in the future.

Uniform sample DNA purity proved critical to the success of the project. Early attempts at assessing amplicon systems were hampered by amplification inhibition. Careful consideration should be placed on what extraction and purification procedures are to be used. Initial attempts at using an extraction/purification technique commonly used in the forensic community failed and it was only through the implementation of a column base purification system (outlined in the Materials and Methods) that reproducible amplification could be produced. Identification of an additional purification step, designed to further reduce amplification inhibitors in processed samples, would thus be a priority.

An accurate and specific DNA quantification protocol should be employed. Although 260/280 absorbance proved to be a rapid and useful process for our initial purposes, it was not sufficiently sensitive to accurately quantify samples with low DNA concentrations. The process is also susceptible to error as a result of contaminating compounds that absorb ultraviolet radiation of 260 nm wavelength. Additionally, its inability to differentiate between DNA from mammalian versus microbial sources means that in real-world applications quantity measurements could potentially be influenced by non-target DNA (bacterial, fungal etc). Much of the “scatter” seen with the data from samples could be directly attributable to variability in the quantification of target DNA. Should an extension of this study be attempted using human tissue/DNA, RT-PCR methods are currently available that would provide very accurate quantification of total human DNA that are unaffected by the presence of microbial or other DNAs. An RT-PCR assay for porcine DNA could have been developed during the course of this project. However, it was decided that doing so would have added unnecessary

complexity, would be expensive both in time and fiscal resources, and would have limited applications beyond the scope of this demonstration study. It was also not the goal of the project to develop a marketable method to determine the PMI for pigs and ultimately the development of RT-PCR for quantification of pig DNA was not necessary to address the underlying question.

One way to remove some of the variability from the data would be to test more samples at each time point. This could include an increase in both the type and number of controlled and field specimens. The intent of this project, as outlined in the introduction, was to determine the feasibility of using DNA degradation for assessing PMI, so the focus on tissue types and incubation temperature could be limited. However, developing an assay for forensic applications would require the inclusion of a wider range of tissue types since the type and quantity of available tissue will vary from one case to another. In a forensic case it may be feasible to collect and process 10 to 20 tissue samples in order to provide a more accurate average decay pattern. However, in order to have suitable and similarly accurate database for comparison, one would need to process a similar number of samples for each data point in the comparison curve. Arguably a study of this scale could have been carried out during the course of this project. However, the intent of this project was never to develop an assay estimating the PMI of pigs in a very accurate fashion and a more limited data set was deemed appropriate at this time. The collection of more complete data sets, requiring the noted level of time and fiscal investment, should be “saved” for a future time when human tissue samples are available for use.

The inclusion of additional large and small amplicons is also likely to provide a more accurate PMI determination. The best predictor of PMI was data associated with the 1300 bp amplicon. The inclusion of amplicons in the 1750 bp and/or 2500 bp range, combined with additional early PMI collections would likely provide additional information regarding signal decay patterns--especially during the early PMI. The addition of a smaller minimum sized control amplicon could also be useful. Although the decrease seen in the 116 bp amplicon was substantially less than that seen with the larger amplicons, the signal for this amplicon did decrease over time. The addition of one or more amplicons in the 50 bp – 100 bp range could provide more stable amplification controls. Additionally, averaging the RFU values for multiple control loci could eliminate experimental variation before determining proportional RFU values for the larger alleles.

It also goes nearly without saying that labeling primers with a fluorescent dye that can be detected using Capillary Electrophoresis (CE) would be a major improvement in the process. CE is more sensitive than is dye staining and would allow for a more precise measurement of low level amplicon signals without the background issues that accompany gel staining and scanning approaches. The original set of RAPD primers was designed with this in mind.

To summarize, based upon the decay profiles obtained using the cytochrome b5 amplicon set, and to a lesser degree the RAPD and cytochrome b mitochondrial amplicons, the evidence suggests that fragment size analysis can provide information related to DNA degradation that, with further development, may prove useful as a tool for estimating the post-mortem interval. In addition to the overall data trend showing an

increase in DNA degradation as a function of an increase in degree/hours, specific data sets appear to suggest a possible mathematical model for that degradation. None of the issues encountered during this project makes developing such an assay insurmountable. However, considering the investment in time and effort required to bring such an assay on-line, the question must be asked as to whether it makes sense to expend the resources to develop it for an animal model, when the same technology can be applied to human samples.

REFERENCES

1. **Afanas'ev, V. N., B. A. Korol, A. Mantsygin Yu, P. A. Nelipovich, V. A. Pechatnikov, and S. R. Umansky.** 1986. Flow cytometry and biochemical analysis of DNA degradation characteristic of two types of cell death. FEBS Lett. **194:**347-50.
2. **Alaeddini, R., S. J. Walsh, and A. Abbas.** 2010. Forensic implications of genetic analyses from degraded DNA-A review. For. Sci. Int. Genet. **4:**148-157.
3. **Ambion Inc.** 2006. Top ten pitfalls in quantitative real-time PCR primer/probe design and use. Ambion TechNotes. **13**.
4. **Amendt, J., R. Krettek, and R. Zehner.** 2004. Forensic entomology. Naturwissenschaften **91:**51-65.
5. **Ameresco Inc.** 1998. Sensitivity is the issue: package insert. Ameresco Inc., Carlsbad, CA.
6. **Ames, C., B. Turnera, and B. Daniela.** 2006. Estimating the post-mortem interval (II): The use of differential temporal gene expression to determine the age of blowfly pupae. Progress in forensic Genetics 11 - Proc. of the 21st Int. ISFG Cong. **1288:**861-863.
7. **Archer, M. S., and M. A. Elgar.** 2003. Yearly activity patterns in southern Victoria (Australia) of seasonally active carrion insects. For. Sci. Int. **132:**173-6.
8. **Ausubel FM, Brent R, Kingston RE, More DD, Seidman JG, Smith JA, Struhl K (ed.)**, (1987). Current protocols in molecular biology, supplement 27, p. 2.4.1. 1st ed. J. Wiley and Sons, New York.

9. **Baccino, E., L. De Saint Martin, Y. Schuliar, P. Guilloteau, M. Le Rhun, J. F. Morin, D. Leglise, and J. Amice.** 1996. Outer ear temperature and time of death. For. Sci. Int. **83:**133-46.

10. **Bahn, S., S. J. Augood, M. Ryan, D. G. Standaert, M. Starkey, and P. C. Emson.** 2001. Gene expression profiling in the post-mortem human brain--no cause for dismay. J. Chem. Neuroanat. **22:**79-94.

11. **Baird, M., I. Balazs, A. Giusti, L. Miyazaki, L. Nicholas, K. Wexler, E. Kanter, J. Glassberg, F. Allen, P. Rubinstein, et al.** 1986. Allele frequency distribution of two highly polymorphic DNA sequences in three ethnic groups and its application to the determination of paternity. Am. J. Hum. Genet. **39:**489-501.

12. **Bar, W., A. Kratzer, M. Machler, and W. Schmid.** 1988. Postmortem stability of DNA. For. Sci. Int. **39:**59-70.

13. **Bass, B., and J. Jefferson.** 2003. The case of the headless corpse. p. 64. *in* Death's Acre: Inside the legendary forensic lab the body farm where the dead to tell tales. G.P. Putnam's Sons, New York, NY.

14. **Batel, R., Z. Jaksic, N. Bihari, B. Hamer, M. Fafandel, C. Chauvin, H. C. Schroder, W. E. Muller, and R. K. Zahn.** 1999. A microplate assay for DNA damage determination (fast micromethod). Anal. Biochem. **270:**195-200.

15. **Batten, J. (ed.).** 1995. p. 115. Mind over murder: DNA and other forensic adventures. McClelland and Stewart, Tornto, Canada.

16. **Bauer, M.** 2007. RNA in forensic science. For. Sci. Int. Genet. **1:**69-74.

17. **Bauer, M., I. Gramlich, S. Polzin, and D. Patzelt.** 2003. Quantification of mRNA degradation as possible indicator of postmortem interval--a pilot study. Leg. Med. **5:**220-7.

18. **Behrensmeyer, A. K.** 1978. Taphonomic and ecologic information from bone weathering. Paleobiology **4:**150-162.

19. **Bell, L. S., M. F. Skinner, and S. J. Jones.** 1996. The speed of post mortem change to the human skeleton and its taphonomic significance. For. Sci. Int. **82:**129-40.

20. **Bender, K., M. J. Farfan, and P. M. Schneider.** 2004. Preparation of degraded human DNA under controlled conditions. For. Sci. Int. **139:**135-40.

21. **Bender, K., P. M. Schneider, and C. Rittner.** 2000. Application of mtDNA sequence analysis in forensic casework for the identification of human remains. For. Sci. Int. **113:**103-7.

22. **Benjamin, R., and W. Watson.** 1996. The application of genetic bit analysis to forensic loci. Proc. of the 7th Annual Promega Human Identification Symp. Promega Corporation, Madison, WI.

23. **Bessetti, J.** 2007. An introduction to PCR inhibitors: package insert. Promega Corporation. Madison, WI.

24. **Billen, M. J., and E. J. Squires.** 2009. The role of porcine cytochrome b5A and cytochrome b5B in the regulation of cytochrome P45017A1 activities. J. Steroid Biochem. Mol. Biol. **113:**98-104.

25. **Biotium Inc.** 2009. Environmentally safe and ultra-sensitive nucleic acid gel stains for replacing EtBr: package insert. Biotium Inc., Haywood, CA.

26. **Biotium Inc.** 2006. GelRed product data sheet: package insert. Biotium Inc., Haywood, CA.

27. **Biotium Inc.** 2008. A summary of mutagenicity and environmental safety test results from three independent laboratories: package insert. Biotium Inc., Haywood, CA.

28. **Blakely, E. L., A. L. Mitchell, N. Fisher, B. Meunier, L. G. Nijtmans, A. M. Schaefer, M. J. Jackson, D. M. Turnbull, and R. W. Taylor.** 2005. A mitochondrial cytochrome b mutation causing severe respiratory chain enzyme deficiency in humans and yeast. FEBS J. **272:**3583-92.

29. **Boy, S. C., H. Bernitz, and W. F. Van Heerden.** 2003. Flow cytometric evaluation of postmortem pulp DNA degradation. Am. J. For. Med. Pathol. **24:**123-7.

30. **Boya, P., K. Andreau, D. Poncet, N. Zamzami, J. L. Perfettini, D. Metivier, D. M. Ojcius, M. Jaattela, and G. Kroemer.** 2003. Lysosomal membrane permeabilization induces cell death in a mitochondrion-dependent fashion. J. Exp. Med. **197:**1323-34.

31. **Bradley, E. J.** 1993. The distribution of 210Po in human bone. Sci. Total Environ. **130-131:**85-93.

32. **Brambillasca, S., M. Yabal, M. Makarow, and N. Borgese.** 2006. Unassisted translocation of large polypeptide domains across phospholipid bilayers. J. Cell Biol. **175:**767-77.

33. **Brion, F., B. Marc, F. Launay, J. Gailledreau, and M. Durigon.** 1991. Postmortem interval estimation by creatinine levels in human psoas muscle. For. Sci. Int. **52:**113-20.

34. **Briskey, E. J., L. L. Kastenchmidt, J. C. Forrest, G. R. Beecher, M. D. Judge, R. G. Cassens, and W. G. Hoekstra.** 2002. Biochemical aspects of post-mortem changes in porcine muscle. J. of Ag. and Food Chem. **14:**201-207.

35. **Bucheli, S. R., J. A. Bytheway, S. M. Pustilnik, and J. Florence.** 2009. Insect successional pattern of a corpse in cooler months of subtropical southeastern Texas. J. For. Sci. **54:**452-5.

36. **Budowle, B., R. Chakraborty, A. M. Giusti, A. J. Eisenberg, and R. C. Allen.** 1991. Analysis of the VNTR locus D1S80 by the PCR followed by high-resolution PAGE. Am. J. Hum. Genet. **48:**137-44.

37. **Burke, W. J., K. L. O'Malley, H. D. Chung, S. K. Harmon, J. P. Miller, and L. Berg.** 1991. Effect of pre- and postmortem variables on specific mRNA levels in human brain. Brain Res. Mol. Brain Res. **11:**37-41.

38. **Campobasso, C. P., G. Di Vella, and F. Introna.** 2001. Factors affecting decomposition and Diptera colonization. For. Sci. Int. **120:**18-27.

39. **Cassel, S. M., and A. Guttman.** 1998. Membrane-mediated sample loading for automated DNA sequencing. Electrophoresis **19:**1341-6.

40. **Catts, V. S., S. V. Catts, H. R. Fernandez, J. M. Taylor, E. J. Coulson, and L. H. Lutze-Mann.** 2005. A microarray study of post-mortem mRNA degradation in mouse brain tissue. Brain Res. Mol. Brain Res. **138:**164-77.

41. **Cengage, G.** 2006. Time of death. eNotes.com. http://www.enotes.com/forensic-science/time-death

42. **Charabidze, D., B. Bourel, V. Hedouin, and D. Gosset.** 2009. Repellent effect of some household products on fly attraction to cadavers. For. Sci. Int. **189:**28-33.

43. **Chen, X., S. Yi, and L. Liu.** 2007. Image analysis for degradation of DNA in retinal nuclei of rat after death. J. Huazhong Univ. Sci. Technolog. Med. Sci. **27:**24-6.

44. **Chen, Y. C., and J. D. Cheng.** 2002. [The relationship between postmortem degradation of marrow DNA in bosom bone and late postmortem interval estimation]. Fa Yi Xue Za Zhi **18:**144-5.

45. **Chiang, P. W., W. J. Song, K. Y. Wu, J. R. Korenberg, E. J. Fogel, M. L. Van Keuren, D. Lashkari, and D. M. Kurnit.** 1996. Use of a fluorescent-PCR reaction to detect genomic sequence copy number and transcriptional abundance. Genome Res. **6:**1013-1026.

46. **Chisholm, H.** 1911. Diurnal variation in body temperature. Encyclopaedia Britannica, 11 ed. Cambridge University Press, Cambridge, England.

47. **Cina, S. J.** 1994. Flow cytometric evaluation of DNA degradation: a predictor of postmortem interval? Am. J. For. Med. Pathol. **15:**300-2.

48. **Clayton, T. M., J. P. Whitaker, and C. N. Maguire.** 1995. Identification of bodies from the scene of a mass disaster using DNA amplification of short tandem repeat (STR) loci. For. Sci. Int. **76:**7-15.

49. **Coe, J. I.** 1993. Postmortem chemistry update. Emphasis on forensic application. Am. J. For. Med. Pathol. **14:**91-117.

50. **Coe, J. I.** 1972. Use of chemical determinations on vitreous humor in forensic pathology. J. For. Sci. **17:**541-6.

51. **Cotran, R., V. Kumar, T. Collins, and S. Robbins.** 1998. Robbins pathologic basis of disease, 6th ed. W.B Saunders Company, Philadelphia, PA.

52. **Coyle, M. H., C. L. Lee, W. Y. Lin, H. C. Lee, and T. M. Palmbach.** 2005. Forensic botany: using plant evidence to aid in forensic death investigation. Croat. Med. J. **46:**606-12.

53. **De María, A., and C. Arruti.** 2004. DNase I and fragmented chromatin during nuclear degradation in adult bovine lens fibers. Mol. Vis. **10:**74-82.

54. **De Saram, G. S. W., G. Webster, and N. Kathirgamatamby.** 1955. Post-mortem temperature and the time of death. J. of Criminalistic, Law, Criminology and Police Sci. **46:**562–577.

55. **Dekeirsschieter, J., F. J. Verheggen, M. Gohy, F. Hubrecht, L. Bourguignon, G. Lognay, and E. Haubruge.** 2009. Cadaveric volatile organic compounds released by decaying pig carcasses (Sus domesticus L.) in different biotopes. For. Sci. Int. **189:**46-53.

56. **Dhawan, A., M. Bajpayee, and D. Parmar.** 2009. Comet assay: a reliable tool for the assessment of DNA damage in different models. Cell Biol. Toxicol. **25:**5-32.

57. **Di Nunno, N., F. Costantinides, S. J. Cina, C. Rizzardi, C. Di Nunno, and M. Melato.** 2002. What is the best sample for determining the early postmortem

period by on-the-spot flow cytometry analysis? Am. J. For. Med. Pathol. **23:**173-80.

58. **Di Nunno, N. R., F. Costantinides, P. Bernasconi, C. Bottin, and M. Melato.** 1998. Is flow cytometric evaluation of DNA degradation a reliable method to investigate the early postmortem period? Am. J. For. Med. Pathol. **19:**50-3.

59. **Didenko, V. V., H. Ngo, and D. S. Baskin.** 2003. Early necrotic DNA degradation: presence of blunt-ended DNA breaks, 3' and 5' overhangs in apoptosis, but only 5' overhangs in early necrosis. Am. J. Pathol. **162:**1571-8.

60. **Dillon, L., and G. F. Anderson.** 1996. Forensic Entomology the Use of Insects in Death Investigations to Determine Elapsed Time Since Death in Interior and Northern British Columbia Regions. Canadian Police Research Centre**:** Technical Report TR-09-96.

61. **Dimo-Simonin, N., and C. Brandt-Casadevall.** 1996. Evaluation and usefulness of reverse dot blot DNA-PolyMarker typing in forensic case work. For. Sci. Int. **81:**61-72.

62. **Dnyaneshwar, W., C. Preeti, J. Kalpana, and P. Bhushan.** 2006. Development and application of RAPD-SCAR marker for identification of Phyllanthus emblica LINN. Biol. Pharm. Bull. **29:**2313-6.

63. **Dubois, A.** 1985. Diet and gastric digestion. Am. J. Clin. Nutr. **42:**1003-5.

64. **Dupuy, B. M., and B. Olaisen.** 1997. A dedicated internal standard in fragment length analysis of hyperpolymorphic short tandem repeats. For. Sci. Int. **86:**207-27.

65. **Eberhardt, T. L., and D. A. Elliot.** 2008. A preliminary investigation of insect colonisation and succession on remains in New Zealand. For. Sci. Int. **176:**217-23.

66. **Elmas, I., B. Baslo, M. Ertas, and M. Kaya.** 2001. Analysis of gastrocnemius compound muscle action potential in rat after death: significance for the estimation of early postmortem interval. For. Sci. Int. **116:**125-32.

67. **Elmas, I., M. B. Baslo, M. Ertas, and M. Kaya.** 2002. Compound muscle action potential analysis in different death models: significance for the estimation of early postmortem interval. For. Sci. Int. **127:**75-81.

68. **Fasco, M. J., C. P. Treanor, S. Spivack, H. L. Figge, and L. S. Kaminsky.** 1995. Quantitative RNA-polymerase chain reaction-DNA analysis by capillary electrophoresis and laser-induced fluorescence. Anal. Biochem. **224:**140-7.

69. **Fermentas Corporation.** 2010. ZipRuler™ Express DNA Ladder Set: package insert. Fermentas Corporation, Burlington, Canada.

70. **Ferris, M. M., R. C. Habbersett, M. Wolinsky, J. H. Jett, T. M. Yoshida, and R. A. Keller.** 2004. Statistics of single-molecule measurements: applications in flow-cytometry sizing of DNA fragments. Cytometry A. **60:**41-52.

71. **Ferslew, K. E., A. N. Hagardorn, M. T. Harrison, and W. F. McCormick.** 1998. Capillary ion analysis of potassium concentrations in human vitreous humor. Electrophoresis **19:**6-10.

72. **Finger, J. M., J. F. Mercer, R. G. Cotton, and D. M. Danks.** 1987. Stability of protein and mRNA in human postmortem liver--analysis by two-dimensional gel electrophoresis. Clin. Chim. Acta. **170:**209-18.

73. **Fleige, S., V. Walf, S. Huch, C. Prgomet, J. Sehm, and M. W. Pfaffl.** 2006. Comparison of relative mRNA quantification models and the impact of RNA integrity in quantitative real-time RT-PCR. Biotechnol Lett. **28:**1601-13.

74. **Foran, D. R.** 2006. Relative degradation of nuclear and mitochondrial DNA: an experimental approach. J. For. Sci. **51:**766-70.

75. **Frank, W. E., and B. E. Llewellyn.** 1999. A time course study on STR profiles derived from human bone, muscle, and bone marrow. J. For. Sci. **44:**778-82.

76. **Frisch, K.** 2001. Childhood Diseases in the Victorian Age. Ancestry Daily News.

77. **Gaensslen, R. E., and National Institute of Justice (U.S.).** 1983. Sourcebook in forensic serology, immunology, and biochemistry. U.S. Dept. of Justice For sale by the Supt. of Docs., U.S. G.P.O., Washington, D.C.

78. **Gallois-Montbrun, F. G., D. R. Barres, and M. Durigon.** 1988. Postmortem interval estimation by biochemical determination in birds muscle. For. Sci. Int. **37:**189-92.

79. **Garlick, J. D.** 1969. Buried Bone, p. 503-512. *In* D. Brothwell, and E. Higgs (ed.), Science in Archaeology: A survey of progress and research. Thames and Hudson, London, England.

80. **Gennard, D. E.** 2007. p. 123. Forensic entomology : an introduction. John Wiley & Sons, Hoboken, NJ.

81. **George, K. A., M. S. Archer, L. M. Green, X. A. Conlan, and T. Toop.** 2009. Effect of morphine on the growth rate of Calliphora stygia (Fabricius) (Diptera: Calliphoridae) and possible implications for forensic entomology. For. Sci. Int. **193**: 21-25.

82. **Gibson, U. E., C. A. Heid, and P. M. Williams.** 1996. A novel method for real time quantitative RTPCR. Genome Res. 6: **6:**995-1001.

83. **Gill, P., A. J. Jeffreys, and D. J. Werrett.** 1985. Forensic application of DNA 'fingerprints'. Nature **318:**577-9.

84. **Gill, P., R. Sparkes, and C. Kimpton.** 1997. Development of guidelines to designate alleles using an STR multiplex system. For. Sci. Int. **89:**185-97.

85. **Goddard, G., J. C. Martin, M. Naivar, P. M. Goodwin, S. W. Graves, R. Habbersett, J. P. Nolan, and J. H. Jett.** 2006. Single particle high resolution spectral analysis flow cytometry. Cytometry A. **69:**842-51.

86. **Graw, M., H. J. Weisser, and S. Lutz.** 2000. DNA typing of human remains found in damp environments. For. Sci. Int. **113:**91-5.

87. **Green, M. A., and J. C. Wright.** 1985. Postmortem interval estimation from body temperature data only. For. Sci. Int. **28:**35-46.

88. **Green, M. A., and J. C. Wright.** 1985. The theoretical aspects of the time dependent Z equation as a means of postmortem interval estimation using body temperature data only. For. Sci. Int. **28:**53-62.

89. **Green, R. L., I. C. Roinestad, C. Boland, and L. K. Hennessy.** 2005. Developmental validation of the quantifiler real-time PCR kits for the quantification of human nuclear DNA samples. J. For. Sci. **50:**809-25.

90. **Haglund, W. D., and M. H. Sorg.** 1997. p. 181. Forensic Taphonomy: The Postmortem Fate of Human Remains. CRC Press LLC, Boca Raton, FL.

91. **Hallcox, J., Welch, A.** 2007. p. 92. Bodies we've buried: inside the National Forensic Academy, the world's top CSI training school, 1st ed. Berkley Press, New York, NY.

92. **Haller, A. C., D. Kanakapalli, R. Walter, S. Alhasan, J. F. Eliason, and R. B. Everson.** 2006. Transcriptional profiling of degraded RNA in cryopreserved and fixed tissue samples obtained at autopsy. BMC Clin. Pathol. **6:**9.

93. **Hardie, D. C., T. R. Gregory, and P. D. Hebert.** 2002. From pixels to picograms: a beginners' guide to genome quantification by Feulgen image analysis densitometry. J. Histochem. Cytochem. **50:**735-49.

94. **Harrison, P. J., P. R. Heath, S. L. Eastwood, P. W. Burnet, B. McDonald, and R. C. Pearson.** 1995. The relative importance of premortem acidosis and postmortem interval for human brain gene expression studies: selective mRNA vulnerability and comparison with their encoded proteins. Neurosci Lett. **200:**151-4.

95. **Heid, C. A., J. Stevens, and K. J. Livak.** 1996. Real time quantitative PCR. Genome Res. **6:**986-994.

96. **Heinrich, M., S. Lutz-Bonengel, K. Matt, and U. Schmidt.** 2007. Real-time PCR detection of five different "endogenous control gene" transcripts in forensic autopsy material. For. Sci. Int. Genet. **1:**163-9.

97. **Henderson, J.** 1987. Factors determining the state of preservation of human remains, p. 249. *in* A. Boddington, A. Garland (ed.), Death, Decay, and Reconstruction. Manchester University Press, Manchester, England.

98. **Henssge, C., and B. Knight.** 2002. The estimation of the time since death in the early postmortem period, 2nd ed. Oxford University Press, New York, NY.

99. **Henssge, C., and B. Knight.** 1995. The estimation of the time since death in the early postmortem period, 1st ed. Arnold, London, England.

100. **Henssge, C., P. P. Lunkenheimer, O. Salomon, and B. Madea.** 1984. [Supravital electrical excitability of muscles]. Z Rechtsmed **93:**165-74.

101. **Higuchi, R., C. Fockler, G. Dollinger, and R. Watson.** 1993. Kinetic PCR analysis: real-time monitoring of DNA amplification reactions. Biotechnology **11:**1026-30.

102. **Hochmeister, M. N., B. Budowle, U. V. Borer, U. Eggmann, C. T. Comey, and R. Dirnhofer.** 1991. Typing of deoxyribonucleic acid (DNA) extracted from compact bone from human remains. J. For. Sci. **36:**1649-61.

103. **Holland, P. M., R. D. Abramson, R. Watson, and D. H. Gelfand.** 1991. Detection of specific polymerase chain reaction product by utilizing the 5'----3' exonuclease activity of Thermus aquaticus DNA polymerase. Proc. Natl. Acad. Sci. USA **88:**7276-80.

104. **Honsho, M., J. Y. Mitoma, and A. Ito.** 1998. Retention of cytochrome b5 in the endoplasmic reticulum is transmembrane and luminal domain-dependent. J. Biol. Chem. **273:**20860-6.

105. **Hudlow, W. R., M. D. Chong, K. L. Swango, M. D. Timken, and M. R. Buoncristiani.** 2008. A quadruplex real-time qPCR assay for the simultaneous assessment of total human DNA, human male DNA, DNA degradation and the

presence of PCR inhibitors in forensic samples: a diagnostic tool for STR typing. For. Sci. Int. Genet. **2:**108-25.

106. **Hughes, C. E., and C. A. White.** 2009. Crack Propagation in Teeth: A Comparison of Perimortem and Postmortem Behavior of Dental Materials and Cracks*. J. For. Sci. **54:**263-266.

107. **Humphreys-Beher, M. G., F. K. King, B. Bunnel, and B. Brody.** 1986. Isolation of biologically active RNA from human autopsy for the study of cystic fibrosis. Biotechnol. Appl. Biochem. **8:**392-403.

108. **Hunsucker, S. W., B. Solomon, J. Gawryluk, J. D. Geiger, G. N. Vacano, M. W. Duncan, and D. Patterson.** 2008. Assessment of post-mortem-induced changes to the mouse brain proteome. J. Neurochem. **105:**725-37.

109. **Hutchins, G. M.** 1985. Body temperature is elevated in the early postmortem period. Hum. Pathol. **16:**560-1.

110. **Imaizumi, K., S. Miyasaka, and M. Yoshino.** 2004. Quantitative analysis of amplifiable DNA in tissues exposed to various environments using competitive PCR assays. Sci. & Justice **44:**199-208.

111. **Inoue, H., A. Kimura, and T. Tuji.** 2002. Degradation profile of mRNA in a dead rat body: basic semi-quantification study. For. Sci. Int. **130:**127-32.

112. **Irwin, D. M., T. D. Kocher, and A. C. Wilson.** 1991. Evolution of the cytochrome b gene of mammals. J. Mol. Evol. **32:**128-44.

113. **Ishii, K., and M. Fukui.** 2001. Optimization of annealing temperature to reduce bias caused by a primer mismatch in multitemplate PCR. Appl. Environ. Microbiol. **67:**3753-5.

114. **Jaffe, E. R.** 1986. Enzymopenic hereditary methemoglobinemia: a clinical/biochemical classification. Blood Cells **12:**81-90.

115. **Jaffe, F. A.** 1989. Stomach contents and the time of death. Reexamination of a persistent question. Am. J. For. Med. Pathol. **10:**37-41.

116. **Janjua, M. A., and T. L. Rogers.** 2008. Bone weathering patterns of metatarsal v. femur and the postmortem interval in Southern Ontario. For. Sci. Int. **178:**16-23.

117. **Jarvis, D. R.** 1997. Nitrogen levels in long bones from coffin burials interred for periods of 26-90 years. For. Sci. Int. **85:**199-208.

118. **Jayaram, A., M. P. Bowen, S. Deshpande, and H. M. Carp.** 1997. Ultrasound examination of the stomach contents of women in the postpartum period. Anesth. Analg. **84:**522-6.

119. **Jeffreys, A. J., J. F. Brookfield, and R. Semeonoff.** 1985. Positive identification of an immigration test-case using human DNA fingerprints. Nature **317:**818-9.

120. **Jia, X., M. Ekman, H. Grove, E. M. Faergestad, L. Aass, K. I. Hildrum, and K. Hollung.** 2007. Proteome changes in bovine longissimus thoracis muscle during the early postmortem storage period. J. Proteome Res. **6:**2720-31.

121. **Johnson, L. A., and J. A. Ferris.** 2002. Analysis of postmortem DNA degradation by single-cell gel electrophoresis. For. Sci. Int. **126:**43-7.

122. **Johnson, S. A., D. G. Morgan, and C. E. Finch.** 1986. Extensive postmortem stability of RNA from rat and human brain. J. Neurosci. Res. **16:**267-80.

123. **Jones, M. D., W. S. James, S. Barasi, and L. D. Nokes.** 1995. Postmortem electrical excitability of skeletal muscle: preliminary investigation of an animal model. For. Sci. Int. **76:**91-6.

124. **Jonuks, T., and M. Konsa.** 2007. The Revival of Prehistoric Burial Practices: Three Archaeological Experiments. Electronic J. of Folklore. **37:**91-110.

125. **Jorgensen, F. G., A. Hobolth, H. Hornshoj, C. Bendixen, M. Fredholm, and M. H. Schierup.** 2005. Comparative analysis of protein coding sequences from human, mouse and the domesticated pig. BMC Biol. **3:**2.

126. **Kaiser, C., B. Bachmeier, C. Conrad, A. Nerlich, H. Bratzke, W. Eisenmenger, and O. Peschel.** 2008. Molecular study of time dependent changes in DNA stability in soil buried skeletal residues. For. Sci. Int. **177:**32-6.

127. **Kanetake, J., Y. Kanawaku, and M. Funayama.** 2006. Automatic continuous monitoring of rectal temperature using a button-type thermo data logger. Leg. Med. **8:**226-30.

128. **Kang, S., N. Kassam, M. L. Gauthier, and D. H. O'Day.** 2003. Post-mortem changes in calmodulin binding proteins in muscle and lung. For. Sci. Int. **131:**140-7.

129. **Katrukha, A. G., A. V. Bereznikova, V. L. Filatov, T. V. Esakova, O. V. Kolosova, K. Pettersson, T. Lovgren, T. V. Bulargina, I. R. Trifonov, N. A. Gratsiansky, K. Pulkki, L. M. Voipio-Pulkki, and N. B. Gusev.** 1998. Degradation of cardiac troponin I: implication for reliable immunodetection. Clin. Chem. **44:**2433-40.

130. **Kellogg, D. E., J. J. Sninsky, and S. Kwok.** 1990. Quantitation of HIV-1 proviral DNA relative to cellular DNA by the polymerase chain reaction. Anal. Biochem. **189:**202-8.

131. **Kent, R. J., and D. E. Norris.** 2005. Identification of mammalian blood meals in mosquitoes by a multiplexed polymerase chain reaction targeting cytochrome B. Am. J. Trop. Med. Hyg. **73:**336-42.

132. **Kimpton, C. P., N. J. Oldroyd, S. K. Watson, R. R. Frazier, P. E. Johnson, E. S. Millican, A. Urquhart, B. L. Sparkes, and P. Gill.** 1996. Validation of highly discriminating multiplex short tandem repeat amplification systems for individual identification. Electrophoresis **17:**1283-93.

133. **Kline, K. H., and P. J. Bechtes.** 1990. Effects of Postmortem Time and Electrical Stimulation on Histochemical Muscle Fiber Staining and pH in the Middle Gluteal Muscle from Beef Cattle. J. of Food Quality **13:**447-452.

134. **Knight, B., and I. Lauder.** 1969. Methods of dating skeletal remains. Hum. Biol. **41:**322-41.

135. **Knight, B. H.** 1963. Specific staining for nucleoprotein in the examination of seminal stains. J. For. Sci. Soc. **3:**107-109.

136. **Koersve, V.** 1951. Presented at the 10th Intern. Ornith. Congr.

137. **Komar, D. A.** 1998. Decay rates in a cold climate region: a review of cases involving advanced decomposition from the Medical Examiner's Office in Edmonton, Alberta. J. For. Sci. **43:**57-61.

138. **Kumagai, A., N. Nakayashiki, and Y. Aoki.** 2007. Analysis of age-related carbonylation of human vitreous humor proteins as a tool for forensic diagnosis. Leg. Med. **9:**175-80.

139. **Laber, T. L., J. M. O'Connor, J. T. Iverson, J. A. Liberty, and D. L. Bergman.** 1992. Evaluation of four deoxyribonucleic acid (DNA) extraction protocols for DNA yield and variation in restriction fragment length polymorphism (RFLP) sizes under varying gel conditions. J. For. Sci. **37:**404-24.

140. **Larkin, B., S. Iaschi, I. Dadour, and G. K. Tay.** 2009. Using accumulated degree-days to estimate postmortem interval from the DNA yield of porcine skeletal muscle. For. Sci. Med. Pathol. **6**:83-92.

141. **Li, X., A. F. Greenwood, R. Powers, and R. S. Jope.** 1996. Effects of postmortem interval, age, and Alzheimer's disease on G-proteins in human brain. Neurobiol. Aging **17:**115-22.

142. **Lin, L. Q., L. Liu, W. N. Deng, L. Zhang, Y. L. Liu, and Y. Liu.** 2000. [An experimental study on the relationship between the estimation of early postmortem interval and DNA content of liver cells in rats by image analysis]. Fa Yi Xue Za Zhi **16:**68-9, 127.

143. **Lipp, R. W., W. J. Schnedl, H. F. Hammer, P. Kotanko, G. Leb, and G. J. Krejs.** 1997. Evidence of accelerated gastric emptying in longstanding diabetic patients after ingestion of a semisolid meal. J. Nucl. Med. **38:**814-8.

144. **Liu, L., X. Shu, L. Ren, H. Zhou, Y. Li, W. Liu, and C. Zhu.** 2007. Determination of the early time of death by computerized image analysis of DNA

degradation: which is the best quantitative indicator of DNA degradation? J. Huazhong. Univ. Sci. Technolog. Med. Sci. **27:**362-6.

145. **Long, R., W. P. Wang, and P. Xiong.** 2005. [Correlation between PMI and DNA degradation of costicartilage and dental pulp cells in human being]. Fa Yi Xue Za Zhi **21:**174-6.

146. **Lonza Rockland Inc.** 2007. SYBR® Green I Nucleic Acid Gel Stain: package insert. Lonza Rockland Inc., Rockland, ME.

147. **Ludes, B., H. Pfitzinger, and P. Mangin.** 1993. DNA fingerprinting from tissues after variable postmortem periods. J. For. Sci. **38:**686-90.

148. **Lundquist, F. (ed.).** 1963. p. 253-293. Methods of Forensic Science, vol. 2. Interscience publishers, London-New York.

149. **Lutz, J.** 2004. 800px-Sus_scrofa_scrofa, p. A domestic pig on an organic farm in Solothurn, Switzerland. Olympus C750 UZ digital camera, vol. 800 × 600 pixels. Wikipedia, Solothurn, Switzerland.

150. **Mackowiak, P. A., S. S. Wasserman, and M. M. Levine.** 1992. A critical appraisal of 98.6 degrees F, the upper limit of the normal body temperature, and other legacies of Carl Reinhold August Wunderlich. JAMA **268:**1578-80.

151. **Maclaughlin-Black, S. M., R. J. Herd, K. Willson, M. Myers, and I. E. West.** 1992. Strontium-90 as an indicator of time since death: a pilot investigation. For. Sci. Int. **57:**51-6.

152. **Madea, B.** 1992. Estimating time of death from measurement of the electrical excitability of skeletal muscle. J. For. Sci. Soc. **32:**117-29.

153. **Madea, B.** 2005. Is there recent progress in the estimation of the postmortem interval by means of thanatochemistry? For. Sc.i Int. **151:**139-49.

154. **Madea, B.** 1990. [Parameters for determining the time of death from post-mortem muscle contraction--precision of assessing time of death]. Beitr. Gerichtl. Med. **48:**423-35.

155. **Madea, B., and C. Henssge.** 1990. Electrical excitability of skeletal muscle postmortem in casework. For. Sci. Int. **47:**207-27.

156. **Madea, B., C. Henssge, W. Honig, and A. Gerbracht.** 1989. References for determining the time of death by potassium in vitreous humor. For. Sci. Int. **40:**231-43.

157. **Madea, B., C. Kreuser, and S. Banaschak.** 2001. Postmortem biochemical examination of synovial fluid--a preliminary study. For. Sci. Int. **118:**29-35.

158. **Madea, B., and A. Rodig.** 2006. Time of death dependent criteria in vitreous humor: accuracy of estimating the time since death. For. Sci. Int. **164:**87-92.

159. **Malik, K. J., C. D. Chen, and T. W. Olsen.** 2003. Stability of RNA from the retina and retinal pigment epithelium in a porcine model simulating human eye bank conditions. Invest. Ophthalmol. Vis. Sci. **44:**2730-5.

160. **Mall, G., and W. Eisenmenger.** 2005. Estimation of time since death by heat-flow Finite-Element model part II: application to non-standard cooling conditions and preliminary results in practical casework. Leg. Med. **7:**69-80.

161. **Mall, G., M. Hubig, M. Eckl, A. Buttner, and W. Eisenmenger.** 2002. Modelling postmortem surface cooling in continuously changing environmental temperature. Leg. Med. **4:**164-73.

162. **Mant, A.** 1987. Knowledge acquired from post-War exhumations, p. 249. *in* A. Boddington, A. Garland (ed.), Death, Decay, and Reconstruction. Manchester University Press, Manchester, England.

163. **Martinez, E., P. Duque, and M. Wolff.** 2007. Succession pattern of carrion-feeding insects in Paramo, Colombia. For. Sci. Int. **166:**182-9.

164. **McDowall, K. L., D. V. Lenihan, A. Busuttil, and M. A. Glasby.** 1998. The use of absolute refractory period in the estimation of early postmortem interval. For. Sci. Int. **91:**163-70.

165. **McNally, L., R. C. Shaler, M. Baird, I. Balazs, P. De Forest, and L. Kobilinsky.** 1989. Evaluation of deoxyribonucleic acid (DNA) isolated from human bloodstains exposed to ultraviolet light, heat, humidity, and soil contamination. J. For. Sci. **34:**1059-69.

166. **Megyesi, M. S., S. P. Nawrocki, and N. H. Haskell.** 2005. Using accumulated degree-days to estimate the postmortem interval from decomposed human remains. J. For. Sci. **50:**618-26.

167. **Melgar, E., and D. A. Goldthwait.** 1968. Deoxyribonucleic acid nucleases. II. The effects of metals on the mechanism of action of deoxyribonuclease I. J. Biol. Chem. **243:**4409-16.

168. **Michaud, J. P., and G. Moreau.** 2009. Predicting the visitation of carcasses by carrion-related insects under different rates of degree-day accumulation. For. Sci. Int. **185:**78-83.

169. **Micozzi, M.** 1991. Postmortem change in human and animal remains : a systematic approach. C.C. Thomas, Springfield, IL.

170. **Micozzi, M. S.** 1986. Experimental study of postmortem change under field conditions: effects of freezing, thawing, and mechanical injury. J. For. Sci. **31:**953-61.

171. **Monna, L., A. Miyao, H. S. Zhong, T. Sasaki, and Y. Minobe.** 1995. Screening of RAPD markers linked to the photoperiod-sensitivity gene in rice chromosome 6 using bulked segregant analysis. DNA Res. **2:**101-6.

172. **Mullis, K., F. Faloona, S. Scharf, R. Saiki, G. Horn, and H. Erlich.** 1986. Specific enzymatic amplification of DNA in vitro: the polymerase chain reaction. Cold Spring Harb. Symp. Quant. Biol. **51 Pt 1:**263-73.

173. **Munoz, D. R., M. de Almeida, E. A. Lopes, and E. S. Iwamura.** 1999. Potential definition of the time of death from autolytic myocardial cells: a morphometric study. For. Sci. Int. **104:**81-9.

174. **Nagamori, H.** 1978. Sex determination from plucked human hairs without epithelial root sheath. For. Sci. Int. **12:**167-73.

175. **Napirei, M., S. Wulf, and H. G. Mannherz.** 2004. Chromatin breakdown during necrosis by serum Dnase1 and the plasminogen system. Arthritis Rheum. **50:**1873-83.

176. **Neis, P., R. Hille, M. Paschke, G. Pilwat, A. Schnabel, C. Niess, and H. Bratzke.** 1999. Strontium90 for determination of time since death. For. Sci. Int. **99:**47-51.

177. **Nelson, E. L.** 2000. Estimation of short-term postmortem interval utilizing core body temperature: a new algorithm. For. Sci. Int. **109:**31-8.

178. **New England Biolabs.** 2010. λ DNA-HindIII Digest: package insert. New England Biolabs, Ipswich, MA.

179. **NFSTC.** 2010. DNA Analyst Training Laboratory Training Manual. Protocol 3.11 Quantifiler Quantitation Procedure.

180. **Niederstatter, H., S. Kochl, P. Grubwieser, M. Pavlic, M. Steinlechner, and W. Parson.** 2007. A modular real-time PCR concept for determining the quantity and quality of human nuclear and mitochondrial DNA. For. Sci. Int. Genet. **1:**29-34.

181. **Niemcunowicz-Janica, A., W. Pepinski, J. R. Janica, M. Skawronska, J. Janica, and E. Koc-Zorawska.** 2007. Typeability of AmpFISTR SGM plus loci in kidney, liver, spleen and pancreas tissue samples incubated in different environments. Adv. Med. Sci. **52:**135-8.

182. **Nokes, L. D., D. Daniel, T. Flint, and S. Barasi.** 1991. Investigations into the analysis of the rate of decay of the compound action potentials recorded from the rat sciatic nerve after death: significance for the prediction of the post-mortem period. For. Sci. Int. **50:**75-85.

183. **Nokes, L. D., T. Flint, J. H. Williams, and B. H. Knight.** 1992. The application of eight reported temperature-based algorithms to calculate the postmortem interval. For. Sci. Int. **54:**109-25.

184. **Oehmichen, M., J. Frasunek, and K. Zilles.** 1988. Cytokinetics of epidermic cells in skin from human cadavers. I. Dependency on the postmortal interval. Z Rechtsmed **101:**161-71.

185. **Ohshima, T., and Y. Sato.** 1998. Time-dependent expression of interleukin-10 (IL-10) mRNA during the early phase of skin wound healing as a possible indicator of wound vitality. Int. J. Legal Med. **111:**251-5.

186. **Osawa, M., N. Yukawa, T. Saito, X. L. Huang, T. Kusakabe, and S. Takeichi.** 1998. Increased complex formation of Gc globulin with actin in plasma from human cadavers. For. Sci. Int. **96:**39-45.

187. **Parsons, T. J., R. Huel, J. Davoren, C. Katzmarzyk, A. Milos, A. Selmanovic, L. Smajlovic, M. D. Coble, and A. Rizvic.** 2007. Application of novel "mini-amplicon" STR multiplexes to high volume casework on degraded skeletal remains. For. Sci. Int. Genet. **1:**175-9.

188. **Peist, R., D. Honsel, G. Twieling, and D. Löffert.** 2001. PCR inhibitors in plant DNA preparations. Qiagen News **3:**7-9.

189. **Penner, G. A., A. Bush, R. Wise, W. Kim, L. Domier, K. Kasha, A. Laroche, G. Scoles, S. J. Molnar, and G. Fedak.** 1993. Reproducibility of random amplified polymorphic DNA (RAPD) analysis among laboratories. PCR Methods Appl. **2:**341-5.

190. **Pera, P., C. Bucca, R. Borro, C. Bernocco, L. A. De, and S. Carossa.** 2002. Influence of mastication on gastric emptying. J. Dent. Res. **81:**179-81.

191. **Perry, W. L., W. M. Bass, W. S. Riggsby, and K. Sirotkin.** 1988. The autodegradation of deoxyribonucleic acid (DNA) in human rib bone and its relationship to the time interval since death. J. For. Sci. **33:**144-53.

192. **Pettenati, M. J., P. N. Rao, S. Schnell, R. Hayworth-Hodge, P. E. Lantz, and K. R. Geisinger.** 1995. Gender identification of dried human bloodstains using fluorescence in situ hybridization. J. For. Sci. **40:**885-7.

193. **Pfeiffer, H., J. Huhne, B. Seitz, and B. Brinkmann.** 1999. Influence of soil storage and exposure period on DNA recovery from teeth. Int. J. Legal Med. **112:**142-4.

194. **Phillips, W. T., U. A. Salman, C. A. McMahan, and J. G. Schwartz.** 1997. Accelerated gastric emptying in hypertensive subjects. J. Nucl. Med. **38:**207-11.

195. **Poloz, Y. O., and D. H. O'Day.** 2009. Determining time of death: temperature-dependent postmortem changes in calcineurin A, MARCKS, CaMKII, and protein phosphatase 2A in mouse. Int. J. Legal. Med. **123:**305-14.

196. **Popova, T., D. Mennerich, A. Weith, and K. Quast.** 2008. Effect of RNA quality on transcript intensity levels in microarray analysis of human post-mortem brain tissues. BMC Genomics **9:**91.

197. **Pounder, D. J.** 1995. Time of death. University of Dundee. http://www.dundee.ac.uk/forensicmedicine/notes/timedeath.pdf

198. **Preece, P., and N. J. Cairns.** 2003. Quantifying mRNA in postmortem human brain: influence of gender, age at death, postmortem interval, brain pH, agonal state and inter-lobe mRNA variance. Brain Res. Mol. Brain Res. **118:**60-71.

199. **Preece, P., D. J. Virley, M. Costandi, R. Coombes, S. J. Moss, A. W. Mudge, E. Jazin, and N. J. Cairns.** 2003. An optimistic view for quantifying mRNA in post-mortem human brain. Brain Res. Mol. Brain Res. **116:**7-16.

200. **Prieto-Castello, M. J., J. P. Hernandez del Rincon, C. Perez-Sirvent, P. Alvarez-Jimenez, M. D. Perez-Carceles, E. Osuna, and A. Luna.** 2007. Application of biochemical and X-ray diffraction analyses to establish the postmortem interval. For. Sci. Int. **172:**112-8.

201. **Proctor, H. C.** 2009. Can freshwater mites act as forensic tools? Exp. Appl. Acarol. **49:**161-5.

202. **Promega, C.** 1998. Certificate of Analysis Gold ST*R 10X Buffer: package insert. Promega Corporation, Madison, WI.

203. **Prusak, B., and T. Grzybowski.** 2004. Non-random base composition in codons of mitochondrial cytochrome b gene in vertebrates. Acta. Biochim. Pol. **51:**897-905.

204. **Querido, D.** 2000. Temperature-correction of abdominal impedance: improved relationship between impedance and postmortem interval. For. Sci. Int. **109:**39-50.

205. **Ramser, J., K. Weising, V. Chikaleke, and G. Kahl.** 1997. Increased informativeness of RAPD analysis by detection of microsatellite motifs. Biotechniques **23:**285-90.

206. **Rodriguez, W. C., 3rd, and W. M. Bass.** 1985. Decomposition of buried bodies and methods that may aid in their location. J. For. Sci. **30:**836-52.

207. **Rozen, S., and H. Skaletsky (ed.).** 2000. Primer3 on the WWW for general users and for biologist programmers. Humana Press, Totowa, NJ.

208. **Sabucedo, A. J., and K. G. Furton.** 2003. Estimation of postmortem interval using the protein marker cardiac Troponin I. For. Sci. Int. **134:**11-6.

209. **Saiki, R. K., S. Scharf, F. Faloona, K. B. Mullis, G. T. Horn, H. A. Erlich, and N. Arnheim.** 1985. Enzymatic amplification of beta-globin genomic sequences and restriction site analysis for diagnosis of sickle cell anemia. Science **230:**1350-4.

210. **Sams, A.** 2002. Post-mortem electrical stimulation of broilers. World's Poultry Sci. J. **58:**147-157.

211. **Sasaki, S., S. Tsunenari, and M. Kanda.** 1983. The estimation of the time of death by non-protein nitrogen (NPN) in cadaveric materials. Report 3: multiple regression analysis of NPN values in human cadaveric materials. For. Sci. Int. **22:**11-22.

212. **Schleyer, F., and J. Brehmer.** 1958. [Examination of the postmortal creatine levels in blood & cerebrospinal fluid in relation to the time & cause of death.]. Medizinische **2:**381-3.

213. **Schleyer, F., and K. Sellier.** 1958. [Studies on the serum hemoglobin content in various venous areas of the dead body.]. Z Gesamte Inn. Med. **13:**805-9.

214. **Schneider, P. M., K. Bender, W. R. Mayr, W. Parson, B. Hoste, R. Decorte, J. Cordonnier, D. Vanek, N. Morling, M. Karjalainen, C. Marie-Paule Carlotti, M. Sabatier, C. Hohoff, H. Schmitter, W. Pflug, R. Wenzel, D. Patzelt, R. Lessig, P. Dobrowolski, G. O'Donnell, L. Garafano, M. Dobosz, P. De Knijff, B. Mevag, R. Pawlowski, L. Gusmao, M. Conceicao Vide, A. Alonso Alonso, O. Garcia Fernandez, P. Sanz Nicolas, A. Kihlgreen, W. Bar, V. Meier, A. Teyssier, R. Coquoz, C. Brandt, U. Germann, P. Gill, J. Hallett, and M.**

Greenhalgh. 2004. STR analysis of artificially degraded DNA-results of a collaborative European exercise. For. Sci. Int. **139:**123-34.

215. **Schoenly, K., and R. Hall.** 2002. Testing Reliability of Animal Models in Research and Training Programs in Forensic Entomology, Part II, Final Report. U.S. Department of Justice Report, National Criminal Justice Reference Service, Rockville, MD.

216. **Schwartz, T. R., E. A. Schwartz, L. Mieszerski, L. McNally, and L. Kobilinsky.** 1991. Characterization of deoxyribonucleic acid (DNA) obtained from teeth subjected to various environmental conditions. J. For. Sci. **36:**979-90.

217. **Sharanowski, B. J., E. G. Walker, and G. S. Anderson.** 2008. Insect succession and decomposition patterns on shaded and sunlit carrion in Saskatchewan in three different seasons. For. Sci. Int. **179:**219-40.

218. **Shu, X., Y. Liu, L. Ren, F. He, H. Zhou, and L. Liu.** 2005. Correlative analysis on the relationship between PMI and DNA degradation of cell nucleus in human different tissues. J. Huazhong Univ. Sci. Technolog. Med. Sci. **25:**423-6.

219. **Siegel, J.** 2006. p 264. Forensic science: the basics. CRC/Taylor & Francis, Boca Raton, FL.

220. **Simonsen, J., J. Voigt, and N. Jeppesen.** 1977. Determination of the time of death by continuous post-mortem temperature measurements. Med. Sci. Law. **17:**112-22.

221. **Singer, V. L., L. J. Jones, S. T. Yue, and R. P. Haugland.** 1997. Characterization of PicoGreen reagent and development of a fluorescence-based

solution assay for double-stranded DNA quantitation. Anal. Biochem. **249:**228-38.

222. **Singer, V. L., T. E. Lawlor, and S. Yue.** 1999. Comparison of SYBR Green I nucleic acid gel stain mutagenicity and ethidium bromide mutagenicity in the Salmonella/mammalian microsome reverse mutation assay (Ames test). Mutat. Res. **439:**37-47.

223. **Son, C. G., S. Bilke, S. Davis, B. T. Greer, J. S. Wei, C. C. Whiteford, Q. R. Chen, N. Cenacchi, and J. Khan.** 2005. Database of mRNA gene expression profiles of multiple human organs. Genome Res. **15:**443-50.

224. **Southern, E. M.** 1975. Detection of specific sequences among DNA fragments separated by gel electrophoresis. J. Mol. Biol. **98:**503-17.

225. **Sparkes, R., C. Kimpton, S. Watson, N. Oldroyd, T. Clayton, L. Barnett, J. Arnold, C. Thompson, R. Hale, J. Chapman, A. Urquhart, and P. Gill.** 1996. The validation of a 7-locus multiplex STR test for use in forensic casework. (I). Mixtures, ageing, degradation and species studies. Int. J. Legal Med. **109:**186-94.

226. **Starkeby, M.** 2004. Ultimate guide to forensic entomology: Introduction to forensic entomology. http://folk.uio.no/mostarke/forens_ent/afterdeath.shtml.

227. **Statheropoulos, M., A. Agapiou, C. Spiliopoulou, G. C. Pallis, and E. Sianos.** 2007. Environmental aspects of VOCs evolved in the early stages of human decomposition. Sci. Total Environ. **385:**221-7.

228. **Statheropoulos, M., C. Spiliopoulou, and A. Agapiou.** 2005. A study of volatile organic compounds evolved from the decaying human body. For. Sci. Int. **153:**147-55.

229. **Stigler, S.** 1972. The Asymptotic Distribution of the Trimmed Mean. The Annals. of Statistics **1:**472-477.

230. **Stokes, K. L., S. L. Forbes, L. A. Benninger, D. O. Carter, and M. Tibbett.** 2009. Decomposition Studies Using Animal Models in Contrasting Environments: Evidence from Temporal Changes in Soil Chemistry and Microbial Activity, p357-377. *in* K. Ritz, L. Dawson, D. Miller (Ed.) Criminal and Environmental Soil Forensics. Springer, NY.

231. **Stokes, K. L., S. L. Forbes, and M. Tibbett.** 2009. Freezing skeletal muscle tissue does not affect its decomposition in soil: evidence from temporal changes in tissue mass, microbial activity and soil chemistry based on excised samples. For. Sci. Int. **183:**6-13.

232. **Straton, K. J., A. Busuttil, and M. A. Glasby.** 1992. Nerve conduction as a means of estimating early post-mortem interval. Int. J. Legal Med. **105:**69-74.

233. **Sugioka, M., H. Sawai, E. Adachi, and Y. Fukuda.** 1995. Changes of compound action potentials in retrograde axonal degeneration of rat optic nerve. Exp. Neurol. **132:**262-70.

234. **Swango, K. L., W. R. Hudlow, M. D. Timken, and M. R. Buoncristiani.** 2007. Developmental validation of a multiplex qPCR assay for assessing the quantity and quality of nuclear DNA in forensic samples. For. Sci. Int. **170:**35-45.

235. **Swango, K. L., M. D. Timken, M. D. Chong, and M. R. Buoncristiani.** 2006. A quantitative PCR assay for the assessment of DNA degradation in forensic samples. For. Sci. Int. **158:**14-26.

236. **SWGDAM.** 2008. Important Notice of Revised Quality Assurance Standards for Forensic DNA. For. Sci. Comm. **10**. http://www.fbi.gov/hq/lab/fsc/backissu/oct2008/standards/2008_10_standards01.htm.

237. **Swift, B.** 1998. Dating human skeletal remains: investigating the viability of measuring the equilibrium between 210Po and 210Pb as a means of estimating the post-mortem interval. For. Sci. Int. **98:**119-26.

238. **Swift, B., I. Lauder, S. Black, and J. Norris.** 2001. An estimation of the post-mortem interval in human skeletal remains: a radionuclide and trace element approach. For. Sci. Int. **117:**73-87.

239. **Tabor, K. L., C. C. Brewster, and R. D. Fell.** 2004. Analysis of the successional patterns of insects on carrion in southwest Virginia. J. Med. Entomol. **41:**785-95.

240. **Tabor, K. L., R. D. Fell, and C. C. Brewster.** 2005. Insect fauna visiting carrion in Southwest Virginia. For. Sci. Int. **150:**73-80.

241. **Takayama, T., I. Nakamura, Y. Watanabe, S. Yamada, K. Hirata, A. Nagai, Y. Bunai, and I. Ohya.** 2003. Quality and quantity of DNA in cadavers' serum. Leg. Med. (Tokyo) **5 Suppl 1:**180-2.

242. **Taylor, R. E., J. M. Suchey, L. A. Payen, and P. J. Slota, Jr.** 1989. The use of radiocarbon (14C) to identify human skeletal materials of forensic science interest. J. For. Sci. **34:**1196-205.

243. **Thierauf, A., F. Musshoff, and B. Madea.** 2009. Post-mortem biochemical investigations of vitreous humor. For. Sci. Int. **192:**78-82.

244. **Thomsen, H., H. J. Kaatsch, and B. Krisch.** 1999. How and why does the platelet count in postmortem blood change during the early postmortem interval? For. Sci. Int. **101:**185-94.

245. **Tomlin, J., N. Brown, A. Ellis, A. Carlsson, C. Bogentoft, and N. W. Read.** 1993. The effect of liquid fibre on gastric emptying in the rat and humans and the distribution of small intestinal contents in the rat. Gut **34:**1177-81.

246. **Trindade-Filhoa, A., C. Mendesa, S. Ferreiraa, S. Oliveirab, A. Vasconcelosb, F. Maiaa, H. Paka, and K. Paulaa.** 2008. DNA obtained from decomposed corpses cartilage: A comparison with skeleton muscle source. For. Sci. Int.: Genetics Supplement Series **1:**456-461.

247. **Troncon, L. E., R. J. Bennett, N. K. Ahluwalia, and D. G. Thompson.** 1994. Abnormal intragastric distribution of food during gastric emptying in functional dyspepsia patients. Gut **35:**327-32.

248. **Trudeau, K.** 2004. PicoGreen DNA Quantitation using the FLUOstar fluorescent plate reader p. 10. Orchid Cellmark Corporation, Nashville, TN.

249. **Tsai, L.-C., M.-T. Huang, C.-T. Hsiao, C.-Y. Lin, S.-J. Chen, C.-I. Lee, and H.-M. Hsieh.** 2007. Species identification of animal specimens by cytochrome b gene. For. Sci. J. **6:**63-65.

250. **Tsokos, M., U. Reichelt, R. Jung, A. Nierhaus, and K. Puschel.** 2001. Interleukin-6 and C-reactive protein serum levels in sepsis-related fatalities during the early postmortem period. For. Sci. Int. **119:**47-56.

251. **Uchigasaki, S., L. Oesterhelweg, A. Gehl, J. P. Sperhake, K. Puschel, S. Oshida, and N. Nemoto.** 2004. Application of compact ultrasound imaging device to postmortem diagnosis. For. Sci. Int. **140:**33-41.

252. **Uhlin-Hansen, L.** 2001. C-reactive protein (CRP), a comparison of pre- and post-mortem blood levels. For. Sci. Int. **124:**32-5.

253. **Van Holde, K. E., J. R. Allen, K. Tatchell, W. O. Weischet, and D. Lohr.** 1980. DNA-histone interactions in nucleosomes. Biophys. J. **32:**271-82.

254. **van Oorschot, R. A., S. J. Gutowski, S. L. Robinson, J. A. Hedley, and I. R. Andrew.** 1996. HUMTH01 validation studies: effect of substrate, environment, and mixtures. J. For. Sci. **41:**142-5.

255. **Vandewoestyne, M., D. Van Hoofstat, F. Van Nieuwerburgh, and D. Deforce.** 2009. Suspension fluorescence in situ hybridization (S-FISH) combined with automatic detection and laser microdissection for STR profiling of male cells in male/female mixtures. Int. J. Legal Med. **123:**441-7.

256. **VanGuilder, H. D., K. E. Vrana, and W. M. Freeman.** 2008. Twenty-five years of quantitative PCR for gene expression analysis. Biotechniques **44:**619-26.

257. **Vass, A. A., W. M. Bass, J. D. Wolt, J. E. Foss, and J. T. Ammons.** 1992. Time since death determinations of human cadavers using soil solution. J. For. Sci. **37:**1236-53.

258. **Verboven, C., A. Rabijns, M. De Maeyer, H. Van Baelen, R. Bouillon, and C. De Ranter.** 2002. A structural basis for the unique binding features of the human vitamin D-binding protein. Nat. Struct. Biol. **9:**131-6.

259. **von Wurmb-Schwark, N., T. Schwark, M. Harbeck, and M. Oehmichen.** 2004. A simple Duplex-PCR to evaluate the DNA quality of anthropological and forensic samples prior short tandem repeat typing. Leg. Med. **6:**80-8.

260. **Wallace, J. R., R. W. Merritt, R. Kimbirauskas, M. E. Benbow, and M. McIntosh.** 2008. Caddisflies assist with homicide case: determining a postmortem submersion interval using aquatic insects. J. For. Sci. **53:**219-21.

261. **Wang, Q., J. Zhang, T. Y. Chen, Z. W. Chen, M. B. Chen, W. C. Lineaweaver, and F. Zhang.** 2006. DNA degradation in nuclei of muscle cells followed by ischemic injury in a rabbit amputation model. Microsurgery **26:**391-5.

262. **Watson, W.** 1994. Personal experience with rapid decomposition associated with acute illness, Dallas, TX.

263. **Waye, J. S., and R. M. Fourney.** 1990. Agarose gel electrophoresis of linear genomic DNA in the presence of ethidium bromide: band shifting and implications for forensic identity testing. Appl. Theor. Electrophor. **1:**193-6.

264. **Wehner, F., H. D. Wehner, M. C. Schieffer, and J. Subke.** 1999. Delimitation of the time of death by immunohistochemical detection of insulin in pancreatic beta-cells. For. Sci. Int. **105:**161-9.

265. **Wehner, F., H. D. Wehner, and J. Subke.** 2001. Delimitation of the time of death by immunohistochemical detection of calcitonin. For. Sci. Int. **122:**89-94.

266. **Wells, J. D., and L. R. Lamotte.** 2001. Estimating the postmortem interval in forensic entomology: The utility of arthropods in legal Investigations. CRC Press, London, England.

267. **Whitney, W. F.** 1897. The Double Staining of Spermatozoa. J. Boston Soc. Med. Sci. **1:**9-10.

268. **Wieberg, D. A., and D. J. Wescott.** 2008. Estimating the timing of long bone fractures: correlation between the postmortem interval, bone moisture content, and blunt force trauma fracture characteristics*. J. For. Sci. **53:**1028-34.

269. **Williams, J. G., A. R. Kubelik, K. J. Livak, J. A. Rafalski, and S. V. Tingey.** 1990. DNA polymorphisms amplified by arbitrary primers are useful as genetic markers. Nucleic Acids Res. **18:**6531-5.

270. **Yadav, J., A. Deshpande, A. Arora, B. K. Athawal, and B. K. Dubey.** 2007. Estimation of time since death from CSF electrolyte concentration in Bhopal region of central India. Legal Medicine **9:** 309-313.

271. **Yamazaki, M., and C. Wakasugi.** 1994. Postmortem changes in drug-metabolizing enzymes of rat liver microsome. For. Sci. Int. **67:**155-68.

272. **Yan, X., R. C. Habbersett, J. M. Cordek, J. P. Nolan, T. M. Yoshida, J. H. Jett, and B. L. Marrone.** 2000. Development of a mechanism-based, DNA staining protocol using SYTOX orange nucleic acid stain and DNA fragment sizing flow cytometry. Anal. Biochem. **286:**138-48.

273. **Ygonaar.** 2006. Ethidium bromide. ACD/ChemStetch, http://en.wikipedia.org/wiki/File:Ethidium_bromide.png.

274. **Ygonaar.** 2006. PicoGreen ([2-[N-bis-(3-dimethylaminopropyl)-amino]-4-[2,3-dihydro-3-methyl-(benzo-1,3-thiazol-2-yl)-methylidene]-1-phenyl-quinolinium]+). . ACD/ChemStetch, http://commons.wikimedia.org/wiki/File:PicoGreen_(topological_formula).png.

275. **Yikrazuul.** 2007. Agarose, the polymere error corrected. vector graphics, http://commons.wikimedia.org/wiki/File:Agarose_polymere.png.

276. **Yoshino, M., T. Kimijima, S. Miyasaka, H. Sato, and S. Seta.** 1991. Microscopical study on estimation of time since death in skeletal remains. For. Sci. Int. **49:**143-58.

277. **Zhao, D., B. L. Zhu, T. Ishikawa, L. Quan, D. R. Li, and H. Maeda.** 2006. Real-time RT-PCR quantitative assays and postmortem degradation profiles of erythropoietin, vascular endothelial growth factor and hypoxia-inducible factor 1 alpha mRNA transcripts in forensic autopsy materials. Leg. Med. (Tokyo) **8:**132-6.

278. **Zhen, J. L., X. D. Zhang, and Q. S. Niu.** 2006. [Relationship between the postmortem interval and nuclear DNA changes of heart muscular cells in mice]. Fa Yi Xue Za Zhi **22:**173-6.

279. **Zimmermann, K., and J. W. Mannhalter.** 1996. Technical aspects of quantitative competitive PCR. Biotechniques **21:**268-72, 274-9.

280. **Zipper, H., H. Brunner, J. Bernhagen, and F. Vitzthum.** 2004. Investigations on DNA intercalation and surface binding by SYBR Green I, its structure determination and methodological implications. Nucleic Acids Res. **32:**103.